

# Statistical Model for Rainfall and Drought Analysis of Tumakuru District, Karnataka State, India Using Geospatial Technology

---

A thesis submitted in fulfillment of the requirement for the degree of

*Doctor of Philosophy*

in

*Geoinformatics*

by

**Sanjay Kumar**

under the supervision of

**Prof. Syed Ashfaq Ahmed**



Department of P.G. Studies & Research in Applied Geology  
Kuvempu University, Jnanasahyadri, Shankaraghatta  
Shivamogga, Karnataka - 577 451

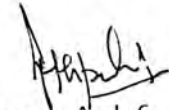
**2022**

*To my beloved family and friends*



## Certificate

This is to certify that the thesis entitled "**Statistical Model for Rainfall and Drought Analysis of Tumakuru District, Karnataka State, India Using Geospatial Technology**" submitted by Mr. Sanjay Kumar for the partial fulfillment of the requirement for the award of Doctor of Philosophy in Geoinformatics to Kuvempu University, Shankaraghatta is a bonafide record of his original work carried out under my guidance and supervision. The matter embodied in this thesis is original and has not been submitted for the award of any other degree/diploma.



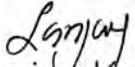
Prof. Syed Ashfaq Ahmed  
Department of Applied Geology  
Kuvempu University  
Shankaraghatta, Shimoga  
Karnataka-577451

Date: 6.12.2022

Place: Shankaraghatta

## Declaration

I hereby declare that the thesis entitles ***"Statistical Model for Rainfall and Drought Analysis of Tumakuru District, Karnataka State, India Using Geospatial Technology"*** carried out by me under the supervision of Prof. Syed Ashfaq Ahmed, Department of Applied Geology, Kuvempu University, Jnanasahyadri, Shankaraghatta is my own work. To the best of my knowledge it contains no materials previously published or written by another person, or substantial proportions of material which have been accepted for the award of any other degree or diploma at Kuvempu University or any other educational institution except where due acknowledgement is made in the thesis. Any contribution made to the research by others, with whom I have worked at Kuvempu University or elsewhere, is explicitly acknowledged in the thesis. I also declare that the intellectual content of this thesis is the product of my own work, except to the extent that assistance from others in the project's design and conception or in style, presentation and linguistic expression is acknowledged.

  
Sanjay Kumar

# Acknowledgement

At the outset, I express my sincere thanks to Kuvempu University and the Department of Applied Geology for the opportunity to complete my long-standing dream of pursuing PhD. The University has been kind enough to provide fellowship and a serene environment conducive for academic progress.

I proudly declare my heartfelt gratitude to my supervisor Prof. Syed Ashfaq Ahmed firstly for choosing me as a research scholar. His exceptional supervision and support have not only made this an enriching adventure but has also made this mammoth of a task tremendously convenient. I appreciate and draw inspiration from your knowledge, patience, availability, and research ideas. For giving me space to confidently develop myself as a researcher thanks to his kindness and strong support, and conceiving the fundamental idea behind the research, I would time and again choose him as my supervisor if given a chance.

Prof. G Chandrakantha, I greatly acknowledge your precious insights during the conception of my research proposal and your support of my whole PhD journey. I appreciate the invaluable contribution of Prof. Govindaraju who shared ideas, spent time discussing research and was a member of my Doctoral committee. Thank you for your inexplicable enthusiasm and assurances that you'll read this thesis. The contribution of the Doctoral Committee members is duly acknowledged. Thanks also goes to the committee members for reading this dissertation and giving valuable feedback to make it better.

I am also deeply indebted to Ms. Jyothika Karkala for spending time in numerous discussions and support, particularly regarding data analysis, MATLAB, R, and programming, which helped me a lot during thesis

writing. I greatly acknowledge her patience and precious insights during my publications. She has enabled refining my approach to problem-solving and the way I present my research. I would like to thank my friends, colleagues, and collaborators for their undying encouragement in every step and involvement in various ways. I wish them all the best of success in their future work.

Harishnaika N has been my companion during the term of Phd both personally and academically. We have worked together on research with the same supervisor. I thank him for his support and all the help rendered at every instance.

During the trying times of the COVID-19 pandemic, Mr. Krishna Kumar S was the one who stood by me and helped me through the tough situations. A huge thanks to a friend like him.

The efforts of Dr. Mohd Sayeed Ul Hasan (Assistant professor, Aliah University, Kolkata) and Mr. Aditya Deshmukh (Research Scholar, UNSW, Australia) in providing me with timely advice and assurance in research are of utmost value to me for which I'll forever be grateful. I owe a lot to my long-time friends Mr. Chirag Arya and Mr. Ashok Sharma for truly supporting me emotionally and financially. A thanks for unburdening me which made this journey a lot smoother.

I owe much to my wife, Naresh, and son Jayesh who sustains me in hard times and champions my success in good times. May everyone have such a family in their life. Nothing would be possible without the blessing and unwavering love and support from my parents, brother, and the rest of my family. Many people have helped directly or indirectly in my entire journey of PhD, who have stood by my side. Although not listed here, you remain loved and special to me.

Sanjay Kumar

# Abstract

Tumakuru district of Karnataka state is situated in the semi-arid climatic region which is considered to be a sensitive zone in response to climate change. The unpredictable weather phenomenon is a cause for major concern as it brings along with it a series of difficulties. This draws our attention to drought which is one of the reasons of concern and needs to be dealt with in an effective manner.

The analysis of the spatiotemporal changes of meteorological drought in the Tumakuru district during 1951-2019 is analysed. To understand the spatial and temporal characteristics of drought, annual and seasonal drought trends were examined using standardized precipitation index. Based on three-seasons, pre-monsoon (Jan-May), southwest monsoon (Jun-Sep), and northeast monsoon (Oct-Dec) along with the annual SPI were calculated. The correlation between precipitation and SPI was similar and strong in nature. The wettest (1962-2006), and driest years (1968, 1954, 1965, 1976) during the study were identified. The higher frequency distribution of the driest years addresses roughly 57% drought years detected for Madhugiri and Tumakuru-1 in SW monsoon of the total years of study, in pre-monsoon Kunigal has 21.73%, and in NE-monsoon it was 50.72% at Kunigal.

A detailed account of frequency, run length, and temporal trend of the drought events are presented in the study from 1981 to 2019 at the 1-, 3-, 6-, 9-, 12-, and 24-month timescale using the Standardized Precipitation Index (SPI) and Standardized Precipitation Evapotranspiration Index SPEI. SPI recorded more drought months in extreme category while SPEI showed longer drought length in moderate and severe category for agricultural and hydrological drought. At 1-month timescale, both the indices reported extreme drought events where Tiptur station in May 2016 (-4.75) and Chikkanayakanahalli

station in March 1992 (-2.76) were the worst-case scenarios.

The trend detection and analysis of rainfall in Tumakuru district during 1952–2019 have been performed using Mann-Kendall (MK), Modified Mann Kendall test (MMK), and Innovative Trend Analysis (ITA) techniques. The significance and slope result of the precipitation trend extracted through the ITA technique is compared with the classical MK method and Sen's approach. The ITA result calculated at a 5% significance level for annual rainfall reported seven stations with a significant increasing trend and three stations having a significant downward trend while one of the stations (Koratagere) shows a non-significantly negative pattern. The rainfall analysis showed that the northern region received the least rainfall while the southern region received the maximum rainfall all except one of the stations had a positive kurtosis. The trend was very well defined by all the methods, though Modified Mann Kendall z statistics showed more occurrences of significant changes in the rainfall pattern. The northeast monsoon carried a significantly decreasing trend at Chikkanayakanahalli station while all of the significantly increasing trends were defined by the Modified Mann Kendall test in the annual, and southwest monsoon season. Seasonal scale evaluation also gives the correct and impressive result using ITA than the Mann-Kendall test.

Homogeneity tests such as the Pettitt test, SNHT, and Buishand test were employed to identify the change point in the rainfall series. The result was found to have the most correlation between the Pettitt test and the Buishand test in comparison to SNHT. Later ARIMA model was run for the precipitation dataset to predict the rainfall value from 2019 to 2029 which showed a decline in the amount of rainfall in the entire study area.

Nowadays there is an increase in the utilization of satellite-based precipitation products which makes it crucial to examine the accuracy of



such products. Although the rain gauge stations with a resolution of 250 × 250 provide precipitation data, the emerging satellite products show bigger promise. The valuation of Tropical Rainfall Measuring Mission (TRMM) data with the gauge data for 11 stations was conducted over the semi-arid region of Karnataka by means of data comparison and the drought indices such as Percent of Normal (PN), Modified China Z Index (MCZI), and Rainfall Anomaly Index (RAI). Comparative analysis was carried out for the monthly data using various statistical methods from the year 1998 to 2019 using the MAE, NSE and Pearson correlation methods. The study focuses on determining the feasibility and reliability of precipitation products in the analysis of drought. There is about 27.13% of similarity amongst the dataset for RAI while only 10.88% of data match for PN index. It was found that the satellite data is most suitable for the large-scale area while there are uncertainties when it comes to regional studies.

In the conditions of monsoon failure and very less rainfall during southwest monsoon, farmers could not able to sown new crops and existing rain-fed crops would be decimated on the field. The study aims at providing informative and practical results to facilitate decision makers for water resource and drought risk management.

## List of Figures

1	<i>Study area with grid stations . . . . .</i>	11
2	<i>Methodology Framework . . . . .</i>	15
3	<i>Percentage occurrence of rainfall at the different season . . . . .</i>	23
4	<i>Evolution of annual rainfall and temporal distribution of SPI . . . . .</i>	25
5	<i>Spatial pattern of annual SPI as a response of drought . . . . .</i>	29
6	<i>Spatial pattern of pre-monsoon SPI as a response of drought . . . . .</i>	30
7	<i>Spatial pattern of pre-monsoon (a,b,c); southwest monsoon (d,e,f); northeast monsoon (g,h,i); and annual (j,k) SPI in response to drought frequency during the period 1951-2019 . . . . .</i>	31
8	<i>Spatial pattern of SW monsoon SPI as a response of drought . . . . .</i>	32
9	<i>Spatial pattern of NE monsoon SPI as a response of drought . . . . .</i>	34
10	<i>Temporal distribution of SPI series at different season . . . . .</i>	35
11	<i>Spatial Distribution of frequency of SPI . . . . .</i>	44
12	<i>Spatial Distribution of frequency of SPEI . . . . .</i>	46
13	<i>Length of dry period in months . . . . .</i>	48
14	<i>Temporal distribution of SPI at different timescale . . . . .</i>	51
15	<i>Temporal distribution of SPEI at different timescale . . . . .</i>	54
16	<i>Interpretation of ITA trend . . . . .</i>	63
17	<i>Graphical representation of pre-monsoon ITA . . . . .</i>	65
18	<i>Minimum and maximum magnitude of trend of time series rainfall in the pre-monsoon (a &amp; b), SW monsoon (c &amp; d), NE monsoon (e &amp; f) and annual (g &amp; h) . . . . .</i>	67
19	<i>Seasonal and annual spatial dispersion of Z, ITA slope and Sen slope . . . . .</i>	68
20	<i>Graphical representation of SW monsoon ITA . . . . .</i>	69
21	<i>Trend comparison of the seasonal and annual ITA . . . . .</i>	70
22	<i>Graphical representation of NE monsoon ITA . . . . .</i>	71
23	<i>Graphical representation of annual ITA . . . . .</i>	72
24	<i>Spatial variability of MMK and ITA with trend indicators . . . . .</i>	74
25	<i>Comparison of Z value of MMK and ITA_R with significance threshold . . . . .</i>	78
26	<i>Comparison of MMK Sen slope and ITA_R slope . . . . .</i>	78
27	<i>Histogram of time series analysis of rainfall with the normal distribution curve . . . . .</i>	83
28	<i>Change point in rainfall series from Pettitt test . . . . .</i>	85
29	<i>Change point in rainfall series from SNHT . . . . .</i>	86
30	<i>Change point in rainfall series from Buishand test . . . . .</i>	87
31	<i>Prediction of spatial rainfall for 2025 and 2029 . . . . .</i>	88

32	<i>Actual rainfall, ARIMA, and predicted rainfall . . . . .</i>	89
33	<i>Methodology used in the study . . . . .</i>	93
34	<i>Spatial distribution of MAE(a), NSE(b), and Pearson Correlation(c) . . . . .</i>	97
35	<i>RMSE of 3B43 and rain gauge dataset for RAI from 1998 to 2019 . . . . .</i>	99
36	<i>Pearson correlation of rain gauge and TRMM 3B43 for RAI . . . . .</i>	100
37	<i>RAI plot for rain gauge versus TRMM from 1998 to 2019 . . . . .</i>	101
38	<i>Pearson correlation of rain gauge and TRMM 3B43 for MCZI . . . . .</i>	103
39	<i>RMSE of 3B43 and rain gauge dataset for MCZI from 1998 to 2019 . . . . .</i>	104
40	<i>Monthly heat map for MCZI . . . . .</i>	105
41	<i>Pearson correlation of rain gauge and TRMM 3B43 for PN . . . . .</i>	108
42	<i>RMSE of 3B43 and rain gauge dataset for PN from 1998 to 2019 . . . . .</i>	109
43	<i>Overlapping temporal distribution of PN with drought severity . . . . .</i>	110
44	<i>RMSE of 3B43 and rain gauge dataset for DI from 1998 to 2019 . . . . .</i>	113
45	<i>Pearson correlation of rain gauge and TRMM 3B43 for DI . . . . .</i>	114
46	<i>DI plot for rain gauge versus TRMM from 1998 to 2019 . . . . .</i>	115
47	<i>Scatter plot of indices . . . . .</i>	118

**List of Tables**

1	<i>Description of Meteorological parameters of Grid stations . . . . .</i>	13
2	<i>Magnitude of precipitation extremes through indices . . . . .</i>	16
3	<i>Descriptive statistics of seasonal rainfall . . . . .</i>	24
4	<i>Evolution of season wise drought frequency . . . . .</i>	28
5	<i>The intensity of SPI series at different timescale . . . . .</i>	28
6	<i>Classification of drought severity based on SPI<sup>1</sup> and SPEI<sup>2</sup> value . . . . .</i>	41
7	<i>Minimum value of SPI and SPEI recorded at different timescale . . . . .</i>	57
8	<i>Detailed statistical description of annual and seasonal rainfall statistics . . . . .</i>	64
9	<i>Description of the Seasonal rainfall variation result for 11 grid stations of Z statistics, ITA slope and Sen's slope with the positive and negative ITA trend during 1952-2019. (The trend at (P&lt;0.05) Significant level is indicated in bold character) . . . . .</i>	66
10	<i>Summary of the statistical test result for Annual rainfall from 1952-2019</i>	73
11	<i>Z and slope value of MMK and ITA_R . . . . .</i>	75
12	<i>Result of homogeneity test . . . . .</i>	84
13	<i>Dry and wet categories of the indices used<sup>3-6</sup> . . . . .</i>	95

## Abbreviations and acronyms

AgriMetSoft	Agricultural and Meteorological Software
ALOS PALSAR	Advanced Land Observing Satellite Phased Array type L-band Synthetic Aperture Radar
ARIMA	Autoregressive Integrated Moving Average
ASCAT	Advanced SCATterometer
ASF	Alaska Satellite Facility
CHIRPS	Climate Hazards Group InfraRed Precipitation with Station data
CN Halli	Chikkanayakanahalli
CZI	China Z Index
DAS	Data Assimilation System
DI	Decile Index
ENSO	El Nino Southern Oscillation
GEOS	Goddard Earth Observation System
GES DISC	Goddard Earth Sciences Data and Information Services Center
GIS	Geographic information system
IDW	Inverse Distance Weighted
IMD	India Meteorological Department
IMERG	Integrated Multi-satellitE Retrievals for GPM
ITA	Innovative Trend Analysis
MAE	Mean Absolute Error
MCZI	Modified China Z Index
MDM	Meteorological Drought Monitoring
MERRA	Modern-Era Retrospective analysis for Research and Applications
MK	Mann-Kendall
MMK	Modified Mann Kendall
NDMA	National Disaster Management Authority
NE	Northeast
NetCDF	Network Common Data Form
NSE	Nash Sutcliffe Efficiency coefficient
PDSI	Palmer Drought Severity Index
PET	Potential evapotranspiration
PN	Percent of Normal
RAI	Rainfall Anomaly Index
RMSE	Root Mean Square Error
RTC	Radiometric Terrain Correction

SM2RAIN	Soil Moisture to Rain
SNHT	Standard Normal Homogeneity Test
SPEI	Standardized Precipitation Evapotranspiration Index
SPI	Standardized Precipitation Index
SPSS	Statistical Package for the Social Sciences
SRI	Standardized Runoff Index
SS	Sen's slope estimator
SSI	Standardized Streamflow Index
SW	Southwest
TRMM	Tropical Rainfall Measuring Mission

## Contents

<b>1</b>	<b>Introduction</b>	<b>6</b>
1.1	Climate Scenario	6
1.2	Monitoring the precipitation extreme: Drought	7
1.3	Description of study area	10
1.4	Why do we need to study drought?	12
1.5	Objective of the research	12
1.6	Data	12
1.6.1	Rain gauge	13
1.6.2	Temperature	13
1.6.3	Satellite	13
1.7	Methodology Framework	14
1.8	Research Significance	16
1.9	Thesis Structure	16
<b>2</b>	<b>Meteorological Drought</b>	<b>18</b>
2.1	Introduction	18
2.2	Methodology	20
2.2.1	Inverse Distance Weighted (IDW)	20
2.2.2	SPI	21
2.3	Results and Discussion	22
2.3.1	Drought characteristics and analysis of SPI	22
2.3.2	Season wise Rainfall Analysis	23
2.3.3	Statistical Parameters and variability analysis of annual rainfall	23
2.3.4	Rainfall Trend and temporal distribution of SPI at Tumakuru district	24
2.3.5	Seasonal detection and monitoring of the wet and dry period	27
2.3.6	Spatial Pattern of Drought	28
2.3.7	Season wise SPI	33
2.4	Conclusion	37
<b>3</b>	<b>Drought Indices</b>	<b>39</b>
3.1	Introduction	39
3.2	Methodology	41
3.2.1	SPI	41
3.2.2	SPEI	43
3.3	Result and Discussion	43
3.3.1	Drought Frequency	43
3.3.2	Run length of drought	47

3.3.3	Temporal evolution of dry period at different timescale . . . . .	50
3.4	Conclusion . . . . .	57
<b>4</b>	<b>Rainfall Trend</b>	<b>59</b>
4.1	Introduction . . . . .	59
4.2	Methodology . . . . .	61
4.2.1	Modified Mann Kendall . . . . .	61
4.2.2	Sen's Slope Estimator . . . . .	62
4.2.3	Innovative Trend Analysis . . . . .	63
4.3	Result . . . . .	64
4.3.1	Pre-monsoon . . . . .	64
4.3.2	Southwest Monsoon . . . . .	66
4.3.3	Northeast Monsoon . . . . .	70
4.3.4	Annual . . . . .	72
4.3.5	Modified Mann Kendall test . . . . .	73
4.3.6	Innovative trend analysis with type-I error removed . . . . .	76
4.4	Discussion and Conclusion . . . . .	77
<b>5</b>	<b>Change Point Detection and Rainfall Forecast</b>	<b>80</b>
5.1	Introduction . . . . .	80
5.2	Methodology . . . . .	81
5.2.1	Pettitt Test . . . . .	81
5.2.2	Standard Normal Homogeneity Test (SNHT) . . . . .	81
5.2.3	Buishand Test . . . . .	82
5.2.4	Autoregressive Integrated Moving Average (ARIMA) . . . . .	82
5.3	Result . . . . .	82
5.3.1	Rainfall time series analysis . . . . .	82
5.3.2	Homogeneity test . . . . .	84
5.3.3	ARIMA . . . . .	88
5.4	Discussion and Conclusion . . . . .	90
<b>6</b>	<b>Validation of IMD and TRMM data for drought analysis</b>	<b>91</b>
6.1	Introduction . . . . .	91
6.2	Methodology . . . . .	93
6.2.1	Mean Absolute Error . . . . .	93
6.2.2	Nash Sutcliffe Efficiency coefficient . . . . .	93
6.2.3	Rainfall Anomaly Index (RAI) . . . . .	94
6.2.4	Modified China Z Index (MCZI) . . . . .	94
6.2.5	Percent of Normal Index (PN) . . . . .	94
6.2.6	Deciles Index (DI) . . . . .	95

6.2.7	Root Mean Square Error (RMSE) . . . . .	95
6.2.8	t-Test . . . . .	95
6.2.9	Pearson Correlation . . . . .	96
6.3	Result and discussion . . . . .	96
6.3.1	Mean Absolute Error . . . . .	96
6.3.2	Nash Sutcliffe Efficiency coefficient . . . . .	98
6.3.3	Pearson Correlation . . . . .	98
6.3.4	Rainfall Anomaly Index . . . . .	98
6.3.5	Modified China Z Index . . . . .	102
6.3.6	Percent of Normal . . . . .	108
6.3.7	Deciles Index . . . . .	113
6.3.8	Comparison of rain gauge and TRMM through indices . . . . .	117
6.4	Conclusion . . . . .	118
<b>7</b>	<b>Conclusion</b>	<b>120</b>
7.1	Outcome of the study . . . . .	120
7.2	Recommendations . . . . .	121
<b>8</b>	<b>Reference</b>	<b>123</b>



## 1. Introduction

### 1.1. Climate Scenario

A vast country such as India experiences various characteristics of climatology. The Himalayan Mountain ranges in the north, the Indo-Gangetic plains, the Peninsular Deccan Plateau, the western Thar Desert, Coastal Plains along with the islands make the six physiographic regions of India's land surface. India deals with a consistently high temperature throughout the summer with the mountain ranges being an exception. Since 1901, the average temperature of India has risen by 0.7°C and the large part of it is due to the greenhouse gases – induced warming, and partially due to the land use and land cover changes and anthropogenic aerosols<sup>7</sup>. Towards the end of the twenty first century, the temperature is projected to rise by around 4.4°C relative to the last three decades. In the Indian Ocean, the sea surface temperature has risen by 1°C from 1951 to 2015 which is significantly higher in comparison to the global rise of 0.7°C. The study of temperature from 1901-2020 revealed that there is an increase in the average annual mean temperature of 0.62°C/100 years. The maximum and minimum temperature increased at a rate of 0.99°C/100 years and 0.24°C/100 years respectively. There is an apparent rise in both the minimum and maximum temperatures in the last 30 years confined mainly to the northern, central, and eastern regions. A small pocket in the north western part has seen a dip in the temperature. Precipitation patterns along the various climate zones of the country cause variations in the winter temperature. The least rainfall of 300 mm is recorded in the arid and semi-arid regions of the west including the desert. High annual rainfall of more than 1500 mm is commonly seen in the wet tropical SW region while the east coast also endures high temperature and high precipitation conditions and is prone to high degree of variation<sup>8</sup>. A greater fluctuation in the seasonal temperature is seen mainly in the central regions. There has been a 6% decline in the Indian summer monsoon relative to 1951-2015, and this decline is especially evident over the Western Ghats and the Indo-Gangetic Plains. Based on multiple datasets and various climate models, there is a clear evidence that the anthropogenic aerosols forcing over the Northern Hemisphere has had its radiative effects causing offset on the summer monsoon precipitation and Greenhouse gases warming<sup>9</sup>.

Heat waves are on a rise in the world and India has been regularly experiencing record high temperatures with an average maximum being 36°C. Climate models have projected that the average number of summer heat waves in India from 2040 to 2069 will rise to about 2.5 events per season and further rise to 3 events by the end of the twenty first century. The west coast of the country is projected to bear brunt<sup>10</sup>. There is a historical trend where an increase in sea surface temperature and

the resultant decrease in the Indian monsoon is strongly influenced by ENSO. Despite the inter-annual fluctuation, the rainfall received over the Indian summer monsoon has stayed stable<sup>11</sup>. Extending from June to September is the SW monsoon which delivers a monthly rainfall of 150 mm to 270 mm on average. The NE monsoon generates about 10 mm to 75 mm of an average monthly rainfall from October to December. The crucial feature of the rainfall regime of India is the huge variability in the inter-annual precipitation which is a result of the climate influence of the Indian Ocean Dipole and El Nino Southern Oscillation (ENSO) on the monsoon<sup>12</sup>.

Historically what should have been an extreme event occurring once every 100 year is going to be a once in 50 year occurrence or event 25 year in most of Asia countries<sup>13</sup>. Most of the annual losses from a disaster in India is associated with flood events. Multiple factors affect the magnitude of the disasters which is highly dependent on physical and socioeconomic vulnerabilities of the people and the asset which is exposed to the disaster<sup>14</sup>. Naumann's research provides a global perspective on how the varying warming of the Earth has affected the drought conditions. With 1.5°C to 2°C of warming the frequency of dry spells is bound to be twice the amount. Many studies have been focused in detail at the changes particularly in Indian Summer Monsoon which is a major contributor to the precipitation amount<sup>15</sup>. Over the past few decades there has been a dramatical increase in the potential risks caused by weather and climate related events leading to loss and damage. A significant rise in the intensity, duration and frequency of extreme weather events are on the rise. Furthermore, it is recognised that merely mitigation and adaptation will not be good enough but rather there is a need to implement management techniques and bring in effective climate risk assessment so that the damage can be addresses and minimized. Many a short term managerial techniques exist and are being implemented but a long term approach to combat the effects of the slow-onset changes due to climate change need to be implemented .

## **1.2. Monitoring the precipitation extreme: Drought**

Defined by the various disaster management organizations in India, disasters can be categorized as human-induced and natural. This classification can be further divided into water and climate related; chemical, nuclear, and industrial related; accident related; geological; and biological related disasters. Some of the typically occurring disasters in India is listed based of the National Disaster Management Plan given by the National Disaster Management Authority (NDMA). Annually 1/8th of the country faces flooding conditions making it one of the highly affected country in the world. The coastline of nearly 7516 km is exposed to about 10% of the global cyclones and

are likely to experience tsunamis. Around 68% of the country is drought prone in varying degrees. Abnormally high temperature (heat waves) are on the rise across the land. India also experiences earthquakes as it is placed on the boundary of two continental plates, while the Himalayan and the Western Ghats bear about 30% of the world's landslides. Thunderstorm, Hail, Dust storm and Cold Wave and Fog are also prevalent<sup>16</sup>.

To select a system of interest, it is eminent to have an understanding of the potential climate risks in the area and the fluctuations in weather patterns leading to an increase in extreme events. Therefore, studying these risks will help in classifying the area into multiple risk zones. Disasters bring along with them a stream of impacts causing loss and damage to property and life. Direct impacts of the disaster refer to the immediate outcome of the event mainly concerning casualties and infrastructure destruction. Indirect impacts of the disaster is not essentially provoked by the event but rather a consequence that follow-on such as poverty induced by loss and others. Drought Background: Drought differs from the rest of the natural disasters since it has slow progression and takes a prolonged time to evolve while having a wide spatial extent and not much structural damage. Hence determining the exact duration and intensity of the disaster tends to be a hard task. Like any other disaster, the effects of drought span the environmental, social and economic sectors and these impacts can be reduced by carrying out mitigation, management and preparedness techniques. Drought is commonly found worldwide with varying duration, intensity, impacts, and contributing factors hence putting focus on development on plans to deal with it in timely and effective manner to avoid water shortage. Drought occurs in areas of high as well as low rainfall in India, where scarcity of water is common even in the Himalayan region. Our country has more than 300 river basins among which some are shared by up to two or more countries and acceleration in drought conditions which eventually cause international water conflicts. In certain regions, drought can leave its impact on recreation and tourism, forest fires, energy sector, transportation, ecosystem, environment, soil erosion, endangering life system and much more. Drought cannot be defined just as a shortage of rainfall but is equally attributed to ineffectiveness in the management of water resources. Lack of water harvesting, over exploitation of water, pollution, increase in impermeable surface, limitation in the recharge of water, encroachment of surface water bodies has only added on to the problem. Due to this about 80 to 90% of the drinking water requirement and about 50% of the irrigation water requirement is met by the groundwater which increases the stress on the sub surface hydrology. Although there is an overall increase in drought events throughout the country, the probabilities varies from 2 years to 15 years in

Rajasthan and Assam respectively.

**Classification of Drought:** Primarily three types of drought are seen in India namely meteorological, agricultural, and hydrological drought. Meteorological Drought is defined when a dry weather pattern is dominant in the area and there is a significant drop in the rainfall with respect to the normal value. Agricultural Drought is in play when the crops tend to become affected by the drought event where the health or yield of the crop is impacted due to lack of soil moisture and insufficient rainfall and increased transpiration. Hydrological Drought deals with the shortage in the water is evident in the surface and the groundwater hydrology system usually occurs due to long term prevalence of the dry spell<sup>17</sup>. Drought risk is the combination of the water shortage in the area and the exposure of the community to the ill effects of drought. It is crucial that the nations take the issue seriously and begin planning accordingly to reduce the vulnerability factor. This can be done through awareness, resource allocation, management and mitigation methods taken up by the administration and the public. It is critical to understand the spatial and temporal pattern of drought in different regions to put in place an early warning system for the disaster which incorporates parameters such as temperature, precipitation, snowpack, soil moisture, surface water storage, stream flow, and ground water level.

**Management in India:** A paradigm shift is apparent in India in recent times concerning the disaster management owing to a large number of casualties and huge economic losses which has made us realise that Disaster Management is crucial if we aim at sustaining the development of the country. Correspondingly, the Government of India has been proactively adopting a multidisciplinary holistic approach to build disaster resilience structures and other initiatives. India need to have a different approach at tackling drought in arid, semi-arid and other regions. It is shocking to realize that Cherrapunji in Meghalaya known for receiving the one of the highest rainfall in the world (over 11000 mm), now for nine months of the year faces drought whereas the wettest region of Jaisalmer District in Rajasthan, known for being one of the driest part of the country now records about 9 cm of annual rainfall. In the Himalayan Mountains, at elevations above 1500 m, the annual precipitation is from 20 to 1000 cm but with the challenge of water storage, the dry season that follows can create scarcity of water. The state of Odisha with average precipitation of 1100 mm is severely affected by drought. This draws attention to the fact that drought is not just a result of water scarcity but an issue deeply related to the water resource management. India is going through an increased propensity for drought over the last 6 to 7 decades owing to the decrease in the summer monsoon rainfall resulting in decreased spatial extent and frequency of rainfall.

Particularly, regions such as central India, southern peninsular, southwest coast, and north-eastern India have been going through twice the amount of drought than usual with an increase of 1.3% in the area affected by drought per decade. By the end of this century, India is expected to witness an increased frequency and intensity of drought conditions as a result of monsoon variability and a rise in the demand for water vapour in the warming atmosphere.

Though Karnataka has reported less number of deaths due to heat waves, the Northern Interior parts are more vulnerable. Air pollution fluctuates partly due to climate and weather abnormalities. The geographical placement of Karnataka is on a tableland that is bounded by the Western Ghats and Eastern Ghats ranges which converge at the Nilgiri hill range. Karnataka states falls within the latitude of 11.5°N and 18.5°N and longitudes of 74°E and 78.5°E neighbouring the states of Maharashtra and Goa in the North and Northwest, Northeast and East by Telangana and Andhra Pradesh, Tamil Nadu in the South and Southeast and Kerala in the South, while the Arabian sea lies on the west. Karnataka can be divided into the regions geographically as the Western Ghats, the Coastal Plains and the Deccan Plateau. With 77% of the area covered by arid and semi-arid regions, drought is a serious issue in need of consideration as two third of the state records rainfall of less than 750 mm yearly. 18 of the 33 districts and 88 among the 176 taluks are in drought prone adding up to 54% of the total area of the state. The limited water resources of the state are stressed and are depleting at a fast pace. With increasing population, and sub-sequential increases in urbanization and industrialization, the demand for water supply has been growing from all the sectors. 45% of the water for irrigation is provided through the ground water. With 64.6% of the area under cultivation and 56.5% of the workforce employed in agriculture, the need for sustainable water resource management is of importance<sup>18</sup>.

Tumakuru district falls in the South Interior region of Karnataka and experience less than average rainfall. There is a high inter-annual variability of rainfall over certain districts including Tumakuru<sup>19</sup>. Tumakuru has a 92% coefficient of variation in rainfall with a precipitation trend of 7.55 mm/day/100yr, minimum temperature trend of 0.321 °C/100yr and maximum temperature trend of 0.403 °C/100yr. Tumakuru has shown an increasing trend in the SW Monsoon while a decreasing trend is observed for the pre-monsoon, NE monsoon and annual normal rainfall<sup>20</sup>.

### **1.3. Description of study area**

The focus of the study lies in Tumakuru District in the South-Eastern part of Karnataka, one of the southern states in India. The geographic extent of the area extends between the latitudes 12°44'31" to 14°21'2" N and longitudes 76°21'2" to 77°30'12" E making up for a total area of 10603 Km<sup>2</sup>. The digital elevation model of

the area as specified in , undulates between 406 m to 1193 m above the mean sea level.

The area characterized as a semi-arid zone, the Koppen-Geiger climate classification categorizes it as arid steppe hot and tropical savannah zone. The precipitation in the area is measured by the 11 grid stations in the 10 taluks of the District as seen in Figure 1. With an average rainfall of 668.74 mm during the 1981-2019 period, the maximum rainfall is observed at Tumakuru in 1962 with 2429.11 mm and minimum rainfall at Gubbi in 1976 with 136.30 mm. The maximum temperature reaches its highest in April at around 33°C and the minimum at 18°C in December. The rate of annual potential evapotranspiration is over 1800 mm and monthly rate is less than 100 mm during December and January while May record over 250 mm monthly. The Eastern part of the Tumakuru district is covered by a narrow range of Granite hills. In the west, the Tumakuru district is covered by a long range of hills running up to South East. The district is surrounded to the north by Anantapur district (Andhra Pradesh state), in the south by Mandya and Ramanagara, in the East by Chikkaballapur and Bangalore, and in the west by Hassan and Chikmagalur.

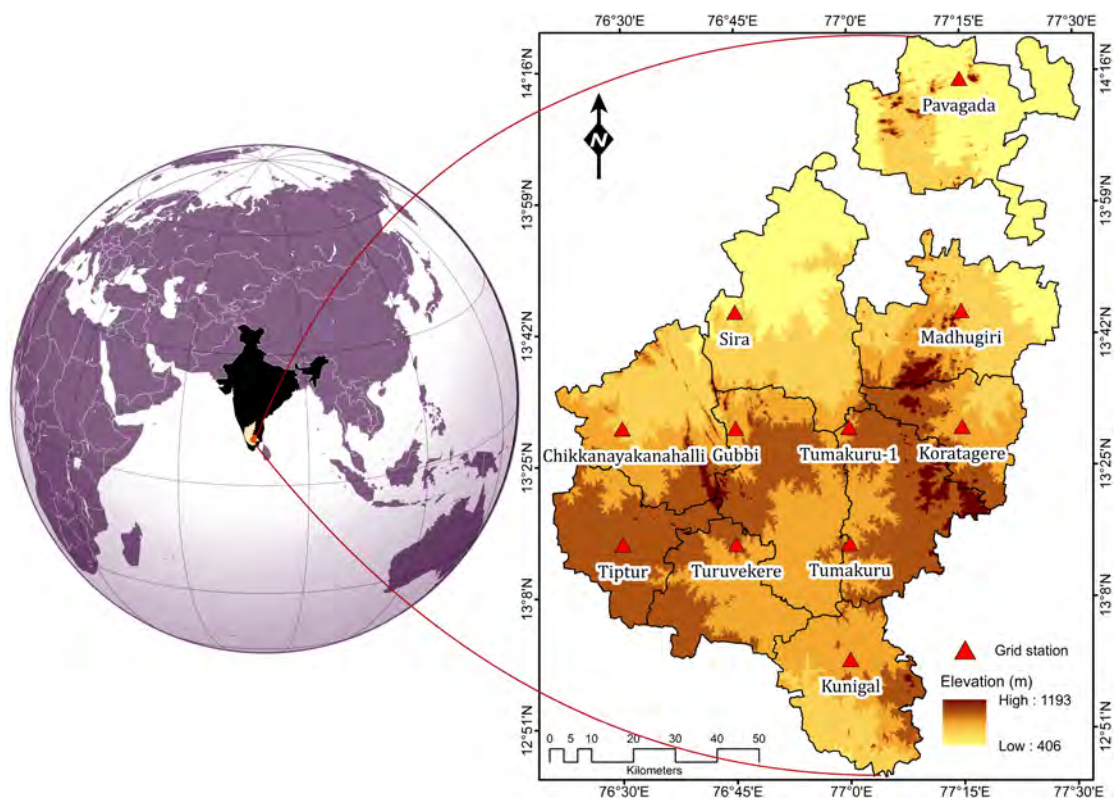


**Figure 1:** Study area with grid stations

In the north, the Tumakuru district is drained by Pennar and lower Tungabhadra and in the south drained by Lower Cauvery river. Jayamangali, Shimsha and Suvarnamukhi are the principal streams found in the district. The district has no

perennial rivers while the streams flowing in the rainy seasons dry up as the seasons' progress. Ragi, groundnut, paddy, horse gram, maize, sunflower, sugarcane makeup of the major crops which are local to the area along with the coconut and arecanut plantations according to the 2009-10 agriculture statistics. Only about 4.3% of the total area is designated as forest which lie mostly in the lower slopes having vegetation inferior than the ones found in the evergreen forests. Open forest comprising of mixed species ranging from dry deciduous to thorny bushes are common to this area while trees tend to be short, and twisted due to scanty rainfall. Barren land and depletion of forest are on the rise in the past decades mainly due to deforestation and overgrazing. The geomorphology of the area covered by denudational uplands are found to be ideal for agriculture, urban settlement, and industrialization.

#### **1.4. Why do we need to study drought?**

Although the Tumakuru District receives a significant amount of rainfall, it is often prone to drought conditions of varying intensities. Lacking the presence of any major river in the area, the agricultural and industrial functioning is mainly dependent on rainfall. Drought conditions have resulted in extreme impacts on the farmer's livelihood and this forms the inspiration for the research.

#### **1.5. Objective of the research**

1. Investigate the drought hazard and prone area of Tumakuru District.
2. Examine the Spatio-temporal Pattern and characteristics of Meteorological Drought.
3. Visualization of seven decadal rainfall variations as a result of climate change using non-parametric tests.
4. Change point detection in the time series data using statistical techniques to identify the vulnerable region and forecast rainfall for the next decade.
5. Implementing a statistical model to evaluate the consistency of TRMM over the Rain Gauge for Drought Monitoring.

#### **1.6. Data**

The scenario of low precipitation over prolonged duration along with changes in atmospheric conditions such as climate change and ocean temperature are the key factors leading to drought. The research prominently observes data concerning rainfall, and temperature collected from multiple sources to assess the drought in the study area. Meteorological data from 11 grid stations were used in the study as mentioned in Table 1.

**Table 1:** Description of Meteorological parameters of Grid stations

Station	Lon	Lat	Elevation (m)	Mean Rainfall (mm)	Min Rainfall (mm)	Max Rainfall (mm)	Min Temp ( <sup>0</sup> C)	Max Temp ( <sup>0</sup> C)
<i>Chikkanayakanahalli</i>	76.5	13.5	660	612.62	273.60	2073.87	18.24	29.38
<i>Gubbi</i>	76.75	13.5	686	551.84	136.30	1091.50	20.76	27.10
<i>Koratagere</i>	77.25	13.5	675	624.41	291.14	1363.19	19.18	31.31
<i>Kunigal</i>	77	13	673	884.31	351.01	1553.00	18.78	30.64
<i>Madhugiri</i>	77.25	13.75	654	585.28	136.84	1247.30	20.22	28.94
<i>Pavagada</i>	77.25	14.25	524	502.04	223.32	2282.16	20.84	33.30
<i>Sira</i>	76.75	13.75	579	628.47	242.80	1286.97	18.60	30.51
<i>Tiptur</i>	76.5	13.25	763	683.90	347.49	1135.34	18.37	30.76
<i>Tumakuru</i>	77	13.25	714	653.35	206.73	1914.99	18.50	30.36
<i>Tumakuru-1</i>	77	13.5	718	796.27	337.02	2429.11	18.94	29.47
<i>Turuvekere</i>	76.75	13.25	741	712.98	275.90	2282.70	18.78	30.44

### 1.6.1. Rain gauge

The ground-based precipitation data were obtained from India Meteorological Department (IMD)<sup>21</sup> with a spatial resolution of 0.25° x 0.25°. Apart from the systemic error due to evaporation, IMD data has been known to be reliable in both spatial and temporal aspects. The daily gridded dataset was collected from 1998 to 2019 and the daily rainfall data is averaged to obtain the monthly data for all the 11 grid stations for meteorological observations in the extent of the study area. The data is available in the .grd file format which is converted to excel readable format by using a C program which is available at ([https://www.imdpune.gov.in/Clim\\_Pred\\_LRF\\_New/Gridded\\_Data\\_Download.html](https://www.imdpune.gov.in/Clim_Pred_LRF_New/Gridded_Data_Download.html)).

### 1.6.2. Temperature

The temperature data are acquired from [POWER | Data Access Viewer \(nasa.gov\)](#) to compute the SPEI. The MERRA-2 temperature data which is assimilated using the GEOS-DAS (Goddard Earth Observation System – Data Assimilation System) is a reanalysis product and has been in operation since 1979.

### 1.6.3. Satellite

ALOS PALSAR – Radiometric Terrain Correction (RTC) Digital Elevation Model having a high spatial resolution of 12.5m is used for calculating the elevation of all stations. It was converted to ellipsoid heights using the ASF Map Ready geoid\_adjust tool<sup>22</sup>. This high-resolution data was used to extract the drainages of the district. The river and stream networks were outlined utilizing the Spatial Analyst tool of ArcGIS software by filling the sinks, generating the flow direction, assessing the flow accumulation,



and depicting the stream and river line. The flow direction is dictated by recognizing the adjoining cells which have the highest positive distance weighted drop<sup>23,24</sup>.

The Tropical Rainfall Measuring Mission (TRMM) was devised to understand the variability and distribution of rainfall in the tropics and the sub-tropics. With the monthly temporal resolution and a spatial resolution of 0.25 degree x 0.25 degree, rainfall data from 1998 to 2019 was obtained from Goddard Earth Sciences Data and Information Services Center (GES DISC) in NetCDF format. ([10.5067/TRMM/TMPA/MONTH/7](https://disc.gsfc.nasa.gov/datasets/10.5067/TRMM/TMPA/MONTH/7)). The TRMM 3B43 provides monthly precipitation values which are obtained by adjusting the 3B42 daily product. The NetCDF format of TRMM data is imported to ArcMap as a raster layer. Later spatial analysis was performed where based on a grid, values from the raster were extracted to points. This step is done so that the grid points from TRMM can be compared to the rain gauge data. The study of meteorological conditions especially when it comes to prediction models heavily depends on long term data patterns and fluctuations. Even though TRMM products such as 3B43 are discontinued, they will still hold prominence when it comes to acquiring long term data.

### 1.7. Methodology Framework

The methodology employed to fulfil the objectives of the research is represented in the flowchart in Figure 2. The ground and satellite based rainfall data is used along with the temperature data for this analysis.

1. Meteorological drought is established using the SPI index and the spatial and temporal aspects are described in detail.
2. The drought indices such as SPI and SPEI and chosen to comparatively assess the parameters of drought such as frequency, run length, and temporal characteristics. A conclusion is drawn at which of the indices is better suited to measure the different aspects of drought.
3. Studying the trend of precipitation is of prominence when it comes to the topic of drought analysis. Rainfall trend is derived using the popular statistical methods such as Mann Kendall Test, Sen's slope, and Innovative trend analysis. Further, the Modified Mann Kendall Test and the improved ITA where the type-1 error is removed is also computed to arrive at an in depth knowledge of the rainfall pattern over the years from 1952 to 2019.
4. Time series analysis is derived to understand the fluctuation in rainfall in the long term. Homogeneity tests such as Pettitt test, SNHT and Buishand test are utilized to understand the extent of the homogeneous nature of rainfall and also giving an insight at the change point in the rainfall trend. Autoregressive

integrated moving average model was used to predict the rainfall for 10 years from 2019 to 2029.

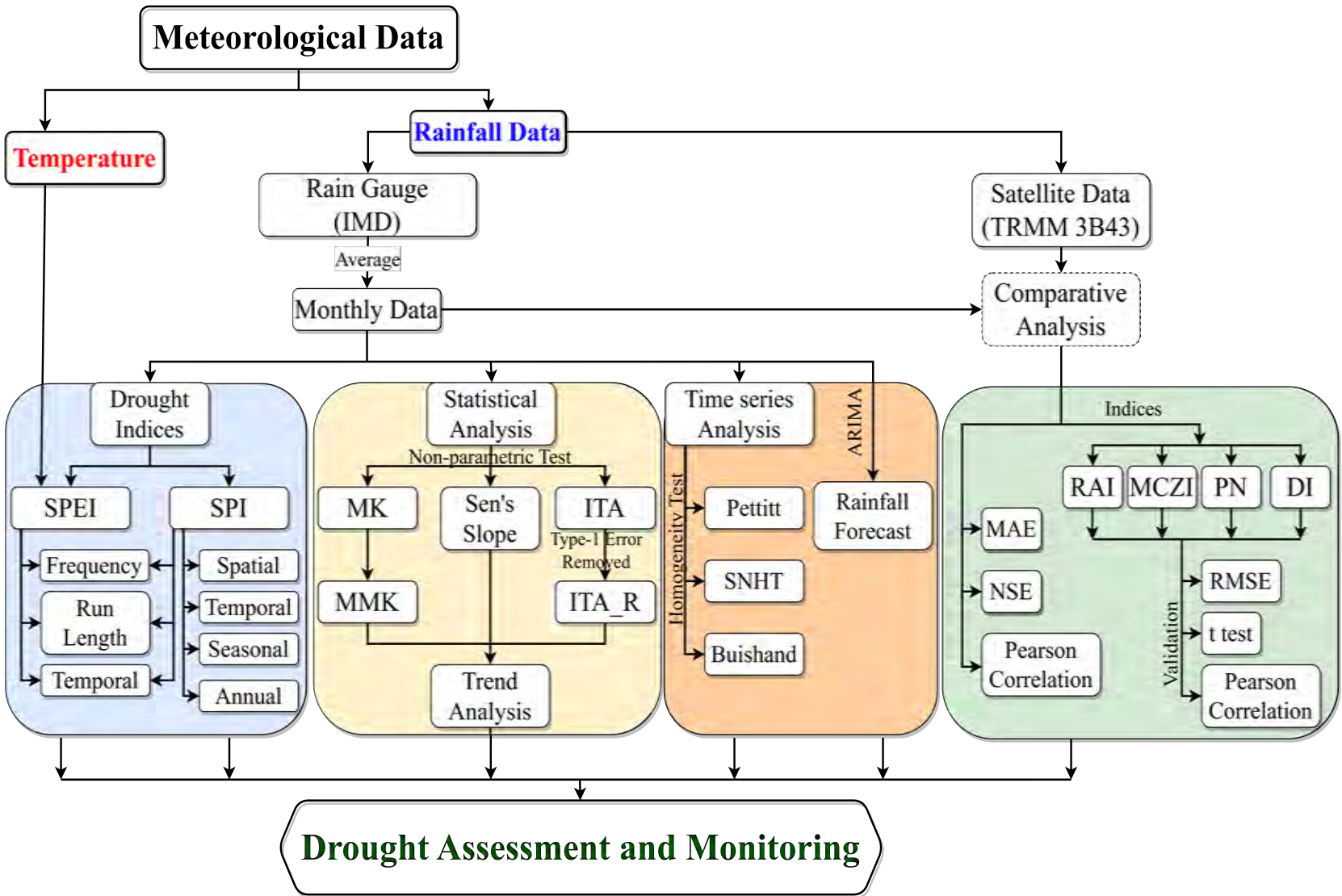


Figure 2: Methodology Framework

5. Multiple options are available to assess the rainfall data. In order to choose the better representation of the ground truth, a comparison of IMD and TRMM precipitation product was conducted. To complete the objective, direct comparison of the data was done based on the MAE, NSE and Pearson correlation. Later the rainfall data were tested for their ability to detect drought accurately using the drought indices such as RAI, MCZI, PN, and DI (Table 2). The results obtained from these indices are evaluated using statistical techniques such as RMSE, t-test, and Pearson correlation.

**Table 2:** Magnitude of precipitation extremes through indices

Category	SPI/SPEI	RAI	MCZI	PN	DI
<i>Extreme wet</i>	$2.0 \leq$	$\geq 4$	$\geq 2.0$	$>115$	9 to 10
<i>Severe wet</i>	1.5 to 2.0	2 to 4	1.5 to 1.99	110 to 115	8
<i>Moderate wet</i>	1.0 to 1.49	0 to 2	1.0 to 1.49	80 to 110	7
<i>Near Normal</i>	-1.0 to 1.0	-	-0.99 to 0.99	70 to 80	5 to 6
<i>Moderate dry</i>	-1.49 to -1.0	-2 to 0	-1.49 to -1.0	55 to 70	4
<i>Severe dry</i>	-2.0 to -1.5	-4 to -2	-1.99 to -1.5	40 to 55	3
<i>Extreme dry</i>	$\leq -2.0$	$\leq -4$	$\leq -2.0$	$<40$	1 to 2

### 1.8. Research Significance

The research aims at contributing to better understanding of drought characteristics such as spatio-temporal aspects, duration, and intensity in Tumakuru District. The knowledge of drought paves way to implement better monitoring and mitigation methods to bring down the socio-economic and agricultural impacts of drought.

### 1.9. Thesis Structure

**Chapter 2** defines the drought prone area of Tumakuru District using the Standardized Precipitation Index as a parameter. The spatial and temporal characteristics of the drought is discussed in detail in the chapter. The drought years for all the 11 meteorological stations are defined.

**Chapter 3** concentrates on studying drought at various time scales such as 1-, 3-, 6-, 9-, and 12- month. The various categories of meteorological, agricultural, and hydrological drought are studied using the drought indices. A comparison is drawn using the Standard Precipitation Index and Standard Precipitation Evapotranspiration Index.

**Chapter 4** focuses on analysing the rainfall trend using the non-parametric tests such as MK, MMK, Sen's Slope, and ITA. The pattern of long time rainfall data is studied and comparison is drawn for the best suited trend detection method.

**Chapter 5** presents the shift in rainfall trend through the homogeneity tests such as Pettitt, SNHT and Buishand. The ARIMA model is employed to forecast the rainfall for a decade.

**Chapter 6** evaluates the reliability of TRMM product over the ground based rain gauge data to study drought characteristics using drought indices.

**Chapter 7** summarises the outcomes of this research. The conclusions of the research and possible applicability of the work is presented in this chapter.

## 2. Meteorological Drought

### 2.1. Introduction

Now-a-days, the scope of development, water resource management, and planning is affected by an adverse change in climatic conditions<sup>25</sup>. Conceptual definition of drought expressed in relative terms e.g. a long period of dry season, whereas operational definition defines the starting of drought, severity, and end of dry periods<sup>26</sup>. Usually drought severity, duration, and its frequency analysis for a given time period comes under operational definition of drought<sup>27</sup>. Drought happens in any environmental zone, and their properties (recurrence, time duration, and seriousness) may vary. Quantitative evaluation of drought characteristics and their improvement is necessary for understanding distinctive types of drought at scales from the local to the worldwide<sup>28</sup>. American Meteorological Society summed up many drought definitions into four types of categories: Hydrological, Meteorological, Agricultural and socio-economic drought<sup>29</sup>. These four classes are related to various segments of the hydrologic cycle<sup>30</sup>. For the most part, precipitation is the primary and major factor in the hydrologic cycle. Drought is defined as the costliest natural disaster characterized by the prolonged insufficiency of rainfall or having significantly less availability of water during a long time over a huge area. In the past, many researchers have investigated the spatial fluctuation of the dry season utilizing drought indices and precipitation attributes<sup>31-41</sup>.

Drought characteristic risk portrayed as having underneath ordinary precipitation because of numerous factors following up on different time scales (months to long time) and it can change spatially as well as a drought can have impacts on different areas, particularly on hydrology, agriculture, environments and society<sup>42</sup>. Hence, drought evaluations depend on the time, severity and affected region. As a hydroclimatic disaster, drought represents terrible intimidation to the economy, environment and society<sup>43</sup>. Meteorological Drought defined by lack of rainfall and duration of this period over a region<sup>44</sup>. When over a region received long term average rainfall value less than 25% of seasonal rainfall, occurs meteorological drought. If this seasonal rainfall average value is between 26% to 50% is known as moderate drought and further, it is classified as severe drought if received rainfall deficit is more than 50% of its long term average value<sup>45</sup>. Meteorological drought restricts the agricultural water resources during drought conditions and it leads to reduction of crop yield<sup>32</sup>. Agriculture is the essential land use across the world, and it is exceptionally sensitive to climate change, and also known as a major cultural, economic and social activities<sup>46</sup>. According to a prediction by 2050 worldwide food demand will be high and indicating that agricultural production should be double<sup>47</sup>. Agriculture drought, generally refers an insufficient quantity of moisture in the soil

to fulfil the need of a particular agriculture crop at a specific point of time. Crop water demand relies upon existing weather conditions, growing stage of plant, biological properties of specific plant and biophysical properties of soil. Many drought indices have been developed and derived to understand the agricultural drought based on combination of temperature, rainfall and soil moisture, in other words soil moisture deficiency is strongly responsible for crop failure<sup>44</sup>. Hydrological Drought is related to the inadequacy of water on the surface and subsurface because of deficiency in precipitation for a long time<sup>48</sup>. The annual precipitation gained by the India was 117.7cm (109%) of normal rainfall which is 118.7 cm since 1901<sup>49</sup>. Only southwest monsoon season from June to September receive more than 75% of annual rainfall<sup>50</sup>, which is known to most rainy season in India and play a vital role for kharif crop<sup>36</sup>.

Rainfall distribution of the Karnataka state vary from 5051 mm to 408 mm. Highest annual rainfall observed at Western Ghats and minimum rainfall observed in the eastern parts of Chitradurga<sup>51</sup>. 13% of total rainfall was received in pre-monsoon season, 71% of the total rainfall received in southwest monsoon and 16% rainfall received during northeast monsoon<sup>52</sup>. The study area, Tumakuru district is one of the district of Karnataka state situated in southeast part of the state. The annual rainfall value of district during 1951-2019 vary from 2429.99 mm (at Tumakuru) to 136.30mm (at Gubbi) and it observed that rainfall increase with the altitude and it decrease as the altitude decrease. The terrain elevation is 720m at Tumakuru-1 and 136.30 at Gubbi. Southwest monsoon is very important rainy season and total 54% of the rainfall received in these four months (June-September). According to Koppen's classification, Tumakuru District witnesses two climatic zones. North Tumakuru lies in very dry which has less than minus 60% moisture availability and adjoining area of Mysore and Tumakuru comes in semi-arid with less than 50% moisture<sup>53,54</sup>. District is categorized into three Agro-climatic zones by University of Agricultural Sciences (UAS) Bangalore. Zone 4 is central dry zone, (Madhugiri, Pavagada, Koratagere, CN Halli, Sira and Tiptur), zone 5 is eastern dry zone (Gubbi and Tumakuru), and zone 6 is southern dry zone (Turuvekere and Kunigal). These different types of agro-climatic zones of the district permit the cultivation of different crops. In the district, kharif is major cropping season and about 70% of the cultivated land occupied by Ragi and Groundnut followed by Maize, Paddy and Red gram and drained by southwest monsoon. When in the south monsoon season does not received the sufficient rainfall during the crop growth, and less rainfall and soil moisture inadequacy causes extreme moisture stress and wilting the plant. The motivation behind this study is to research precipitation inconsistency and its spatial pattern over the Tumakuru district. In this research, the SPI was adopted due to its great characteristics in drought recognition. Standardized Precipitation Index

(SPI) was broadly used during the primary decade of the 21st century<sup>55</sup>. Standardized Precipitation Index work on the basis of probability of rainfall for any time scale. Due to its ability to compute for different time scale, this index is very useful for long term hydrological and short term agriculture drought<sup>56,57</sup>. SPI index suited to compare the different conditions of drought with many time scales. Previous many researches have been done on meteorological drought in the country but no one seems attempted earlier on spatio-temporal change and expansion of drought on Tumakuru district. So, the overall purpose of this research to endow the explication of the various time scale drought variability in meteorological drought over Tumakuru district through Standardized Precipitation Index (SPI). Particular objectives are following (1) investigating the spatial and temporal distribution of meteorological drought in the district; (2) characteristics of rainfall in the Tumakuru district during 1951-2019 through applying the SPI technique; and (3) understanding the variation in rainfall characterizing the changes in drought pattern. This research work confers in-depth perusal of the trend in rainfall variations using Standardized Precipitation Index technique over 69 years of precipitation data as well as output of pattern of rainfall and wettest and driest years in the study area.

## 2.2. Methodology

### 2.2.1. Inverse Distance Weighted (IDW)

Spline interpolation methods is known to produce extreme value of data along edges of the study region and the kriging interpolation technique revealed that the tendency of kriging method has to underestimated the data value, compared with real values<sup>58</sup>. To avoid these above error, IDW method was used in this research. The benefit of IDW is that it is simple to understand, easy in computation and has more efficient. Disadvantage is that there is no error indication and if the distributed sampled point is uneven, and output quality of result can decrease. The IDW technique is a basic and deterministic interpolation technique that works based on Tobler's First Law of Geography<sup>59</sup> that expects that sample values near to the unmeasured points have more impact on the interpolated value than farther points.

$$Z_j = \frac{\sum_i z_i / d_{ij}^n}{\sum_i 1 / d_{ij}^n} \quad (1)$$

$Z_j$  is indicating the unknown value and it reminds to estimate the value of unsampled points.  $z_i$  is the value of the known point.  $d_{ij}$  is the Euclidean distance from unsampled points to a known point.  $n$  is a user-selected exponent that directly influencing the weight of  $Z_j$  and is working as a medium of the inverse of spatial and temporal in between unsampled points and nearer points.

### 2.2.2. SPI

Standardized Precipitation Index was created by<sup>1</sup> to demonstrate the precipitation deficiency at various time scales that indicate the meteorological drought which entirely depends on rainfall data. The SPI is widely used to express the characteristics of the probability and amount of precipitation that include the long-term monthly rainfall data at multiple time scales. Two primary benefits emerge from the utilization of the SPI index. At first, SPI depends on precipitation data only and ease of computing<sup>60</sup>. Second, the index makes it conceivable to depict drought on different time scales<sup>61</sup>. The fundamental analysis of the SPI is that it depends entirely on precipitation information, not considering different factors that play a vital role to decide drought conditions like wind speed, evapotranspiration and temperature data, etc. The calculation and analysis of Standardized Precipitation Index (SPI) compute through Meteorological Drought Monitoring (MDM) software which is developed by Agricultural and Meteorological Software (AgriMetSoft)<sup>62</sup>. MDM was downloaded from <https://agrimetsoft.com/MDM>. The standardized precipitation Index used  $\Gamma$  distribution probability to detect the variation in precipitation. This long-time rainfall data needs to be fitted in gamma probability that transformed into a normal distribution through equal probability transformation. The higher positive value of SPI with more than median precipitation indicates the wet sequences and the higher negative value less than median precipitation corresponds to dry periods. The formula includes  $\Gamma$  distribution probability density function is formulated by:

$$f(x_i) = \frac{1}{\beta^\alpha \Gamma(\alpha)} x_i^{\alpha-1} e^{-x_i/\beta} \quad (2)$$

In this formula,  $\alpha > 0$  is the shape and  $\beta > 0$  is the scale parameters as well as  $x$  indicate the monthly amount of precipitation. Where  $x_i$  indicate the precipitation within  $i$  consecutive months.

$$x_i^j = \sum_{k=i}^i P_{jk}, j = 1, 2, 3, \dots, N \quad (3)$$

Here  $P_{jk}$  indicate the precipitation data value of  $k^{th}$  month of the  $j^{th}$  year.  $N$  denotes the number of years. The value near the normal distribution curve having a larger value of shape parameter. For the estimation of  $\alpha$  the gamma functions  $\Gamma$  expressed by:

$$\Gamma(\alpha) = \int_0^\infty y^{\alpha-1} e^{-y} dy \quad (4)$$



Therefore, fitting the gamma distribution to a given frequency of rainfall sum for a station to be estimated  $\alpha$  and  $\beta$ <sup>63</sup> using maximum likelihood for estimating the optimal values of and parameters adopting the maximum likelihood methods<sup>64</sup>:

$$\alpha = \frac{1}{4A} \left( 1 + \sqrt{1 + \frac{4A}{3}} \right) \quad (5)$$

$$\beta = \frac{\bar{x}_i}{\alpha} \quad (6)$$

$$A = \ln(\bar{x}_i) - \frac{1}{n} \sum_{j=1}^n \ln((x_i)_j) \quad (7)$$

Where  $\bar{x}$  showing the amount of mean precipitation and  $n$  is the observation record number.  $A$  is determined through the above formula. The wet intensity and dry periods corresponding threshold for SPI<sup>1</sup> can be classified based on SPI categories respectively as shown in Table 2 .

### 2.3. Results and Discussion

#### 2.3.1. Drought characteristics and analysis of SPI

Drought intensity, frequency and duration of drought are generally used to depict the characteristics of drought. The intensity of drought shows the seriousness of drought during the drought duration, which can be determined by the aggregated deficiency with the SPI value continuously below 0. Drought frequency alludes to the quantity of drought in a particular period, which is determined by the proportion of the number of drought months that occurred in the total months in a particular period. Duration of drought shows the number of months lies in drought conditions from the start to the end of the dry season.<sup>65</sup> The result from the SPI program has been a huge contribution of ArcMap GIS to create drought severity maps for the study area. To acquire a spatial coverage of the drought index, each point of the rain gauge station is allocated a region of impact using the IDW technique. By permitting joins between spatial feature and attribute information, a drought severity map with the spatially varying seriousness has generated. To describe the temporal change in drought during pre-monsoon, SW monsoon, and NE monsoon were averaged at each rainfall stations for each SPI accumulation period (January-May, June-September and October- December respectively). At that point, the annual SPI value was averaged of monthly aggregated SPI.

### 2.3.2. Season wise Rainfall Analysis

Pre-monsoon season from January to May have contributed not much significant amount of precipitation (19% of the total rainfall); maximum average rainfall was 191.7mm in Kunigal and minimum average of rainfall detected 84.3mm in Pavagada. As portrayed in Figure 3, SW monsoon (June-September) season had leading rainfall season in the study area that contributes about 54% of the aggregate precipitation (where almost 25% contributed by the Kunigal and Tumakuru) which evident the presence of higher rainfall. SW monsoon had mean rainfall varying from 465 mm in Kunigal to 284 mm in Pavagada. During the NE monsoon (October to December), 27% rainfall of total had been recorded.

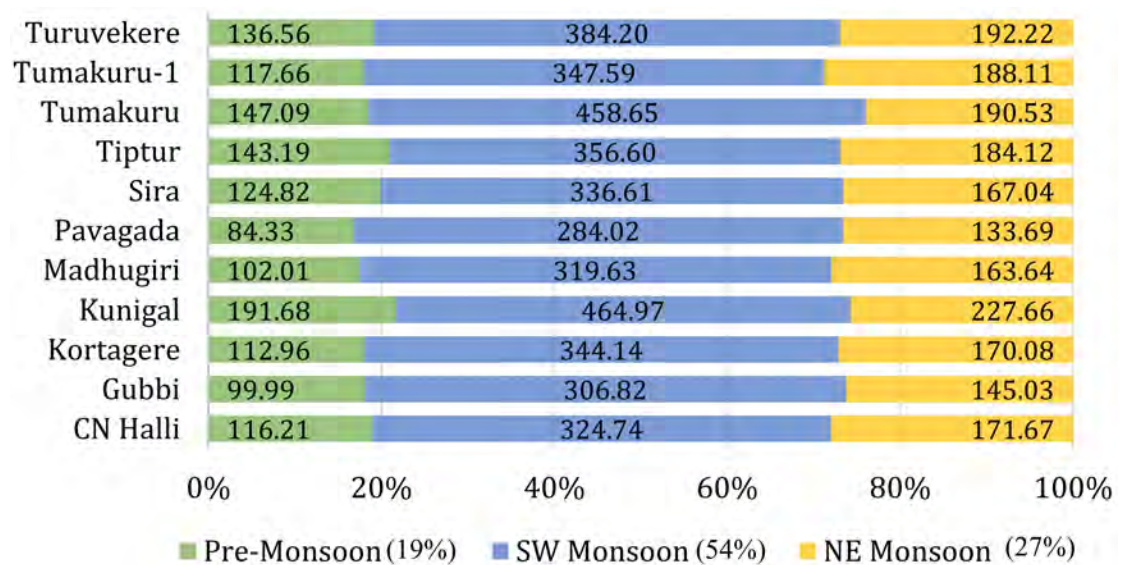


**Figure 3:** Percentage occurrence of rainfall at the different season

The mean seasonally precipitation (October–December) in the investigation region from 1951 to 2019 was 227.7mm and a minimum average of 133.7 mm for Kunigal and Pavagada. While the result of NE monsoon presented the highest value of average rainfall 749 mm in Kunigal (1956), however, 1.9 mm observed as the minimum average rainfall in 1965.

### 2.3.3. Statistical Parameters and variability analysis of annual rainfall

Statistical parameters of rainfall in Tumakuru district at 11grid points/ stations during 1951– 2019 are summed up in Table 3. The minimum ever recorded precipitation was 136.30 mm for Gubbi stations (in 1976- the driest year) and the maximum precipitation observed at Tumakuru which was 2429.11mm (in 1962- the wettest year). The average annual precipitation of the study area is varying from 884.31 mm/year (Kunigal) with 257.8mm standard deviation and 502.04 mm/year rainfall (Pavagada) with 275.4 mm standard deviation.

**Table 3:** Descriptive statistics of seasonal rainfall

Stations	Pre-monsoon			SW Monsoon			NE Monsoon		
	Max	Min	Mean	Max	Min	Mean	Max	Min	Mean
<i>CN Halli</i>	470	6	116.2	1461	86.7	324.7	421	20	171.7
<i>Gubbi</i>	343	2.6	100	619.9	56.3	306	421	6.2	145
<i>Koratagere</i>	272	1.5	113	811.3	110	344.1	451	18	170.1
<i>Kunigal</i>	376	57	191.7	1213	162	465	749	42	227.7
<i>Madhugiri</i>	392	4	102	867.8	127	319.6	498	2.9	163.6
<i>Pavagada</i>	372	15	84.3	1702	64.5	284	402	1.9	133.7
<i>Sira</i>	783	9.6	124.8	677.9	128	336.6	537	10	167
<i>Tiptur</i>	346	47	143.2	879.2	98.8	356.6	421	32	184.1
<i>Tumakuru</i>	483	34	147.1	1767	187	458.7	402	26	190.5
<i>Tumakuru-1</i>	765	0	117.7	981.5	55.9	347.6	605	42	188.1
<i>Turuvekere</i>	374	36	136.6	1672	91	384.2	421	37	192.2

#### 2.3.4. Rainfall Trend and temporal distribution of SPI at Tumakuru district

The  $R^2$  (Figure 4) values showed the relationship of Y and X axes of rainfall, the patterns of yearly precipitation were not as significant at all stations and it is showing that there is a slight shortage of extreme drought over the whole Tumakuru district. The yearly precipitation showed a mixed type of fluctuation. Annual pattern of SPI and rainfall clearly indicate that linear regression equation of Tiptur station showing the highest positive slope value of  $R^2$  comes about 0.1887 which explain that 18% of variability in the annual rainfall and gradually it has significant increasing trend. Tiptur area were detected under the dryness condition during 1956- 61 and the result of Tiptur rainfall trend line variation illustrated relatively higher significant trends with values of 4.222 mm/year. The average of annual SPI -0.63 in Chikkanayakanahalli (2003) and 1993-97, 2001-2003 have been found the continuous drought year and yearly precipitation decreased at the rate of -1.194mm/year in the Chikkanayakanahalli stations with a large fluctuation in 1962 and the  $R^2$  value (0.0088) of the station indicate most of the negative trends in this station.  $R^2$  value of rainfall variability indicate the 0.0088% variation in rainfall during 69 years of study.

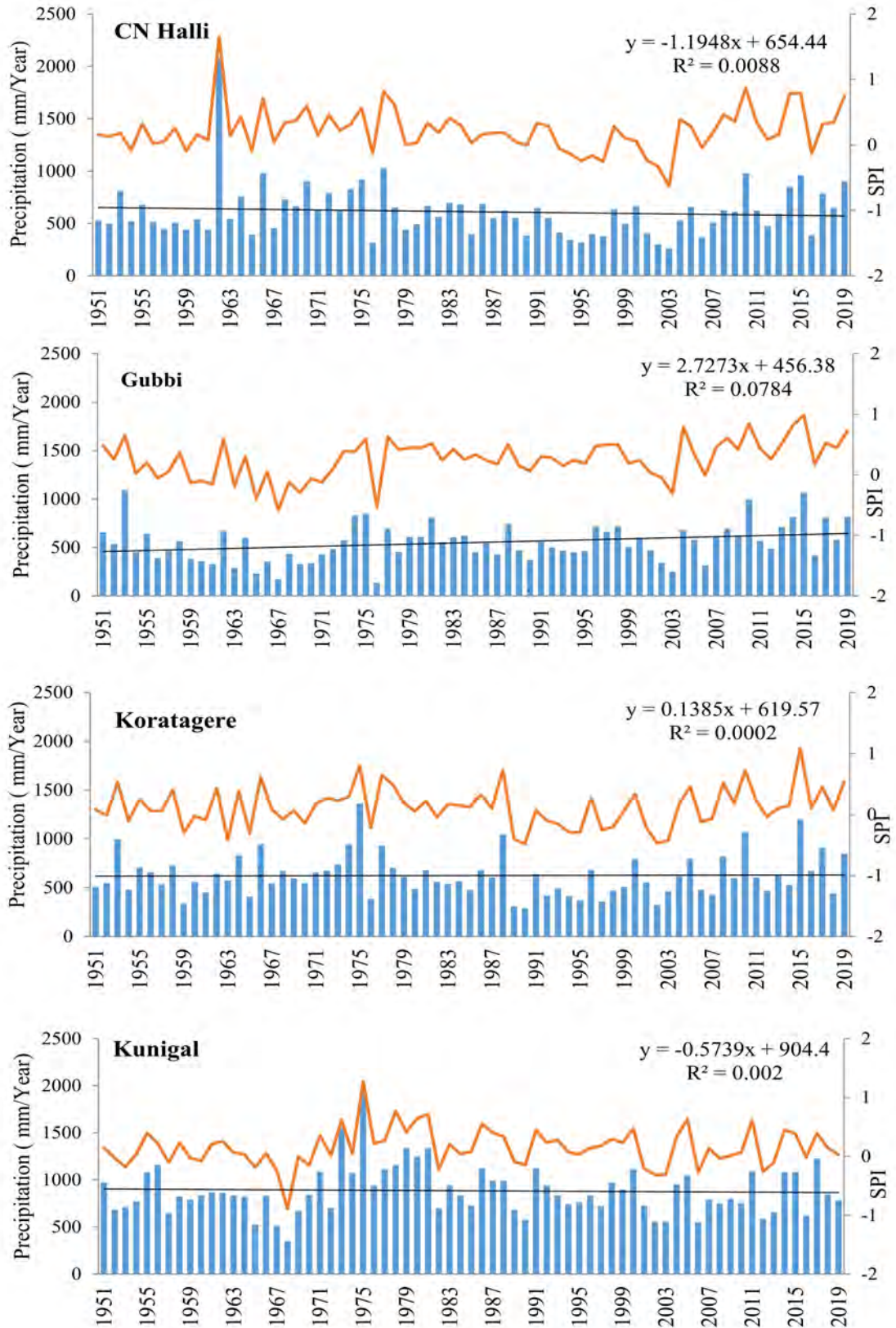


**Figure 4:** Evolution of annual rainfall and temporal distribution of SPI

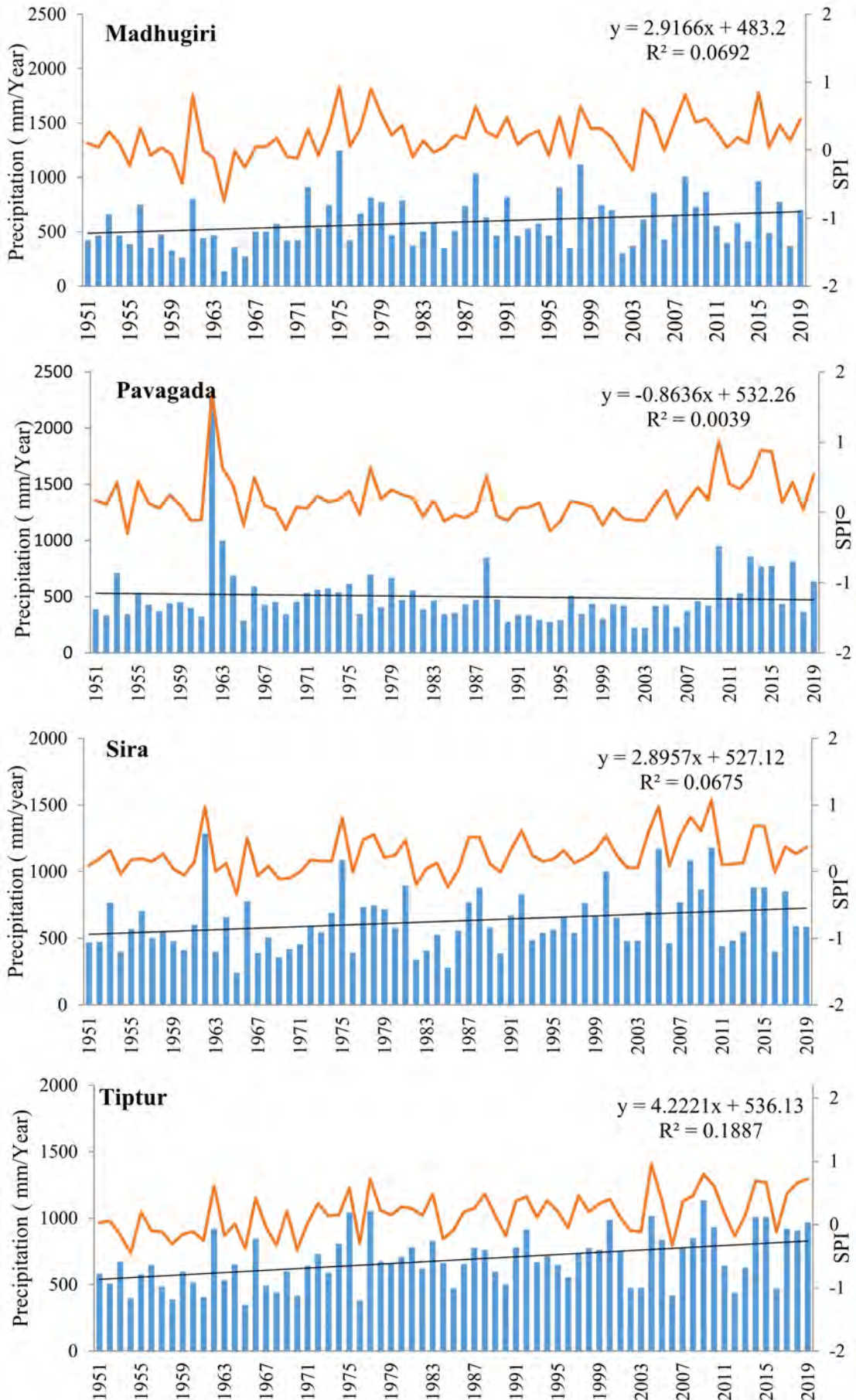
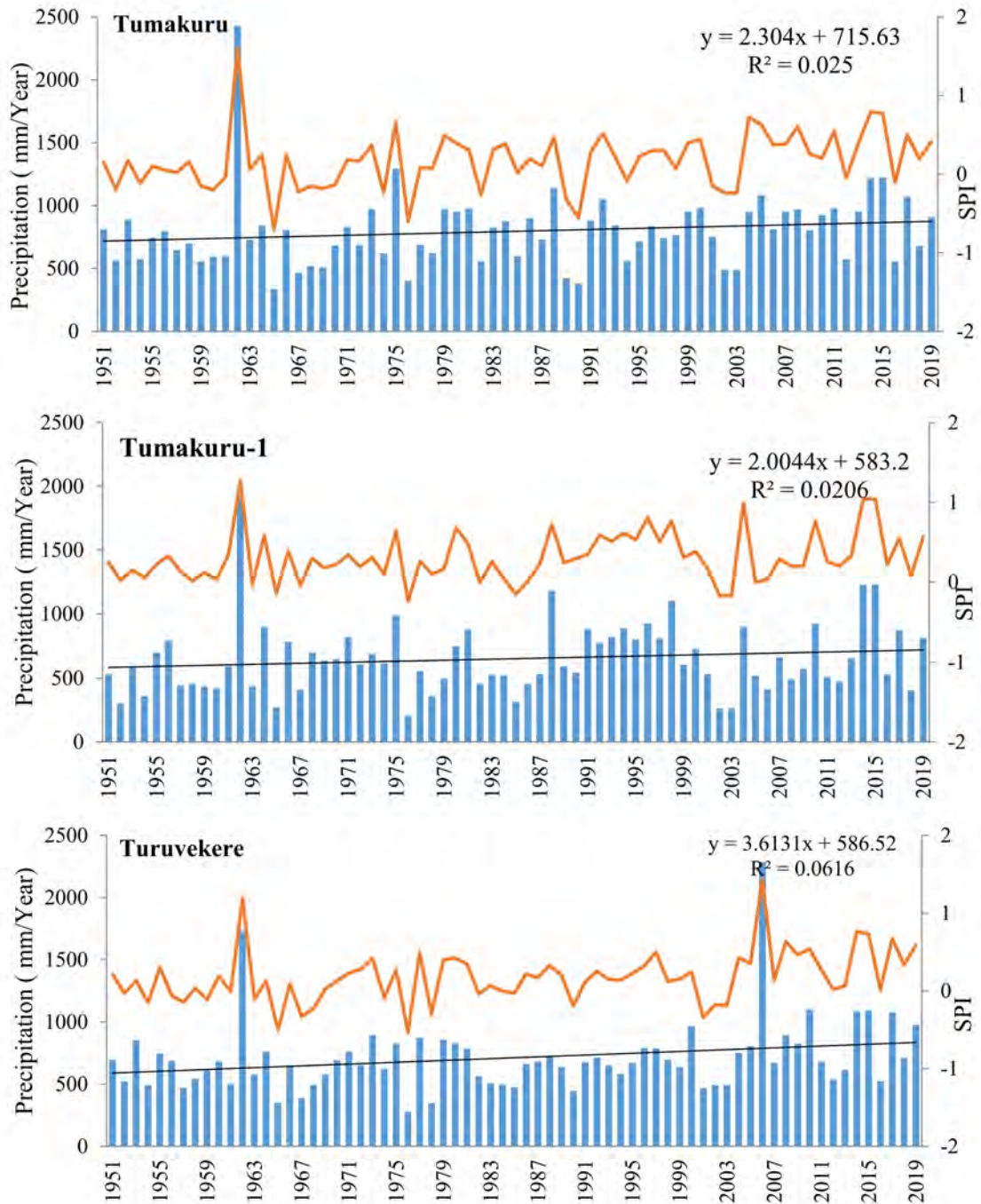


Figure 4: continued



**Figure 4:** continued

### 2.3.5. Seasonal detection and monitoring of the wet and dry period

In this research from 1951 to 2019, the Standardized Precipitation Index (SPI) has been calculated based on the season as well as annually and a spatial interpolation map has been prepared. The severity of drought has varied with time and a blend of wetness and dryness years have been noticed. Within 69 years of the research period, Tumakuru-1 has observed only one station having not a single drought year in pre-monsoon. Apart from that, none of the stations from all three seasons has been untouched from drought. Therefore, each season during the research period

has experienced some serious or moderate drought. The entire pre-monsoon season has encountered a maximum of 15 years of drought in Kunigal (Table 4). The highest SPI detected in 2006 at Turuvekere which was 2.76 in SW monsoon, and the lowest SPI was -1.74 observed in 1965 at Tumakuru-1 in NE monsoon.

**Table 4:** Evolution of season wise drought frequency

Stations	Pre-monsoon	SW Monsoon	NE Monsoon
<i>CN Halli</i>	7	34	28
<i>Gubbi</i>	4	32	26
<i>Koratagere</i>	9	34	28
<i>Kunigal</i>	15	31	35
<i>Madhugiri</i>	11	39	32
<i>Pavagada</i>	7	38	28
<i>Sira</i>	4	38	25
<i>Tiptur</i>	10	30	32
<i>Tumakuru</i>	16	32	35
<i>Tumakuru-1</i>	0	39	23
<i>Turuvekere</i>	10	32	30

**Table 5:** The intensity of SPI series at different timescale

Category	Pre-Monsoon	SW Monsoon	NE Monsoon	Annual
<i>Minimum SPI Value</i>	-0.58 (2003)	-1.71 (1954)	-1.74 (1965)	-0.89 (1968)
<i>Maximum SPI Value</i>	1.98 (2004)	2.85 (1962)	1.72 (1956)	1.70 (1962)
<i>Positive SPI Frequency</i>	65	39	46	60
<i>Negative SPI Frequency</i>	16	39	35	25

### 2.3.6. Spatial Pattern of Drought

**Annual:** The spatial extension of annual SPI drought years portrayed in the Figure 7 indicates the wettest condition (j) and driest condition (k) of the area. During 1951-1955, the district had wetness. Moreover, the dryness between 1952-1953 was existing in Tumakuru, Tiptur and Kunigal grid stations. Similarly, during 1963, 1972, 1983, 2006 and 2007 almost whole district was overwhelmed by severe drought except Turuvekere grid station. The dryness in the years 1956, 1959, 1961 concentrated in the southwest part of the area suffered with severe drought. In 1957-1958, 1960, 1964-1968, 1979, 1980, 1987, 1988, 1999, 2003, 2008, 2015 and 2019 wetness was found in most part of the district, with some drought in 1967 at Gubbi and Turuvekere (Figure 5). While the North-eastern part of the district, from 1984-1987, 1994, 1999, 2000, 2004 and 2018 Pavagada grid station presented the severe drought. Moderate drought events occurred in 1959 (except Pavagada),

1961(except the northern part of Madhugiri), 1972, 1981 (except Kunigal), 1983, 2016 and most of the eastern part of the district in 2018 and the remaining stations observed as wetter during 1954, 1958, 1964, 1968, 1988, 1999, 2008, 2015, and 2019.

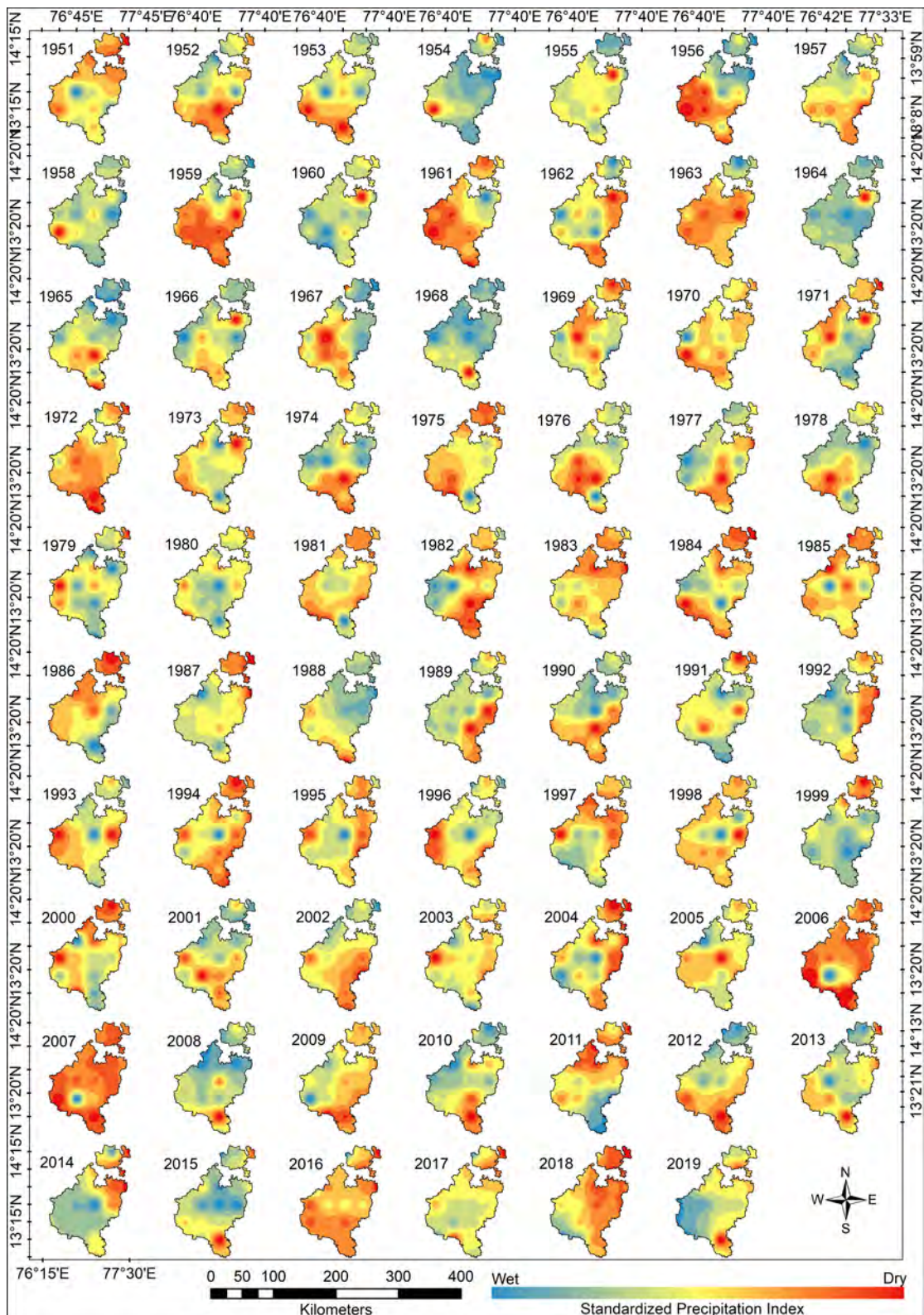


**Figure 5:** Spatial pattern of annual SPI as a response of drought



**Pre-monsoon:** To characterize the drought intensities of the SPI, the classification of drought given in Table 5 is utilized. Figure 6, show the driest(a), wettest (b) and normal (c) condition of the drought.

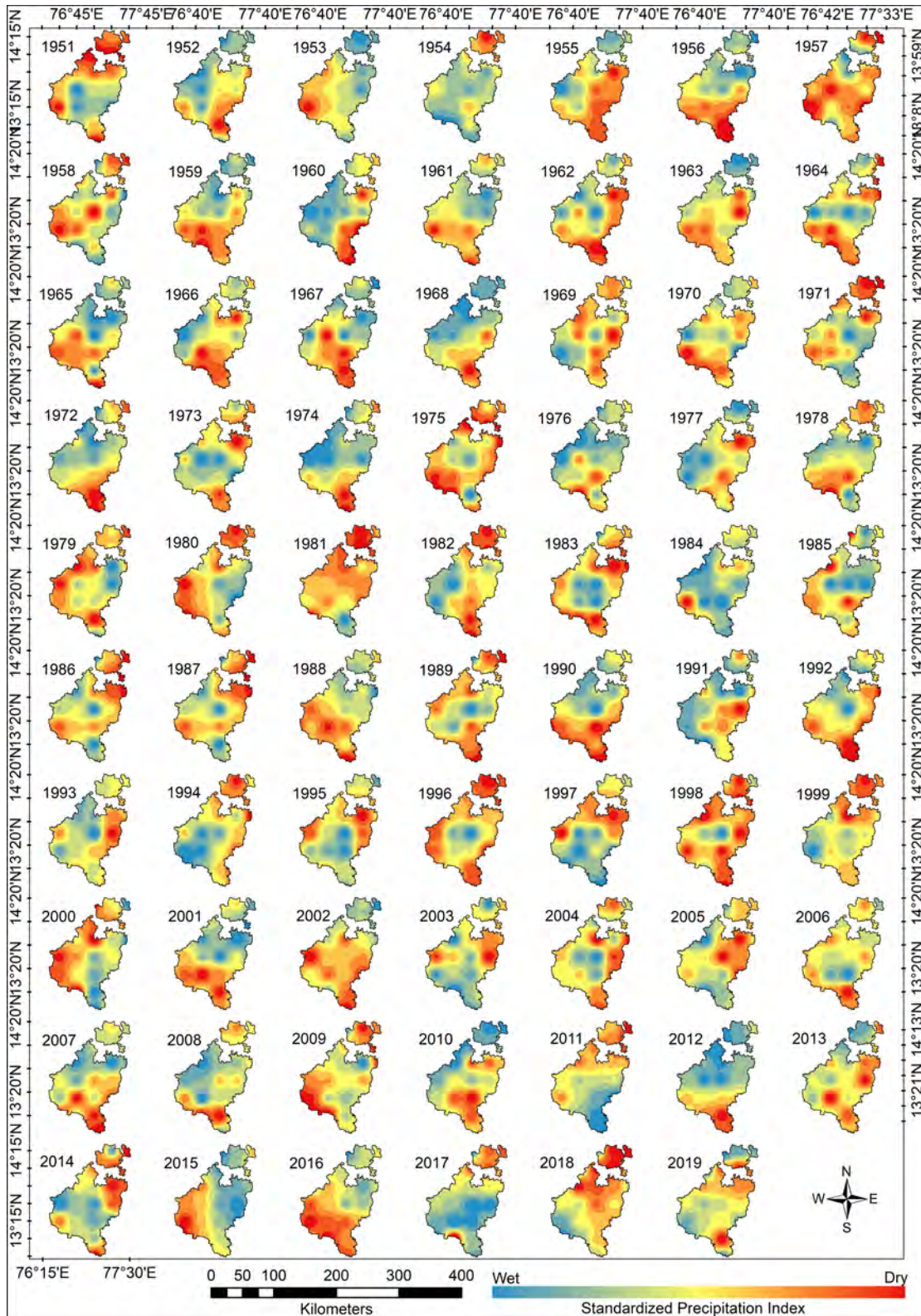


**Figure 6:** Spatial pattern of pre-monsoon SPI as a response of drought

Southern part of the district is struck by the drought in years 1955, 1956, 1957, 1959, 1966, 1967, 1988, 1990, 1998, 2001, 2002, 2015 and 2016. It means, mostly south and south-eastern parts of the district is affected by drought events during the investigation period (1951–2019). The years 1955, 1957, 1981, 1988 and 2002 imprint the most fragile dry years. The year 1998 was most awful year when most of the district was under dry condition, followed by the years 1957 and 1981 with the highest percentage of the total area of the district, influenced by drought events.

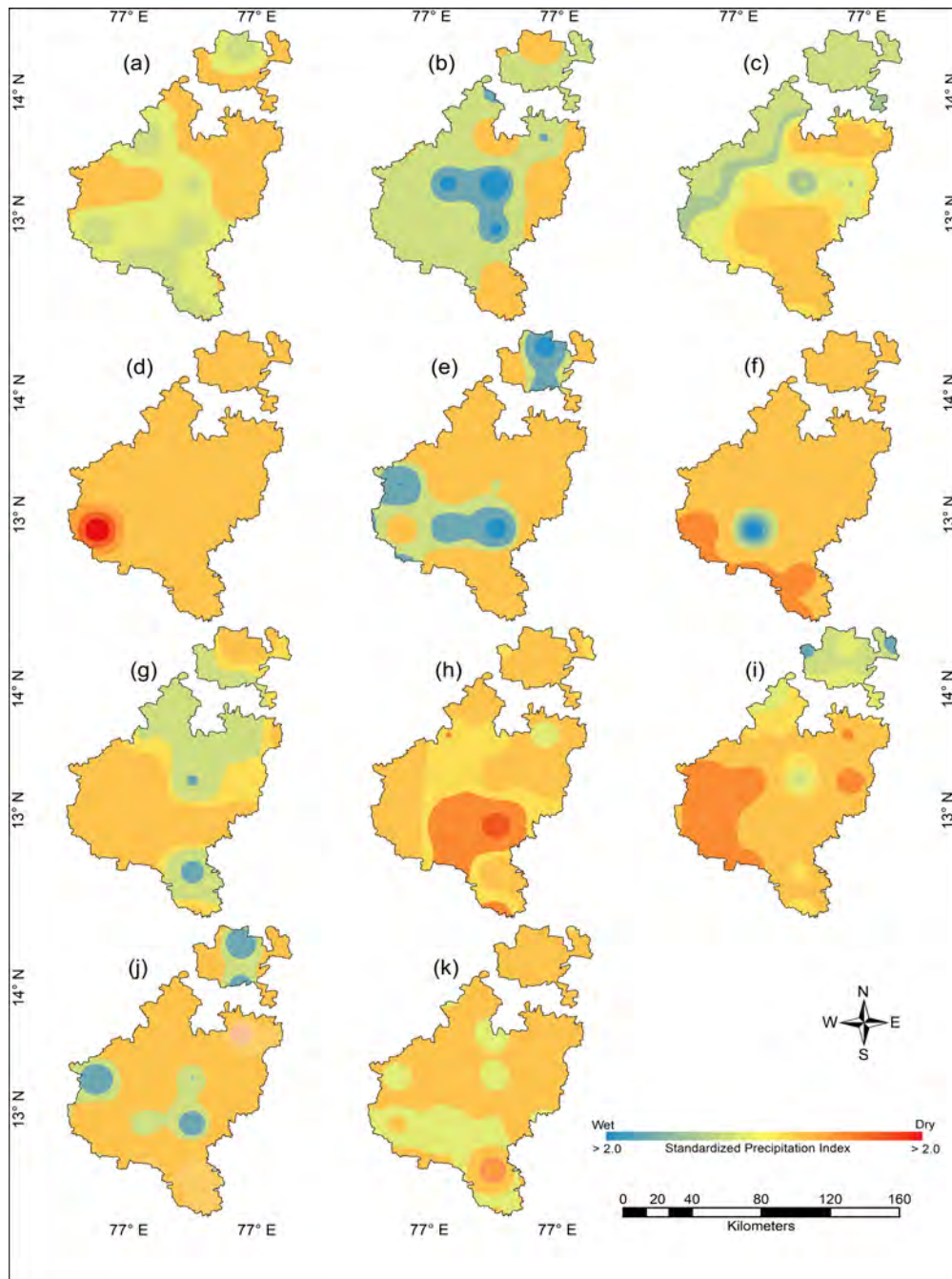


**Figure 7:** Spatial pattern of pre-monsoon (a,b,c); southwest monsoon (d,e,f); northeast monsoon (g,h,i); and annual (j,k) SPI in response to drought frequency during the period 1951-2019

**SW monsoon:** The years 1955, 1963, 2006, 2009 and 2018 addresses the driest period of the SW monsoon season and 1954, 1964, 1967, 1978, 1981, 1984, 1986, 1987, 1989, 2007 2008, 2013, 2014 and 2015 addresses the retreating period of dryness (Figure 8).

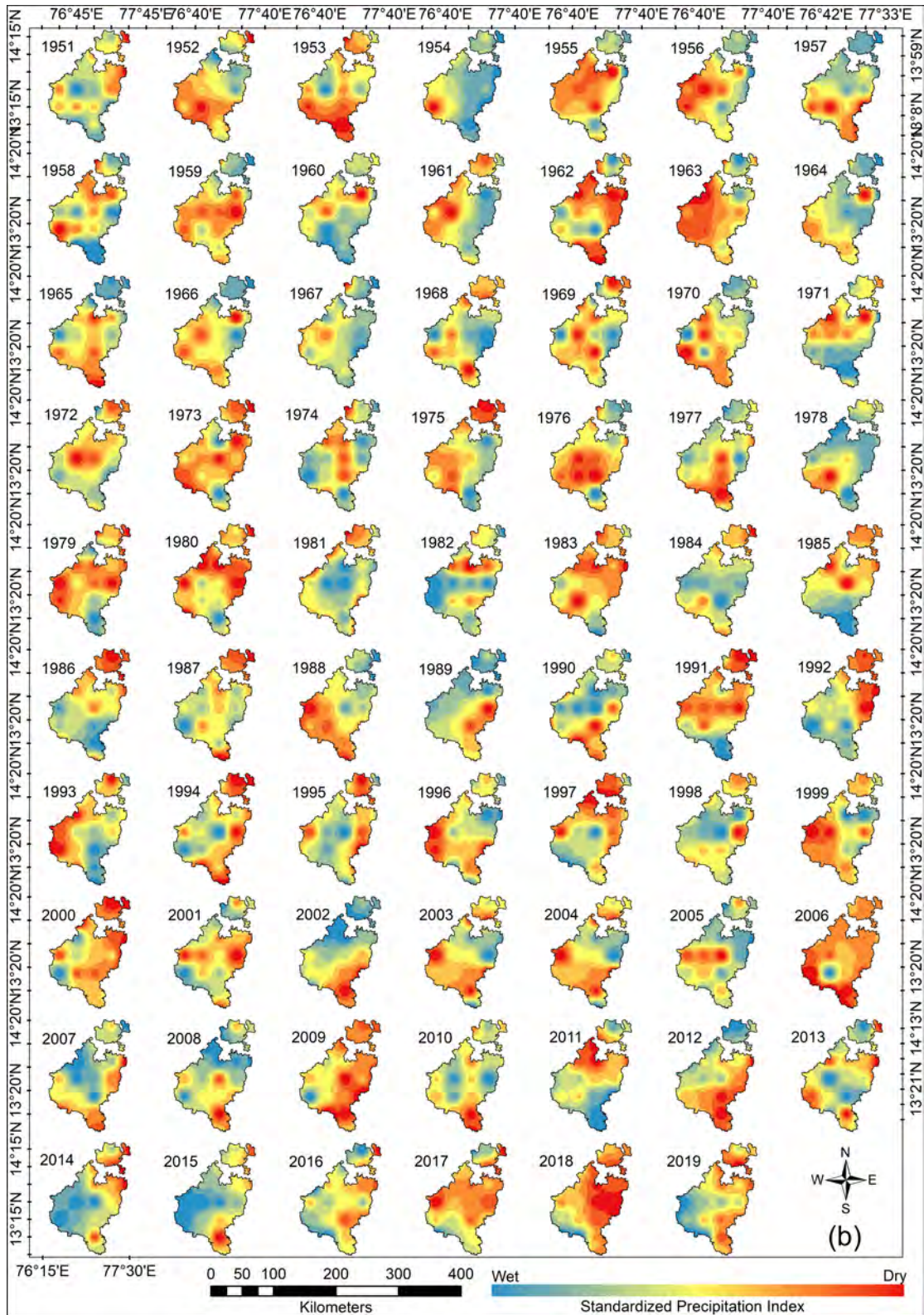


**Figure 8:** Spatial pattern of SW monsoon SPI as a response of drought

From a drought perspective, 2006 and 2018 were more effective because of their impact on meteorological drought. The year 1967 had a more noteworthy number of grid stations under wetness compared to the rest of the years in the time scale. The year 2006 had almost all number of grid points under drought except Turuvekere. Even though in 2018 Turuvekere and neighbour station Tiptur come under wet conditions (Figure 7). Further, the extent of the region under severe and moderate drought was huge in 2006. Some other years having broad dry territories in SW monsoon including 1953, 1955, 1959, 1963, 1973, 1979, 1991, 2009 and 2018. During these years, 1955, 1963, 1973, and 2018 were accounted wide spreading dry years in the district.

**NE monsoon:** The spatial variability of northeast monsoon drought severity is presented in Figure 7 with the average of season SPI. Results showed that district experienced very wet to severe dry conditions in almost years under examinations though the wet condition was seen in this season for the years 1953, 1958, 1959, 1964, 1987, 1988, 1989, 1999, 2001, 2004, 2010 and 2011, 2012, 2013, 2017, 2018 and 2019 (Figure 9). The highest positive SPI in NE monsoon was noticed 1.72 at Kunigal in 1956 and the lowest mean SPI was observed -1.74 at Tumakuru grid station in 1965 (Table 5). Severe drought conditions were knowledgeable about almost all the grid stations of the district during the years of 1954, 1996, 1998 2005, 2006 and 2008. In the period of 69 years spatial dissemination of drought frequency, Gubbi was the critical grid station that encountered the most continuous drought years from 1965-1971.

#### 2.3.7. Season wise SPI

In Chikkanayakanahalli, the strongest wet event noticeably in 1962 that is 2.20 (extremely wet) for SW monsoon, in 1962 was 1.70 (very wet) for pre-monsoon and 1.30 (moderately wet) in 1966 for NE monsoon. Various drought hazard frequencies with  $SPI \leq 1.00$  were observed in the SW monsoon. It was seen that 2003 was characterized by moderate drought with  $SPI - 1.29$  in past 69 years which was the driest year in this station. In Gubbi, moderate drought events occurred with  $SPI -1.37$  in SW monsoon in the year of 1976 as well as  $SPI < -1$  observed in 1961 and 1972 respectively. In addition, the continuous drought detected in the SW monsoon during years from 1965-1972. NE monsoon also appeared under the moderate drought in 1959 with the  $SPI -1.22$ . The most positive value of SPI in Gubbi was reported 1.74 in 2004, which shown the wettest year of this station in NE monsoon. Koratagere station experienced maximum number of drought years in SW monsoon. It was seen that normal drought events with  $SPI \leq 1$  was examined in 2003 (-0.58, pre-monsoon) and 1989 (-0.98, NE monsoon). But moderate drought was identified in 1990 (SW monsoon) with  $SPI -1.19$ . Highest negative SPI -1.58 was

observed in the SW monsoon at Kunigal. In pre-monsoon, the station experienced a short time drought than SW monsoon.

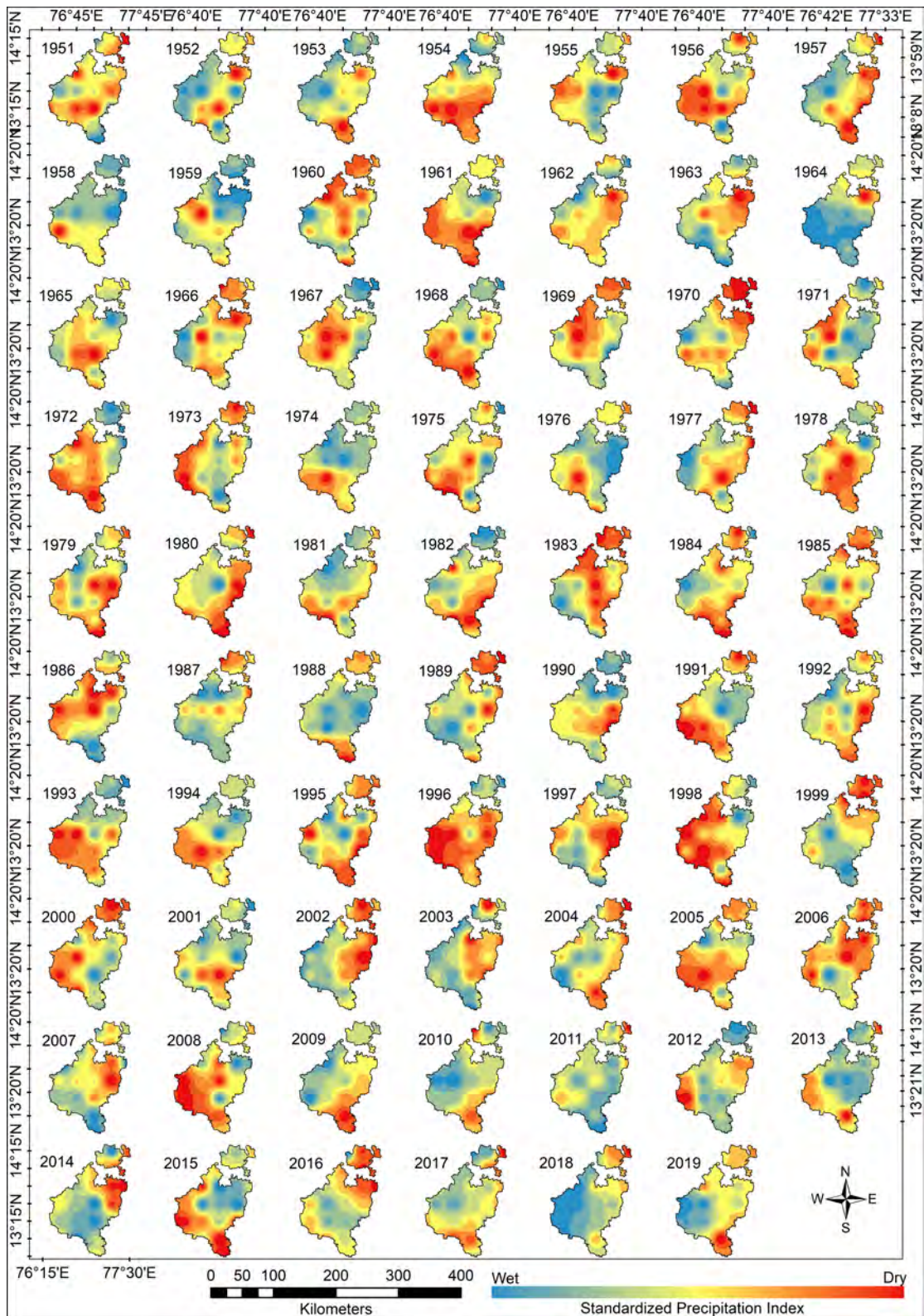


**Figure 9:** Spatial pattern of NE monsoon SPI as a response of drought

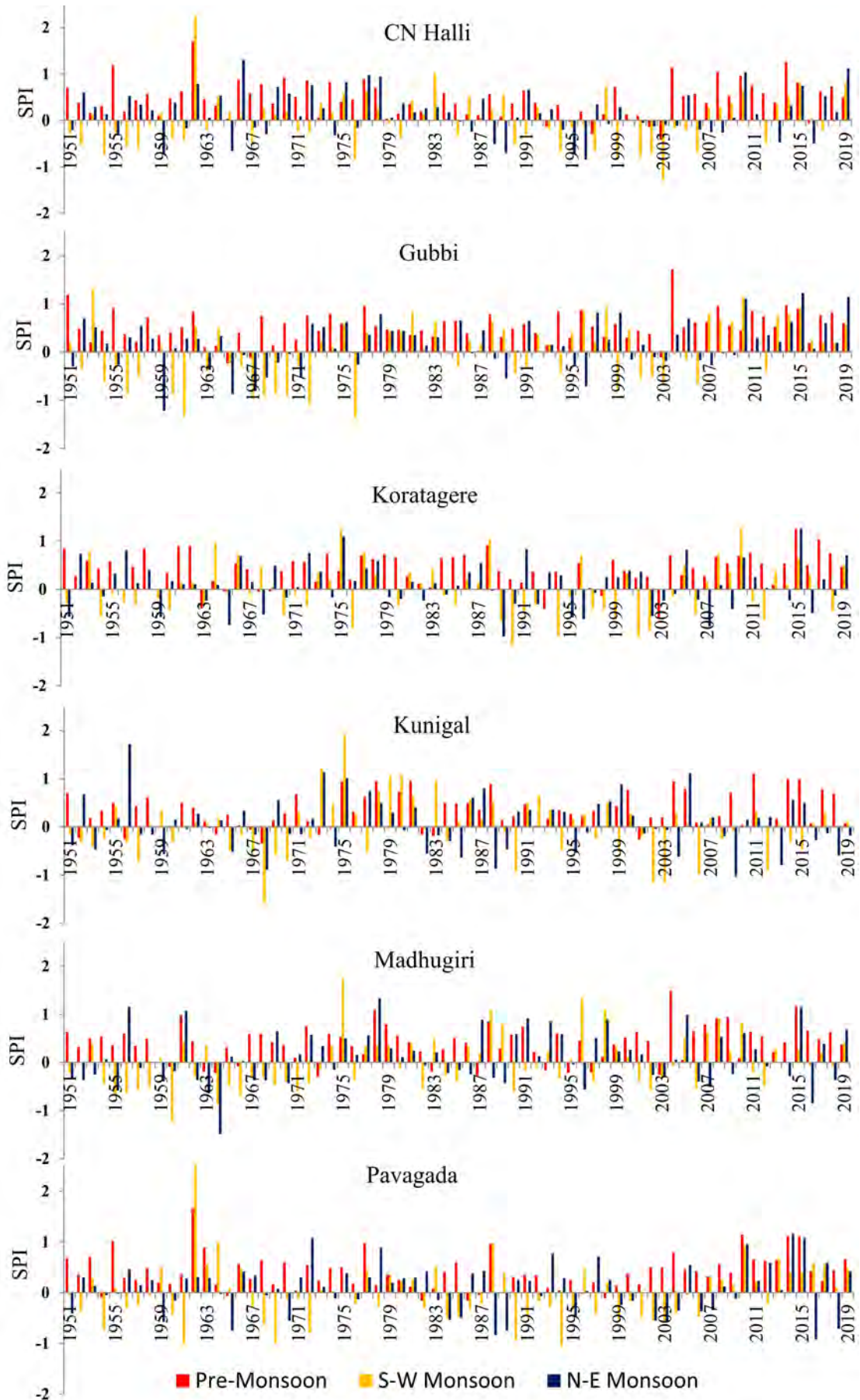


**Figure 10:** Temporal distribution of SPI series at different season

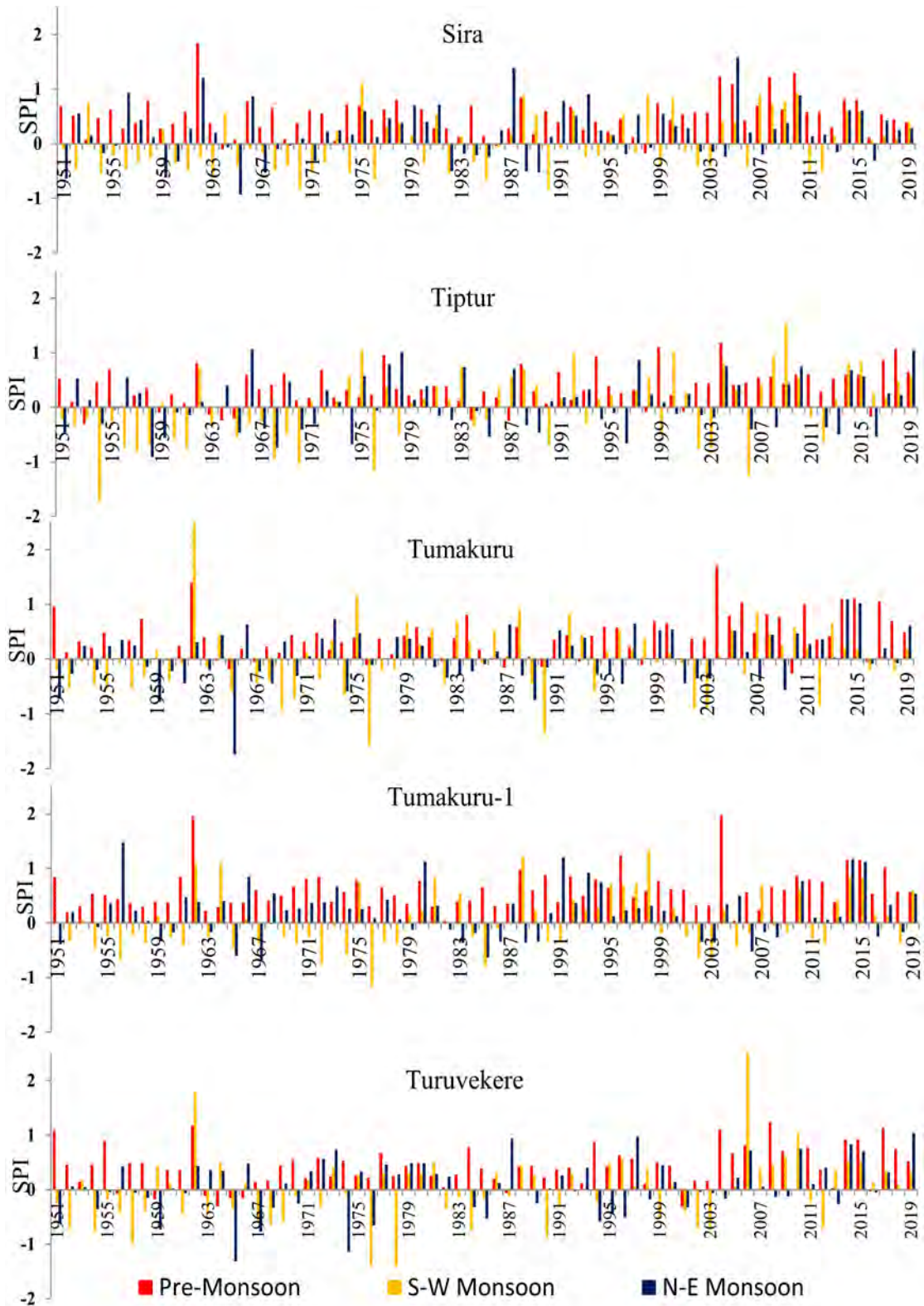


**Figure 10:** continued

Hence, moderate and near-normal drought frequently happened in this station. Only 2009 was the year that faced moderate drought in NE monsoon that had SPI -1.03 (Figure 10). In Madhugiri, 1975 was witnessed the most wetness year with SPI

1.75 compared to all seasons and the driest season was the NE monsoon with SPI -1.49 in 1964. The SPI trend of pre-monsoon exhibits an upward trend in 2004 (1.48) and downward in 1973 (-0.29). In Pavagada SPI increased toward the positive in 1962 up to 2.79 and drastically decreased in 1963 (0.55) at SW monsoon. The SW monsoon moderate drought years were 1961 and 1994. Sira grid station only one of the stations that shown the non-huge expanding pattern and recognized without moderate or extreme drought events during the research period. All seasons of this station were under near-normal drought. Tiptur grid station was identified most of the negative SPI in SW monsoon compared to all grid stations. Moderate drought events occurred in 1954, 1970, 1976 and 2006. The maximum SPI 1.53 for SW monsoon was in the year 2009. The highest negative SPI were detected in 1954 that was -1.71, -1.04 in 1970, -1.15 in 1976 and -1.26 observed in 2006. While pre-monsoon and NE monsoon seasons had recognized the near-normal drought with the minimum SPI recorded -0.31 (pre-monsoon) in 1953 and -0.91(NE monsoon) in 1958. At Tumakuru station most of the years identified as near normal and moderate drought in all three seasons as compared to other stations. In the pre-monsoon there were 16, SE-monsoon has 32 and NE monsoon has 35 years of drought. While moderate drought events were recognized in SW monsoon and NE monsoon. SW monsoon witnessed moderate drought in 1976 and 1990 with SPI -1.58 and -1.35 respectively. Tumakuru has maximum SPI 2.85 in SW monsoon. Tumakuru-1 is the only station that had positive value in pre-monsoon without any single drought year. Tumakuru-1 had the highest SPI 1.98 and a minimum SPI 0.04 in pre-monsoon. SW monsoon result illustrated the maximum SPI 1.32 in 1998 and the minimum SPI -1.17 in 1975. The NE monsoon distribution of the SPI found the near-normal drought with a minimum SPI -0.68 in 1967 and moderately wet conditions found with a maximum SPI 1.48 in 1956. Analysis of time series SPI of Turuvekere indicates how the pattern of dryness and wetness were changed during 1951-2019. The SPI increased 2006 with 2.76 in SW monsoon, while the pattern of SPI in pre-monsoon was varying between moderate wet to near normal drought with SPI 1.24 to -0.31 (Figure 10).

#### **2.4. Conclusion**

In this research SPI computation based on the IMD (India Meteorological Department) monthly precipitation data shows well characterize historical drought in the entire district. This study detected significant wetness periods at some particular seasons and years in the entire district. However, the SPI demonstrates a genuinely huge negative pattern in some years. The patterns of precipitation were showed the annual precipitation of Chikkanayakanahalli, Kunigal, and Pavagada diminishing but the trend of precipitation in Gubbi, Madhugiri, Sira, Tiptur, Tumakuru, Tumakuru-1 and Turuvekere were increasing. Precipitation changes in



the Koratagere remain almost constant. Spatially, the entire district showed a dry pattern in 1961, 1963, 2006 and 2007 at annual analysis, while the year 2006 was more articulated in SW monsoon as well as with multiple grid stations in NE monsoon. 2006 was the driest year that contributed to almost every season as a drought year except pre-monsoon. Wetness and Dryness patterns were identified through the SPI based on season and annual time scales, and the spatial variability was assessed by applying the IDW interpolation technique by using ARC/Map software. In terms of the spatial distribution of drought the study reveals that the frequency of drought most of the years occurs in southwest monsoon. In Karnataka state arid and semi-arid zones are mostly dependent on the southwest monsoon for agriculture crop. The majority of kharif crop in district like Tumakuru are early and growing stage in these four months (June-September) of southwest monsoon. Due to water deficiency during the growing stage from emergence to maturity (In India it is defined as four consecutive weeks), due to high moisture stress plant can't survive. The result of the study found that in arid and semi-arid zones like Tumakuru district, this type of behaviour of climate change during the growing stage of agriculture plant, means that meteorological drought can easily change into agricultural drought. Therefore, southwest monsoon is most devastating season in these zones. The Standardized Precipitation Index can define nicely the variation of drought in Tumakuru. Results of the study not just helpful for understanding the spatial and temporal change in drought characteristics but also helpful in drought prediction and drought monitoring etc.

### 3. Drought Indices

#### 3.1. Introduction

Climate change has paved way for the increase in the frequency of extreme weather conditions driving the community towards vulnerability. In recent years, such events make a severe impact not only on the environment but also on the world economy. At varying intensity and magnitude, hydro-meteorological disasters have been occurring all over the world. Fluctuations in the temporal and spatial distribution of rainfall along with the rise in temperature have caused persistent aridity with long-lasting environmental consequences like drought. Drought is one of the most influencing phenomena and poses a threat to human lives more than other natural disasters and it is broadly considered the least understood and the most complex of all environmental hazards<sup>66</sup>. Drought identification and its assessments are most difficult to explore because of the lack of a universally accepted method for qualifying and measuring drought effects<sup>67</sup>. Drought has long-term severe impacts on water resources, ecosystem, economies, society, and agriculture that leads to loss of the economy, shortage of food availability and drinking water, increased land degradation, and a forest fire that causes diseases and epidemics<sup>68</sup>. As per the International Disaster Database statistics, the worldwide loss of nearly 221 billion dollars per annum from 1960 to 2016 was caused by drought<sup>69</sup>. The frequency, intensity, and severity of drought have noticed a significant positive trend due to the increasing global warming<sup>70</sup>. Accordingly, it is necessary to monitor the drought occurrences and understand the indices of drought assessment to reduce and avoid the unnecessary loss of money and lives.

Various indices are developed and suggested for drought assessment e.g., Standardized Precipitation Index (SPI)<sup>1</sup>, Palmer Drought Severity Index<sup>71</sup>(Palmer, 1965), Standardized Streamflow Index<sup>72</sup>, Percent of Normal Precipitation Index<sup>73</sup>, Regional Drought Area Index<sup>74</sup> and Standardized Precipitation Evapotranspiration Index (SPEI)<sup>2</sup>. Every index defines specific characteristics. A standardized precipitation index (SPI) can recognize the characteristics of drought activity within a region and has the ability to quantify the drought severity at multiple timescale. The SPI indicates that rainfall is the only major variable affecting the duration, frequency, and intensity of drought. Ref.<sup>2</sup> proposed the first improved index for drought identification and analysis as SPEI to study the effects of climate change on drought parameters. SPEI takes into consideration the impact of evapotranspiration on drought characteristics, while the different timescale nature of the SPEI empowers the identification of various types of droughts and its impacts<sup>75-77</sup>. Various studies have been carried out on SPEI and SPI in recent years. An increase in the duration, occurrences, and severity of drought in India was witnessed under the

warming climate situation when studied at different time periods<sup>78</sup>. Ref.<sup>36</sup> analyzed the drought variability using SPI in India. The result indicated an increasing trend in July and highlighted the severe drought year of 1987. The study regarding the changes in the drought characteristics with respect to the geomorphology was carried out using SPI and SPEI in China at differing time and space scales<sup>79</sup>. Ref.<sup>80</sup> stated that there was consistency in SPI and SPEI values with the increasing timescale while there was a larger difference in between the indices at shorter timescales. Ref.<sup>81</sup> used the meteorological indices to follow the progress of the extreme drought event of 2018 in Ireland. It was the most severe event in the 1981 to 2018 period when the soil moisture deficit index reached a maximum value of 94.3 mm. The influence of the atmospheric circulation pattern on the drought scenario is studied using SPI<sup>82</sup>. The analysis showed that the dry event had a higher frequency in December month. The drought pattern of Oklahoma at 6-month timescale is studied using SPEI by Ref.<sup>83</sup>. The moisture conditions varied sustainably which was evident in the shorter timescales. Over the mainland of Spain,<sup>84</sup> characterized the drought events using SPI and SPEI. The duration and magnitude of drought were higher for SPEI than SPI at the 1-, 3-, and 6- month time scales. The study of the long-term hydroclimatic condition in Chile was assessed by<sup>85</sup> using the SPEI. A breaking point was seen in the mid-20th century with an increase in interannual variability and less intense wet events. The impact of climate change with respect to the groundwater drought was investigated by<sup>86</sup> using SPI and SPEI and realized that there was a negative effect on the groundwater levels. The intensity-duration-frequency curve is employed to obtain better knowledge about the relationship between the parameters<sup>87</sup>.

In general, some major factors such as topography, atmospheric circulation, geology, distance from the ocean, and geography are highly responsible for climate change and the climate of Tumakuru district which is characterized as arid and semi-arid. An assessment of the spatial and temporal pattern of the meteorological drought in Tumakuru is studied by<sup>88</sup> which revealed that most of the drought occurred during the southwest monsoon season resulting in a devastating outcome. The dry season starts in November lasting till the end of May and the rainy season extends from June to October in Tumakuru. Due to the arid and semiarid climatic zone of Tumakuru district, the ecological environment conditions are very delicate and permeable to climate change<sup>89</sup>. Drought conditions are a frequent meteorological hazard in Tumakuru and affect the agriculture production that causes the agricultural drought. Therefore, it is crucial to examine and observe the varying conditions of drought characteristics over time to avoid disaster risk. How do the SPEI and SPI describe the different characteristics and behavior of drought

varieties in the study area? What are the applicability and characteristics of both these indices at multiple timescales? These discoveries need further investigation. The major aim of this study is the computations of the SPEI and SPI of 11 meteorological grid stations at 1-, 3-, 6-, 9-, 12-, and 24-month timescale in Tumakuru district from 1981 to 2019. The study analyzes and compares the performance and reliability of these indices. The primary goals of the study are: (1) to examine the differences in the spatial and temporal characteristics of drought computed through SPEI and SPI at different time scales, and (2) to investigate the consistency and relevance of the SPEI and SPI in drought assessment and the relationship between drought intensity, severity, and frequency at Tumakuru district. There has been no prior research regarding drought in the study area hence making it of greater importance for a better water management system. It is expected that the study would give the appropriate ideas to select the feasible index for drought monitoring.

### 3.2. Methodology

In this study, R studio software<sup>90</sup> has been used with SPEI version 1.7 package which has a different program to compute both SPI and SPEI. Fitting the P (precipitation) and PET (potential evapotranspiration) data series to an appropriate probability distribution is the main function of computing these indices. Then this fitted data series is converted into a standard value that defines the SPEI and SPI (Table 6).

**Table 6:** Classification of drought severity based on SPI<sup>1</sup> and SPEI<sup>2</sup> value

SPI/SPEI values	Category
2.0	<i>Extremely wet</i>
1.5 to 2.0	<i>Very wet</i>
1.0 to 1.49	<i>Moderately wet</i>
-1.0 to 1.0	<i>Nearly normal</i>
-1.49 to -1.0	<i>Moderate dry</i>
-2.0 to -1.5	<i>Severe dry</i>
-2.0	<i>Extreme dry</i>

#### 3.2.1. SPI

The index was firstly introduced by<sup>1</sup> that has been generally utilized to monitor the Spatio-temporal pattern of drought. SPI can demonstrate the amount of rainfall at a particular time period in a selected region and suggested by World Meteorological Organization to be utilized globally. The stable result, simple calculation, and dependency of only rainfall data are some advantages of SPI. SPI depends on the probability distribution of rainfall utilizing the gamma probability. For the chosen

frequency distribution of rainfall, a gamma probability density function is defined as:

$$g(x) = \frac{1}{\beta^\alpha \Gamma(\alpha)} x^{\alpha-1} e^{-\frac{x}{\beta}}, x > 0 \quad (8)$$

Where  $\alpha$  defines the shape and  $\beta$  defines the scale parameter.  $x$  is the quantity of precipitation and the gamma function is defined as

$$\Gamma(\alpha) = \int_0^\infty x^{\alpha-1} e^{-x} dx \quad (9)$$

Using the maximum likelihood method, the suitable values of  $\alpha$  and  $\beta$  are calculated.

$$\hat{\alpha} = \frac{1}{4A} \left( 1 + \sqrt{1 + \frac{4A}{3}} \right) \quad (10)$$

$$\hat{\beta} = \frac{\bar{x}}{\hat{\alpha}} \quad (11)$$

$$A = \ln(\bar{x}) - \frac{\sum \ln(x)}{n} \quad (12)$$

Where  $n$  denotes the total number of samples of rainfall. A function can then be derived to calculate the cumulative probability of rainfall for a given month using:

$$G(x) = \int_0^x g(x) dx = \frac{1}{\beta^\alpha \Gamma(\alpha)} \int_0^x x^{\alpha-1} e^{-x/\beta} dx \quad (13)$$

The SPI is calculated as:

$$SPI = S \frac{t - (c_2 t + c_1) + c_0}{[(d_3 t + d_2)t + d_1]t + 1.0} \quad (14)$$

$$t = \sqrt{\ln \frac{1}{G(x)^2}} \quad (15)$$

where  $x$  denotes the amount of rainfall and  $G(x)$  is the precipitation probability distribution concerning the  $\Gamma$  function.  $S$  indicates the minus and plus coefficient of cumulative probability distribution. When  $G(x) > 0.5$ ,  $S = 1$  and when  $G(x) \leq 0.5$ ,  $S = -1$ .  $c_0 = 2.5155$ ,  $c_1 = 0.8028$ ,  $c_2 = 0.0103$ ,  $d_1 = 1.4327$ ,  $d_2 = 0.1892$ ,  $d_3 = 0.0013$ .

### 3.2.2. SPEI

The method to compute the SPEI was first developed by Ref.<sup>2</sup> as the enhancement of the SPI. Taking into account the change in surface evaporation and the impact of temperature, SPEI improves on the SPI by replacing the monthly rainfall in SPI with the difference between the Potential Evapotranspiration (PET) and rainfall data. The following method demonstrates the probability distribution function of log-logistic probability which makes SPEI provide a characterized and suitable analysis of drought severity. The probability density function is expressed by the following equation:

$$f(x) = \frac{\beta}{\alpha} \left( \frac{x - \gamma}{\alpha} \right) \left[ 1 + \left( \frac{x - \gamma}{\alpha} \right) \right]^{-2} \quad (16)$$

Where  $\alpha$  denotes scale,  $\beta$  the shape, and  $\gamma$  the origin. The probability distribution function can therefore be given as:

$$F(x) = \left[ 1 + \left( \frac{\alpha}{x - \gamma} \right)^\beta \right]^{-1} \quad (17)$$

Following which SPEI can be calculated as:

$$SPEI = w - \frac{c_0 + c_1w + c_2w^2}{1 + d_1w + d_2w^2 + d_3w^3} \quad (18)$$

When  $P \leq 0.5$ ,  $w = \sqrt{-2 \ln(P)}$ , and when  $P > 0.5$ ,  $w = \sqrt{-2 \ln(1 - P)}$ ,  $c_0 = 2.5155$ ,  $c_1 = 0.8028$ ,  $c_2 = 0.0203$ ,  $d_1 = 1.4327$ ,  $d_2 = 0.1892$ ,  $d_3 = 0.0013$ .

## 3.3. Result and Discussion

### 3.3.1. Drought Frequency

The purpose of this research was to compute the frequency distribution to recognize the frequently affected area by drought, on the premise of the frequency of the SPI and SPEI for individual eleven stations and various timescale. The frequency was determined based on the occurrences percentage distribution of drought categories (moderate, severe, and extreme) at various timescale (1-, 3-, 6-, 9-, 12-, and 24-month) over Tumakuru region from 1981 to 2019. The spatial distribution and extent of drought events (%) for different SPI and SPEI timescale with drought categories are shown in Figure 11 and Figure 12. The outcomes of this study stated that for a selected timescale extreme drought happened less frequently at every station and mild drought existed more frequently than other drought categories. Time-series comparison of both indices indicates the sensitivity

and ability to find out the temporal and spatial pattern of drought in any specified region. In this research, both SPI and SPEI concurred on the pattern and directional variability of drought although the indices showed different intensities.

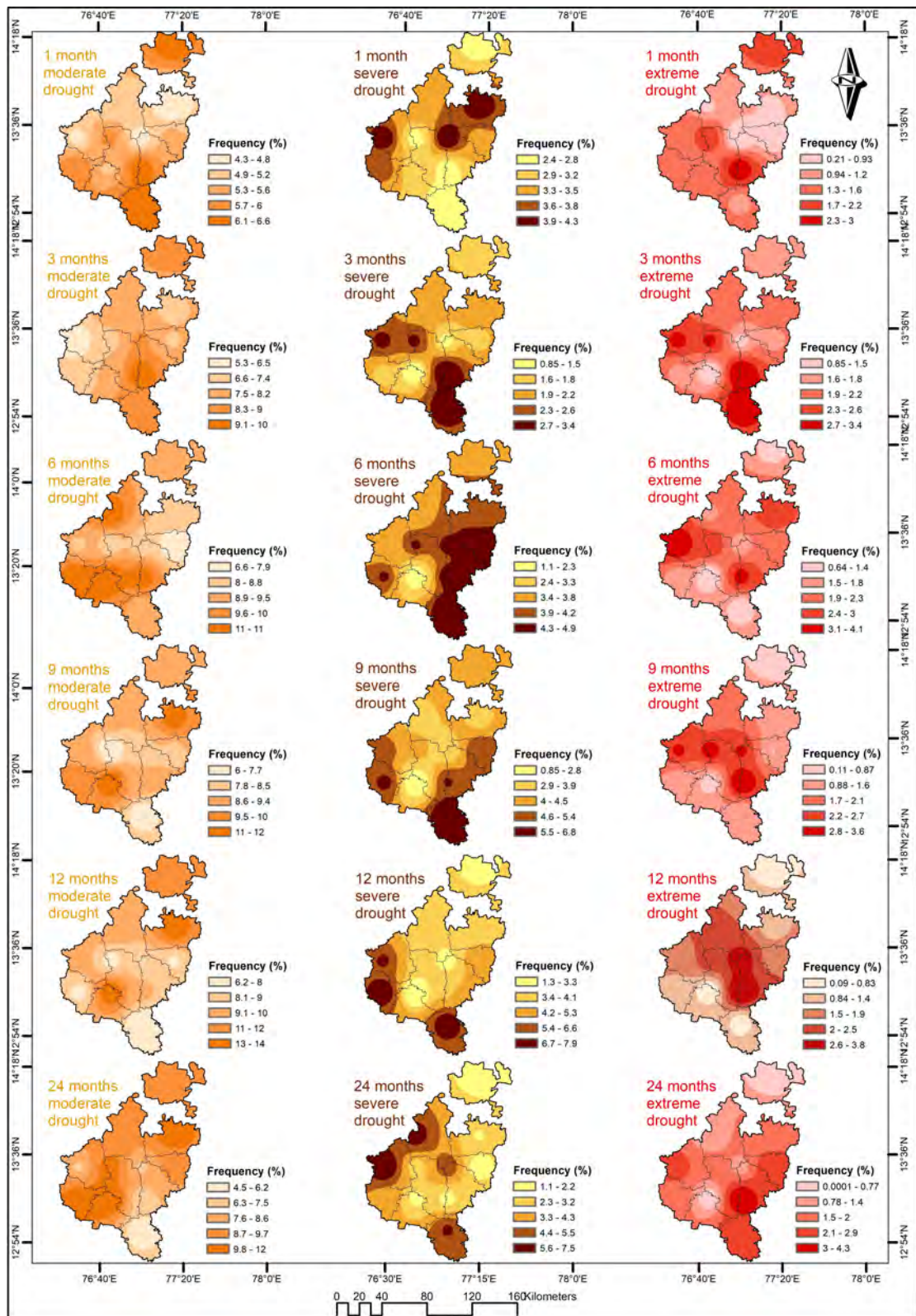


**Figure 11:** Spatial Distribution of frequency of SPI

When comparing the SPEI to SPI, SPEI recognized the more frequent drought spells in the moderate and severe categories while SPI discovered the greater number of dry months and frequency under the mild and extreme categories. The result of the SPEI expresses the significant role portrayed by the temperature fluctuation in the drought analysis but the SPI claims importance in drought analysis when temperature data is missing. The frequency of drought at the various timescale was analyzed from the spatial distribution perspective. The SPI and SPEI results for the frequency analysis barely showed any similarity at any of the timescales barring a few exceptions at 1- and 3-month for moderate drought and 6-month for severe drought.

For SPI, at the 1-month timescale, the maximum drought event of moderate-intensity occurred in the southern part of the district, the severe intensity at Chikkanayakanahalli and Madhugiri, and extreme intensity at Tumakuru. At the 3-month timescale, severe drought expanded in Chikkanayakanahalli and extreme drought at Kunigal and Tumakuru stations while moderate drought noted the highest frequency of about 10%. A major chunk of the South and Southeastern part of the area is affected by a 6-month severe drought. As per the 9-month timescale, Kunigal was highly affected by severe drought and extreme drought affected Chikkanayakanahalli, Gubbi, Tumakuru and Tumakuru-1. Kunigal, Tiptur, and Chikkanayakanahalli were influenced by severe drought and Tumakuru and Tumakuru-1 by extreme drought at the 12-month timescale. Extreme drought condition tends to occur at higher frequency as the timescale is increased from 1-month to 24-month. The 24-month severe drought occurred frequently in the Northwest direction and moderate drought in the North and Southwest region of the district.

The spatial distribution of SPEI with moderate drought occurred over 40% of the area majorly in the South and Southeast parts for a 3-month timescale. Pavagada station recorded the highest frequency of moderate drought at all the timescales featuring the effect of the climatic condition as the region lies in the arid steppe hot climatic zone according to Köppen-Geiger Climate classification. The severe drought frequency is predominantly indicated in the greater part of the South and Southeastern region at the 6-, 9-, 12-, and 24-month timescale. Extreme drought is evident in Madhugiri for all the timescales and extreme drought at slightly less intensity is observed at Chikkanayakanahalli for all the timescales except for the 3-month. For all the timescale except 12-month, moderate and severe drought finds better representation in SPEI while SPI tends to give better results for the extreme drought category. The similarity in SPI and SPEI was observed for the moderate, severe, and extreme intensities at the 12-month timescale. Pavagada station



receives the least mean rainfall in the study area and the frequency of the moderate drought is high in the area whereas apart from significant extreme meteorological drought, the rest of the timescale does not express intense dry periods as seen in SPI and SPEI.

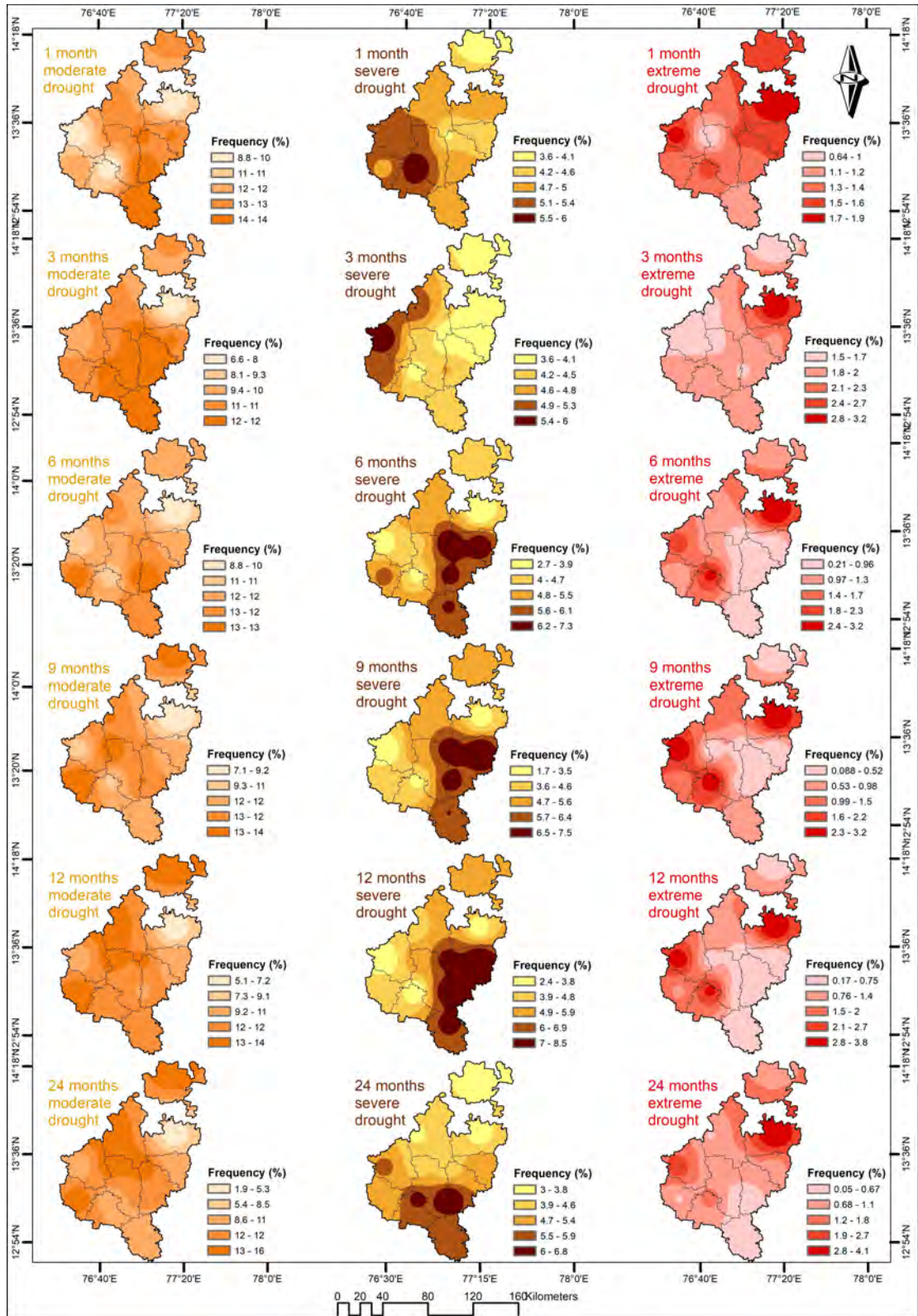


**Figure 12:** Spatial Distribution of frequency of SPEI

Although Kunigal recorded the highest mean rainfall, there is a higher frequency of moderate meteorological drought. There is a greater frequency of severe category of agricultural and hydrological drought as discovered by SPI and SPEI. From this observation, we can deduce that the mean rainfall although highest at Kunigal station may have occurred over a very short period of time giving room to the more frequent occurrence of drought events. There is also no clear association of the fluctuation of the drought frequency with the mean rainfall in the area.

### 3.3.2. Run length of drought

The SPI and SPEI values were calculated in hopes of finding their potential application in the analysis of the dry periods and also drought risk monitoring and management for the time scale 1-, 3-, 6-, 9-, 12-, and 24-months from 1981 to 2019 were utilized to construct the graphs portraying the maximum run length (in months) for various drought categories. The period over which a certain level of wetness persists denotes the duration of drought and serves as a crucial tool in the planning of water resources. According to Figure 13, for the hydrological and agricultural drought conditions SPI showed greater drought months in the extreme category than SPEI while at the same time, SPEI observed longer drought run length than SPI in the moderate and severe category.

Madhugiri station experienced a prolonged drought of extreme intensity throughout the year 2019 from January to December which is upheld by the consistently negative ( $<-2.0$ ) SPEI value in all time scales except for 1 month. Particularly in the 24-month timescale, extreme drought persisted from January 2018 to December 2019. From December 2002 to April 2004, Tumakuru-1 and Koratagere showed continuous severe drought conditions in the 12-month timescale. The station Turuvekere recorded severe to extreme drought for an extended duration from December of 2016 to December 2019. The entire study area was affected by severe drought during the years 2016-17 in all the timescales. The continuous moderate drought was found in the year 1986 at Tumakuru-1 and Pavagada, in 1991 at Turuvekere and Chikkanayakanahalli, in 2003 at Chikkanayakanahalli, Kunigal, Sira, Tiptur, Tumakuru, and Turuvekere and in 2012 at Gubbi. Rabi season was greatly affected by severe drought as seen from the SPEI value at 6-month timescale while Madhugiri faced extreme drought. The SPEI value for 1- and 3-month are more pronounced than SPI.

During the years 2002 and 2003 most of the study area suffered drought conditions categorized using SPI as severe and extreme mostly in 6-, 9-, 12-, and 24-month timescale.

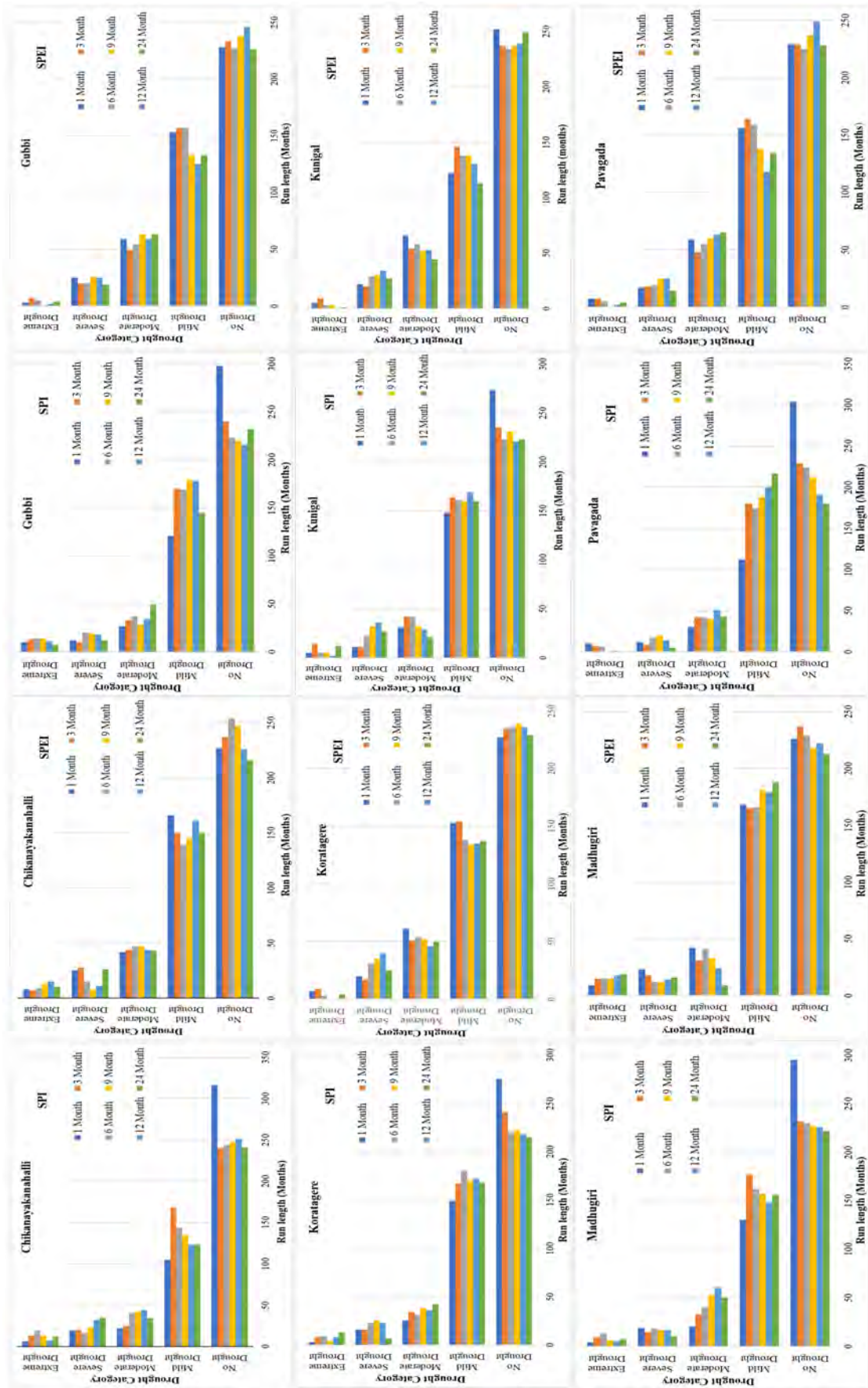


**Figure 13:** Length of dry period in months

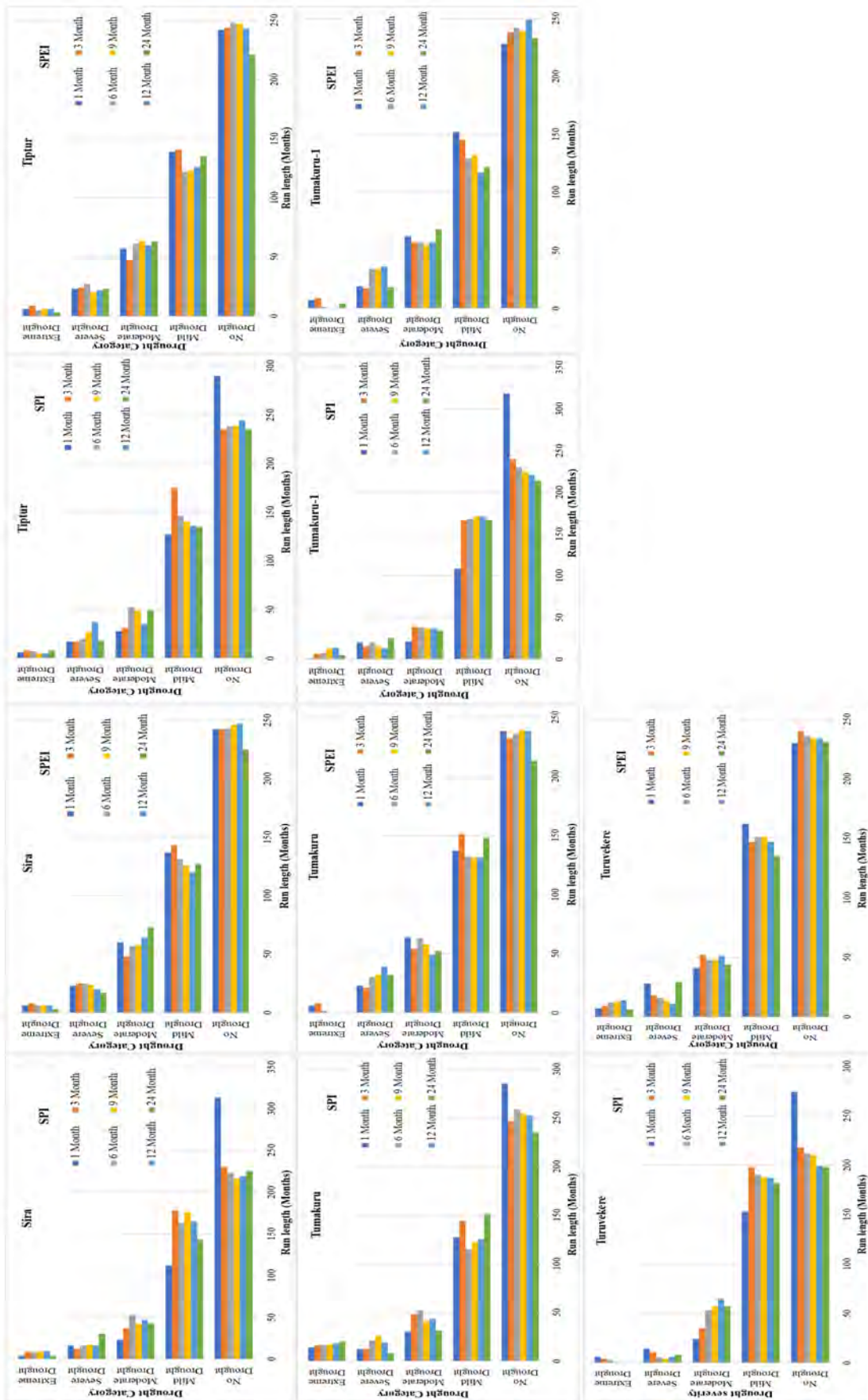
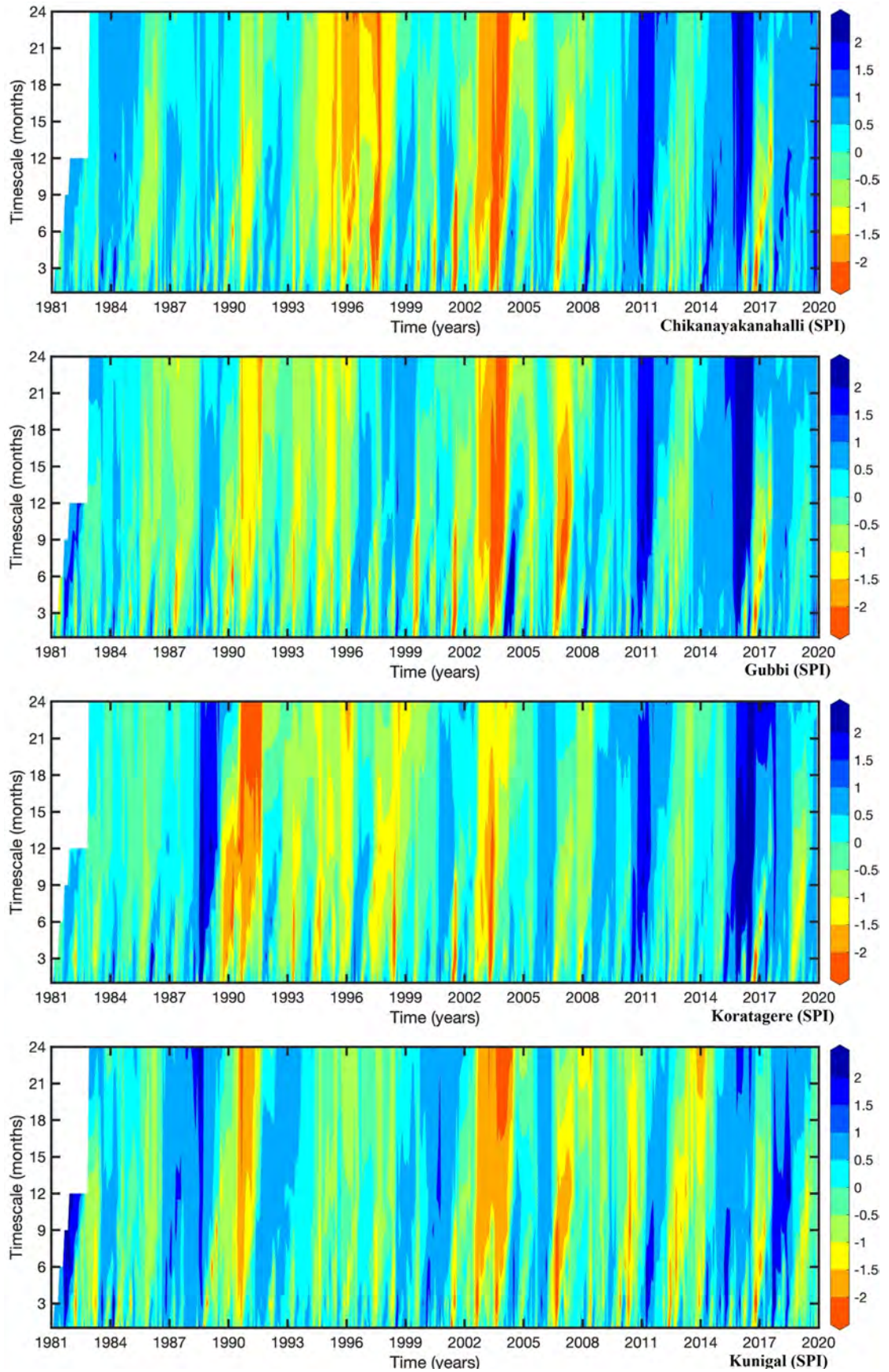


Figure 13: continued

This pattern was recorded prominently during the southwest monsoon season (July to December). The longest run length of nearly 46 months for moderate and severe drought was observed at Sira station from September 1983 to July 1987 for the 24-month timescale. Meteorological drought persisted from August to December in 2002 and 2003 at the stations Tumakuru and Tumakuru-1 which was moderate, severe, and extreme in character along with Tumakuru enduring severe drought from April 1990 to November 1990. Tumakuru is the sole station that witnessed extreme 6-month drought in continuity during January-December of 1990. At the shorter time scale, the meteorological drought has a good representation in SPEI in comparison to SPI. When comparing the agricultural drought, more stations revealed severe and some extreme events in SPEI. The variation of results from SPI and SPEI though inevitable finds similarities when it comes to a longer time scale indicating the hydrological drought. The key factor that sets SPEI apart from SPI is the inclusion of evapotranspiration parameters by including the temperature data. This brings about a huge change in the resulting value. The evaporation of water from the surface also affects the onset of drought which can be quantified using the SPEI. The evapotranspiration creates a demand on the available water which is clearly observed during periods of water scarcity which is further reflected in the increased SPEI values. Also, the drought period found in SPI was further amplified when seen in SPEI. With rainfall being the only parameter, more of extreme drought condition is extracted than when the potential evapotranspiration (PET) is included. The longer timescale holds a greater duration than the shorter timescale of drought in 55% of the stations for SPEI. The rest of the station at the longer timescale noted a lower duration of drought which greatly impacted the short-term water resource than the long term. It is not necessary that the longest drought period cause the most impact as the intensity of the drought needs to be taken into consideration. The relationship between the duration of drought and mean rainfall is erratic in the region.

### 3.3.3. Temporal evolution of dry period at different timescale

The drought occurrence in the study area over the years has seen fluctuations and these are directly related to the meteorological parameters affecting the region. The analysis of the temporal pattern at various time scales (1-, 3-, 6-, 9-, 12-, 24-month) from 1981 to 2019 as shown in Figure 14 and Figure 15 helps us obtain a better understanding of the dry conditions in the area which in turn paves a way to monitor and mitigate further deterioration in the condition. From 1981 to 2019, the early 1990's, the early 2000s, and late 2010s are the years that stand out in the entire study area showing prominent dry periods. The worst of extreme drought event at the 1-month scale according to SPI and SPEI occurred in Tiptur in May 2016 (-4.75) and Chikkanayakanahalli in March 1992 (-2.76) respectively.



**Figure 14:** Temporal distribution of SPI at different timescale

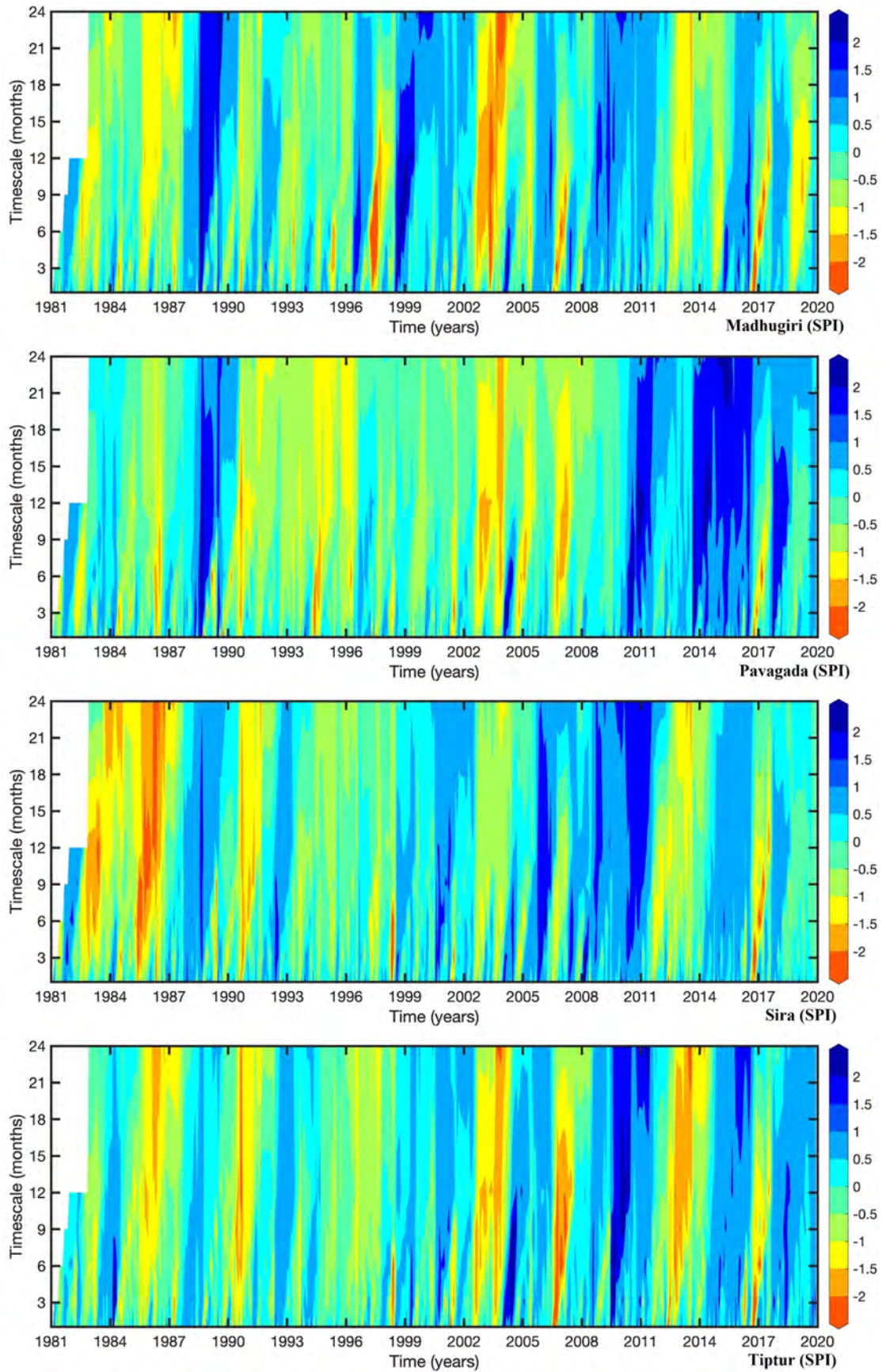


**Figure 14:** continued

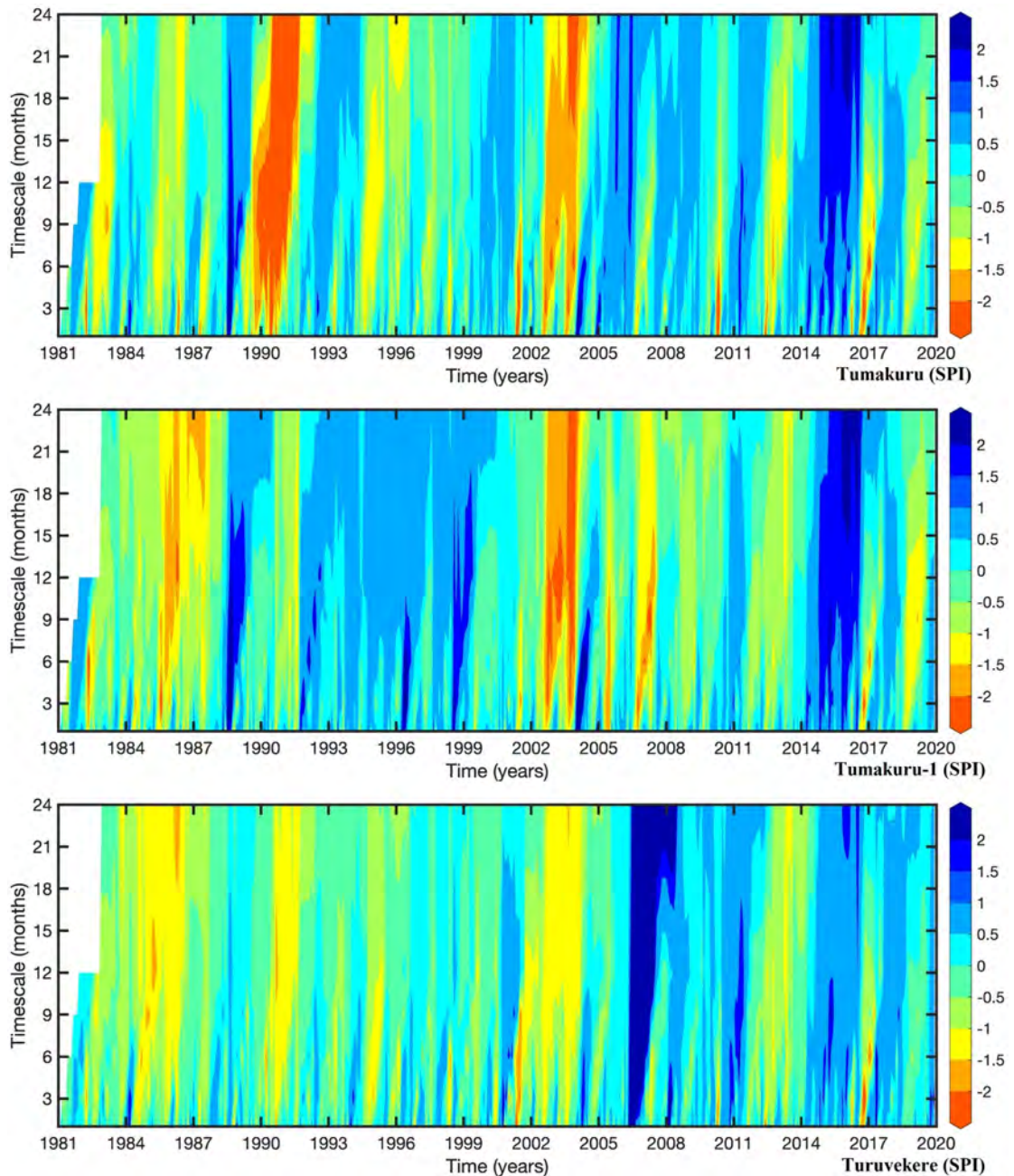


**Figure 14:** continued

For the 3-month timescale, the lowest value for SPI was at Chikkanayakanahalli in July 2001 (-4.21) and for SPEI at Gubbi in April 1983 (-2.71). SPI at Koratagere in May 2003 (-4.16) and SPEI at Gubbi in September 2003 (-2.79) are the minimum at the 6-month timescale. Chikkanayakanahalli in September 2003 noted an SPI value of -3.38 and Madhugiri in May 2019 noted an SPEI value of -2.59 for the 9-month timescale. SPI for Tumakuru in July 1990 was -3.91 and SPEI for Chikkanayakanahalli in February 2017 was -2.54 which were the least values in the 12-month timescale. At the timescale of 24-month, Tumakuru in September 1990 showed -3.61, and Madhugiri in May 2019 showed -2.28. The intensity of drought is



significantly more in SPI in comparison to SPEI at all the stations and timescales which is denoted by the negative value of the indices.

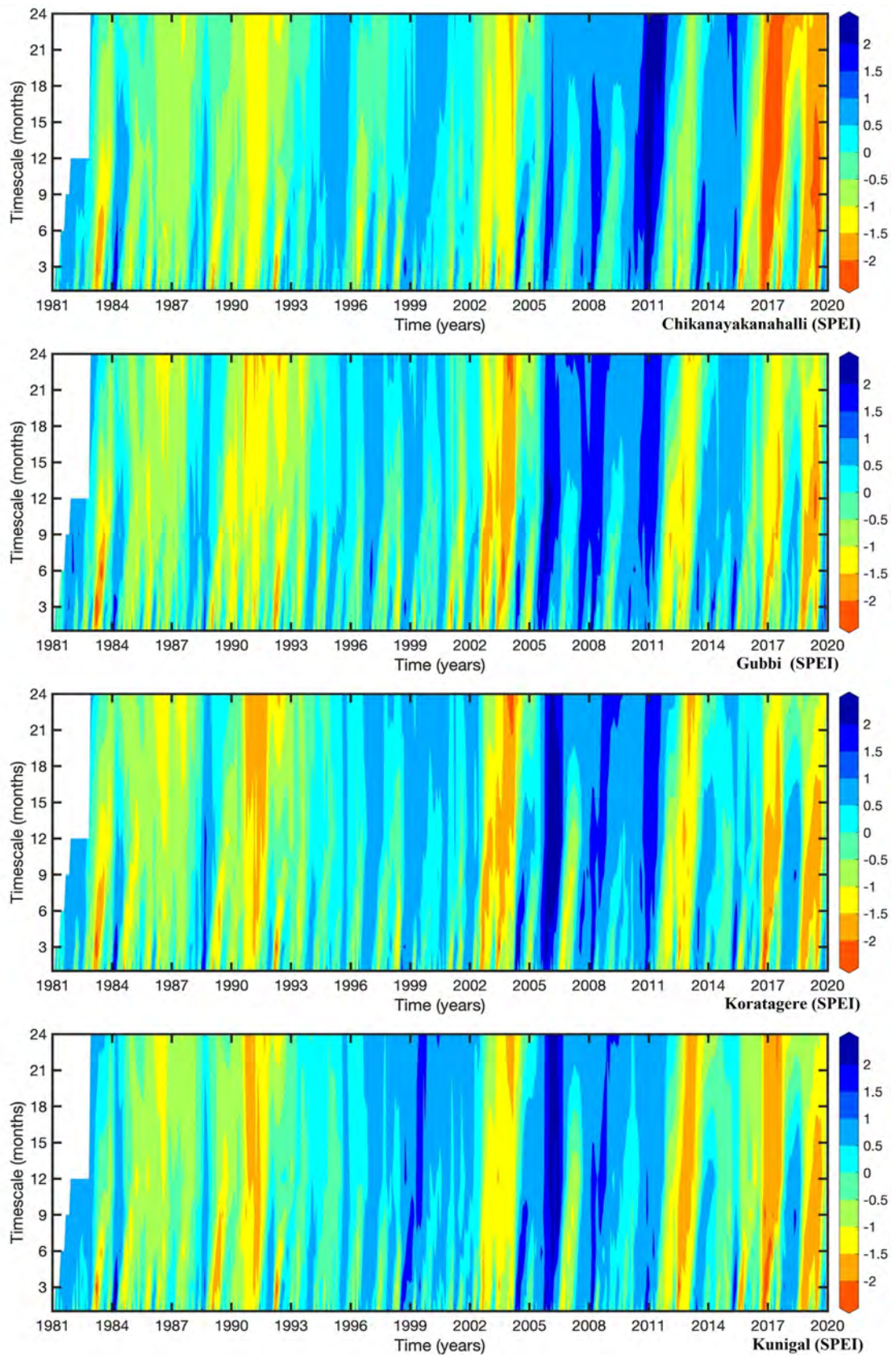


**Figure 15:** Temporal distribution of SPEI at different timescale

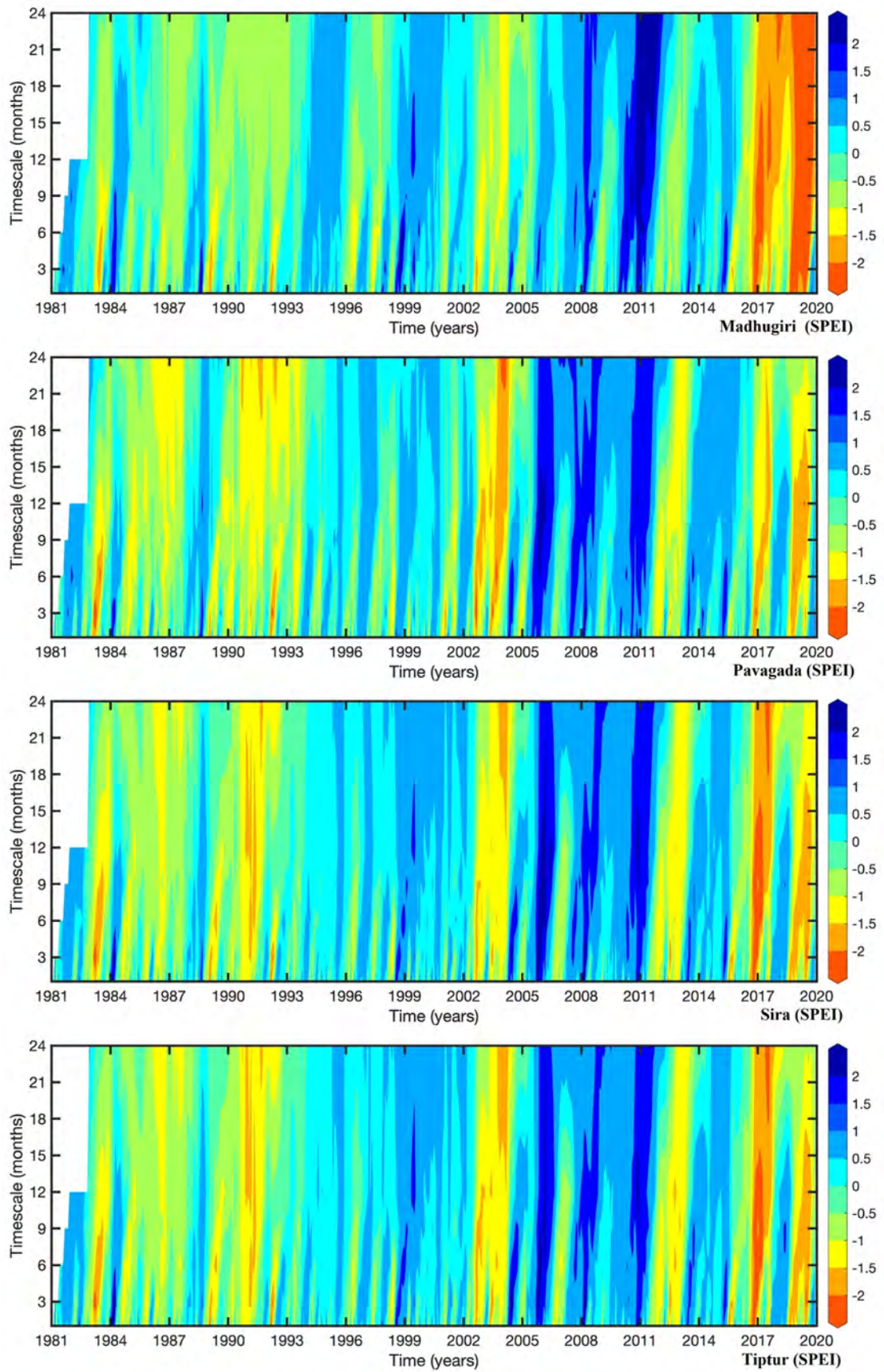


**Figure 15:** continued

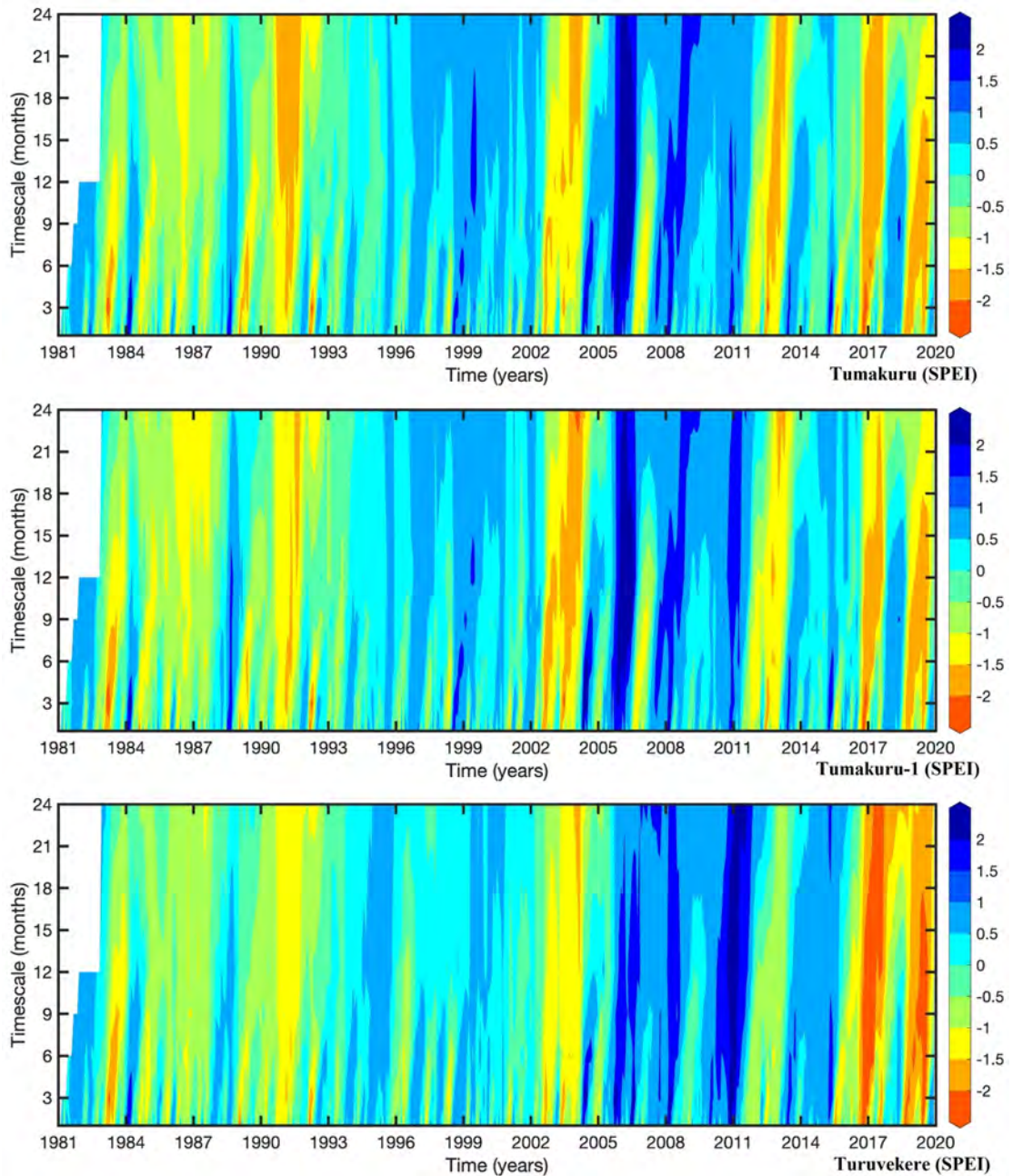


**Figure 15:** continued

A common trend is seen where the extreme drought event at all the stations and at every time scale was prominently featured by SPI than SPEI. The smaller time scales showed lower values for both SPI and SPEI and the value increased when proceeding toward the longer timescale. May to July seem to be the worst affected months across the timescales for SPI and February and March as per SPEI values. Tumakuru station did not record any extreme drought events successively for the 9-, 12- and 24-month timescale for SPEI. Koratagere and Tumakuru-1 at the 9- and 12-month timescale showed zero extreme drought events. SPI did not capture any extreme drought events at Pavagada for 9- and 24-month and at Turuvekere for 12-

and 24-month timescale. A stark difference between SPI and SPEI can be observed from the temporal graph at the various timescale. A similar dry spell was found at all the stations in 2016 and 2017 for the SPEI value whereas, at the same time, SPI recorded mostly no drought condition. SPI value is prominent in 2003 showing extreme conditions at all stations except Sira, while SPEI showed mainly mild drought conditions. The large fluctuation was frequently observed in the indices at the shorter timescale which also showed a large difference between the intensity (Table 7). For the longer timescale, there was a slight difference between the SPI and SPEI intensity, and the fluctuation tended to be gentle. The climate change and subsequent increase in global warming find better representation in SPEI rather than SPI, as the former includes the effects of temperature on PET along with precipitation, while the latter shows no attention to the effect of evaporation on drought.

**Table 7:** Minimum value of SPI and SPEI recorded at different timescale

Timescale	Least SPI		Least SPEI	
	Station	Year	Station	Year
1-month	-4.75 at Tiptur	Aug 2006	-2.76 at CN Halli	Mar 1992
3-month	-4.21 at CN Halli	July 2001	-2.71 at Gubbi	Apr 1983
6-month	-4.16 at Koratagere	May 2003	-2.79 at Gubbi	Sep2003
9-month	-3.38 at CN Halli	Sep 2003	-2.59 at Madhugiri	May 2019
12-month	-3.91 at Tumakuru	Jul 1990	-2.54 at CN Halli	Feb 2017
24-month	-3.61 at Tumakuru	Sep 1990	-2.28 at Madhugiri	May 2019

### 3.4. Conclusion

Drought being one of the hydro-meteorological disasters has been a successively recurring event across the state of Karnataka with varying magnitude and intensity. Climate change resulting in the spatial and temporal variation of temperature and precipitation has been the driving force for such events. The major difference between the indices is that SPEI includes the evapotranspiration parameter along with rainfall while SPI is solely dependent on rainfall only. This difference is minor when concerning the meteorological drought but when dealing with agricultural and hydrological drought, the climatic water balance comes into question drawing prominence to SPEI over SPI. This study analyzed the drought severity at the 1-, 3-, 6-, 9-, 12-, and 24-month timescales by drawing a comparison between SPI and SPEI.

a. The outcome of the drought frequency study indicated that SPI showed more frequent extreme dry periods while SPEI gave a better result for moderate and severe drought in all the timescale.

b. SPI and SPEI showed greater fluctuation and had a poor correlation for the shorter timescale representing the meteorological drought as there was a large difference in their values; SPEI gives the best result since it deals with the increase in the water demand caused by the PET as a result of rising temperature. For the longer time scale, there is a mild fluctuation between the indices, and the difference between them also considerably decreased. By this, we can conclude that the drought conditions at the longer timescale given by SPI and SPEI tend to be more consistent.

c. Although precipitation has a great role in the determination of drought, evapotranspiration has an unforgettable part to play in the spatio-temporal variability of soil moisture giving rise to agricultural drought which is best portrayed in the 6- and 9-month timescale of SPEI. While SPI and SPEI serve different purposes, the former needs to be utilized with caution and whereas the latter is extremely useful wherever the effects of evapotranspiration are in play.

The present study aims at defining the difference between the two indices SPI and SPEI by evaluating the data of Tumakuru District, India. As they serve a different purposes, no clear conclusion can be drawn on which index is the better identifier of the drought condition. The research gives an understanding of the most suitable index to criticize drought in the study area but this may not be extended to other regions as the index is dependent on the variability of climatic conditions and regional characteristics. The correlation of SPEI and SPI facilitates policymakers and planners in the planning and execution of innovative water conservation structures and effective drought mitigation structures.

## 4. Rainfall Trend

### 4.1. Introduction

Global warming has affected and continuously changed the magnitude and distribution of hydrometeorological variables such as rainfall, temperature, and humidity. As per the Intergovernmental Panel statement about Climate Change<sup>91</sup>, the hydrological cycle at the regional and global scale is changing due to the rising surface temperature. The impacts of climate change can be illustrated as an output of the analysis of physical variables like geophysical, oceanographic, and hydrometeorological; resulting in water deficiency in certain areas, and it may be responsible for floods in certain regions<sup>92</sup>. The food security and economy of the nations such as India are relying on the ideal accessibility of rainfall. Therefore, precise statistics and information about rainfall trends and its pattern are necessary for the management and utilization of water resources<sup>93-95</sup>. The fluctuations in the climatic variables are bound to cause startling changes in the hydrological conditions, which have been identified in the arid or semi-arid region of India, Tumakuru district for example. These impacts of climate changes in the environment stimulate the frequency of drought events, intensive floods, and sometimes severe storms. Hence fore, the long-term trend identification and its slope analysis has been a key input for many climate change-induced events such as water resource management, drought assessment and/or monitoring, as well as flood mitigation.

The Mann-Kendall (MK) test<sup>96</sup>, Innovative Trend Analysis (ITA)<sup>97</sup>, Linear Regression analysis<sup>98</sup> and Sen's slope estimator (SS)<sup>99</sup>, are the major adopted trend test techniques in neoteric research. Globally, numerous studies have been conducted with gridded rain gauge data to explore the rainfall trend via MK, ITA, and SS. MK Test and Sen's slope was utilized by<sup>100</sup> to evaluate the hydrometeorological parameters and identify parameters influencing groundwater availability. Water budget was also analysed to study the ground water drought in the Ganga basin. An improved MK test for hydrological data was proposed by<sup>101</sup> which turned out to have more advantages than the other methods available for trend detection for precipitation time series data. To study the impact of changing climatic conditions on rainfall in Vietnam,<sup>102</sup> employed the techniques of Innovative Polygon Trend Analysis which are developed from ITA along with MK methods. Ref.<sup>103</sup>, (2018) worked on implementing the MK test on precipitation and temperature data to analyze the trend and Theil-Sen slope for the estimation of magnitude. Further Pettitt-Mann-Whitney test helped identify the change point. Several other studies concerning a similar subject have been carried out in India<sup>104,105</sup>, Bangladesh<sup>106</sup>, China<sup>107</sup>, Kyrgyzstan<sup>108</sup>, Algeria<sup>109</sup> to name a few. Ref.<sup>100</sup> utilized Sen's slope

estimate and MK test to identify the groundwater influencing parameters in the Ganga basin. The study also included the determination of water budget, storage, and groundwater flow analysis. Ref.<sup>110</sup> implemented multiple statistical techniques such as the MMK test, Linear Regression, ITA, Sen's slope, Pearson's Coefficient of Skewness, Weibull's Recurrence Interval, and others to analyze the monthly, seasonal, and decadal rainfall trend in Hill Agro-Climatic Region and West Coast Plain of India. Ref.<sup>111</sup> investigated the fluctuation in the rainfall trend due in the semi-arid region of Chhattisgarh state in India. MMK test along with discrete wavelet transformation was utilized to achieve the result of the study. Ref.<sup>112</sup> Examined the rainfall trend using the MMK test and determined other indices for multiple precipitation datasets to evaluate the variability of rainfall in Ethiopia. Ref.<sup>113</sup> studied the rainfall variability using MK, MMK, Sen's slope, ITA, and other methods in Maharashtra. The study concluded that although various methods were successful in identifying the trend, ITA was able to observe trends given by all the other methods. Ref.<sup>93</sup> worked on forecasting rainfall and analyzing the trend in India. Ref.<sup>93</sup> conducted a comparative evaluation of several machine learning models when applied to rainfall forecasting under different time horizons. Ref.<sup>114</sup> employed MK and ITA methods to analyze the precipitation trend in Sri Lanka. The results obtained from both tests indicated a similar percentage of increasing and decreasing trends in the region. Further, the ITA was said to be better suited as it depicted trends at different values. Ref.<sup>115</sup> worked on the trend of extreme flood events in northern Sweden through statistical analysis.

In addition to the above mentioned method, there are numerous types of trend analysis methods recommended for trend measurement but very few of the studies have focused on India, especially on the ITA approach<sup>116</sup>. Ref.<sup>117</sup> studied the trend in the northwest and peninsular region of the country during 1901-2019 and mentioned an increasing rainfall trend on monsoon and annual scale. Similar studies were conducted by Ref.<sup>118</sup> during 1871-2008 through MK and SS methods and not much difference was found in the trend. However, the MK trend technique equations, unlike the ITA, a categorization in the time series data is not feasible and it derives only monotonic trend in the dataset<sup>119</sup>. While following ITA, the long-term trend patterns, such as negative, positive, and trendless possibilities could be analysed, whereas distinctive trend movement has not been assessed in the MK. In the present study, we have focused to analyse the long-term seasonal as well as the annual pattern of rainfall, by implementing both MK and ITA methods to figure out the best fit trend model to analyse the long-term rainfall pattern. The current study aims to understand the rainfall pattern in the semi-arid region of Karnataka, India from 1952 to 2019 using the MMK, Sen's slope, and ITA methods. In addition, Sen's

estimator was also utilized to assess the long-term trend magnitude. The present research on trend analysis has met the required confidence interval of 95% ( $\pm 1.96$  as the threshold for trend) with a significant level of =5%. Hence, the trend analysis result of long-term rainfall pattern in 11 meteorological grid stations for 68 years from 1952 to 2019 will be a key input for assessing the spatio-temporal variability in the Tumakuru district in India. A large part of the population is dependent on agriculture relying on rainfall in this area due to lack of any major rivers. This study will be beneficial not only for analysing the trend but also have an impact on the socio economic conditions of the people. Having a better understanding of the rainfall scenario makes a good basis to build a better monitoring system for extreme events and better water management systems.

## 4.2. Methodology

The methodology of this research follows the non-parametrical tests to analyze the trend pattern and detect the change point in the region from 1952 to 2019. The daily rainfall data were averaged to get the monthly value upon which the trend analysis was conducted. The following methods were adopted to fulfill the objective.

### 4.2.1. Modified Mann Kendall

To analyze the non-normally distributed time series rainfall gridded data for temporal tendencies, the MK test<sup>96,120</sup> is employed. Along with a significance value, this non-parametric test facilitates the identification of an increasing or decreasing pattern. The Mann Kendall statistics quantify any trend which is present by testing whether the time series lies in the confidence interval defined for the null hypothesis of the significance level.

$$S = \sum_{k=1}^{n-1} \sum_{l=k+1}^n \text{sgn}(x_l - x_k) \quad (19)$$

Where  $n$  refers to the length of the rainfall data,  $x_l$  and  $x_k$  denote the sequential data values.

$$\text{sgn}(x_l - x_k) = \begin{cases} 1, & \text{if } (x_l - x_k) > 0 \\ 0, & \text{if } (x_l - x_k) = 0 \\ -1, & \text{if } (x_l - x_k) < 0 \end{cases} \quad (20)$$

For the random variable distribution, the statistics approximate the normal distribution when  $n \geq 8$  where the mean is given by  $E(S)$  and variance by  $Var(S)$ .

$$E(S) = 0 \quad (21)$$

$$Var(S) = \frac{n(n-1)(2n+5) - \sum_{k=1}^m t_k(t_k-1)(2t_k+5)}{18} \quad (22)$$



Where the number of ties for the extent  $k$  is given by  $t_k$  and the number of tie groups is given by  $m$ . Further, test statistics are obtained by  $Z_S$ .

$$Z_S = \begin{cases} \frac{S-1}{\sqrt{Var(S)}}, & \text{if } S > 0 \\ 0, & \text{if } S = 0 \\ \frac{S+1}{\sqrt{Var(S)}}, & \text{if } S < 0 \end{cases} \quad (23)$$

A positive  $Z_S$  indicates an increasing trend while a negative  $Z_S$  indicates a decreasing trend. This study is performed for an  $\alpha$  value of 0.05 giving a 5% significance level. With the standard normal variate given by  $Z_{1-\frac{\alpha}{2}}$ , if  $|Z_S| > Z_{1-\frac{\alpha}{2}}$ , the null hypothesis for no trend is rejected. If  $|Z_S| > 1.96$ , the null hypothesis is rejected. To address the issue of misinterpretation caused by the serial autocorrelation in the data, the modified MK test was devised. This method gives an empirical variance of test statistics<sup>121</sup>.

$$V^*(S) = Var(S) \cdot \frac{n}{n_S^*} = \frac{n(n-1)(2n+5)}{18} \cdot \frac{n}{n_S^*} \quad (24)$$

The correction of  $n/n_S^*$  is given for the autocorrelation in the data calculated as

$$\frac{n}{n_S^*} = 1 + \frac{2}{n(n-1)(n-2)} \sum_{k=1}^{n-1} (n-k)(n-k-1)(n-k-2)\rho_S(k) \quad (25)$$

Where the autocorrelation function of the rank of observations is given as  $\rho_S(k)$  and  $n$  is the length of the data. By comparing the standardized test statistics  $Z_S$ , the significance of the trend is tested. The parent correlation function  $\rho(k)$  defines the autocorrelation of ranks of observation  $\rho_s(k)$ .

$$\rho(k) = 2\sin\left(\frac{\pi}{6}\rho_S(k)\right) \quad (26)$$

#### 4.2.2. Sen's Slope Estimator

Sen's slope is based on a non-parametric median which quantifies the magnitude of the trend<sup>122</sup>. The slope is given by the following equation.

$$\beta = \text{Median} \left[ \frac{x_a - x_b}{a - b} \right] \text{ for all } b < a \quad (27)$$

For years  $a$  and  $b$ , the consecutive data values are defined as  $x_a$  and  $x_b$  respectively.  $\beta$  for the trend slope of the data denotes the magnitude.

#### 4.2.3. Innovative Trend Analysis

The rainfall series is divided into two halves giving the first half series and second half series. Both the series are arranged in ascending order and the values are plotted on a graph with the initial half series on the horizontal axis and on the vertical axis, the latter half series is plotted. Figure 16 details the trends that are found in the data<sup>99,123,124</sup>.

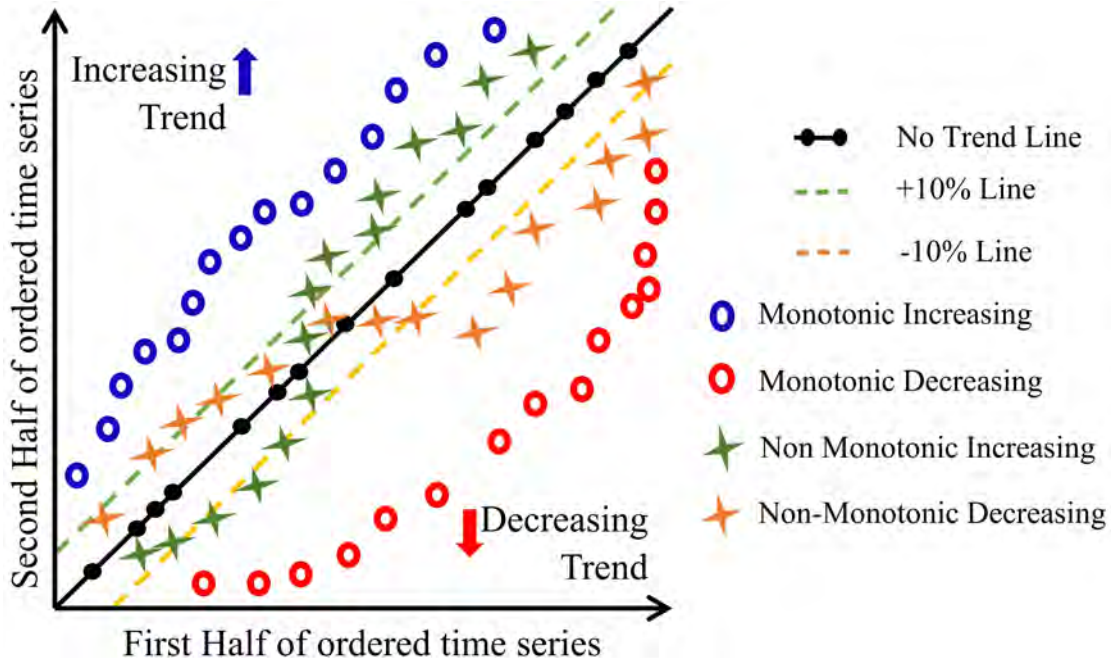


**Figure 16:** Interpretation of ITA trend

In the ITA method proposed by Sen, the critical trend is assumed by the null hypothesis. The slope for series a and b are determined by

$$s = \frac{2(\bar{b} - \bar{a})}{n} \quad (28)$$

The expected value is given as

$$E(s) = \frac{2(E(\bar{b}) - E(\bar{a}))}{n} \quad (29)$$

The variance, covariance, and standard deviation for the series are calculated.

$$\sigma_s^2 = \frac{4}{n^2}(E(\bar{b}^2) + E(\bar{a}^2) - 2Cov(\bar{a}\bar{b}) - 2E(\bar{a})E(\bar{b})) \quad (30)$$

$$\sigma_s = \frac{2}{n}(Var(\bar{a}) + Var(\bar{b}) - 2Cov(\bar{a}\bar{b}))^{\frac{1}{2}} \quad (31)$$

The  $z$  value of the ITA is adjusted for the type-I error and is calculated as

$$z_{ITA\_R} = \frac{s - E(s)}{\sigma_s} = \frac{s}{\sigma_s} \quad (32)$$

The  $z$  values greater than 1.65 are considered an increasing trend while  $z > 1.96$  are significantly increasing.  $z > 2.58$  are a very significantly increasing trend. Similar values are defined for the negative values for the decreasing trend.

### 4.3. Result

The rainfall data analysis was carried out for the Tumakuru district from 1952 to 2019. The result shows the analysis of the time series precipitation data and the trend for each of the 11 grid stations present in the study area. The preliminary investigation of the statistical scenario of time series rainfall dynamics in Tumakuru district indicates that few stations do not qualify for the normal distribution assumptions. Though the annual rainfall dataset is entirely positively skewed, the kurtosis value has shown negative results in very few instances for both seasonal as well as annual rainfall data (Table 8). Hence, it is important to implement a non-parametric method to investigate the rainfall trend.

**Table 8:** Detailed statistical description of annual and seasonal rainfall statistics

Stations	Annual		Kurtosis			
	SD	Skewness	Annual	Pre monsoon	SW monsoon	NE monsoon
<i>CN Halli</i>	256.9	2.80	13.44	5.89	20.99	-0.04
<i>Gubbi</i>	196.4	0.48	0.34	3.50	-0.65	1.00
<i>Koratagere</i>	214.5	1.07	1.29	0.03	2.03	0.32
<i>Kunigal</i>	261.3	1.15	2.77	-0.57	2.83	4.65
<i>Madhugiri</i>	223.1	0.68	0.11	3.41	3.06	0.40
<i>Pavagada</i>	279.1	4.03	22.44	6.50	27.09	0.84
<i>Sira</i>	224.3	0.87	0.45	22.43	-0.28	1.24
<i>Tiptur</i>	196.0	0.28	-0.77	1.98	0.71	-0.17
<i>Tumakuru</i>	294.2	2.50	12.09	2.42	17.00	-0.23
<i>Tumakuru-1</i>	281.8	1.51	4.39	15.95	2.10	1.92
<i>Turuvekere</i>	294.1	2.83	11.83	1.03	16.63	-0.56

#### 4.3.1. Pre-monsoon

The statistical description of the kurtosis value for 11 grid stations in the study area is depicted in Table 8, where Kunigal is the only station to have a negative kurtosis value of -0.57 in the pre-monsoon. Table 9 shows pre-monsoon seasonal trend results of MK Z value, ITA slope, and Sen's slope. The SS magnitude indicates that the highest value recorded is in the Tumakuru station whereas the lowest value is in Chikkanayakanahalli (CN Halli) with 1.34 mm/year and -0.16 mm/year respectively (Figure 18). The stations such as Tiptur, Tumakuru, and Tumakuru-1 has shown

significant increasing trends with Z value 2.41, 3.31, and 2.61 respectively, with a fixed threshold of  $p < 0.05$ .

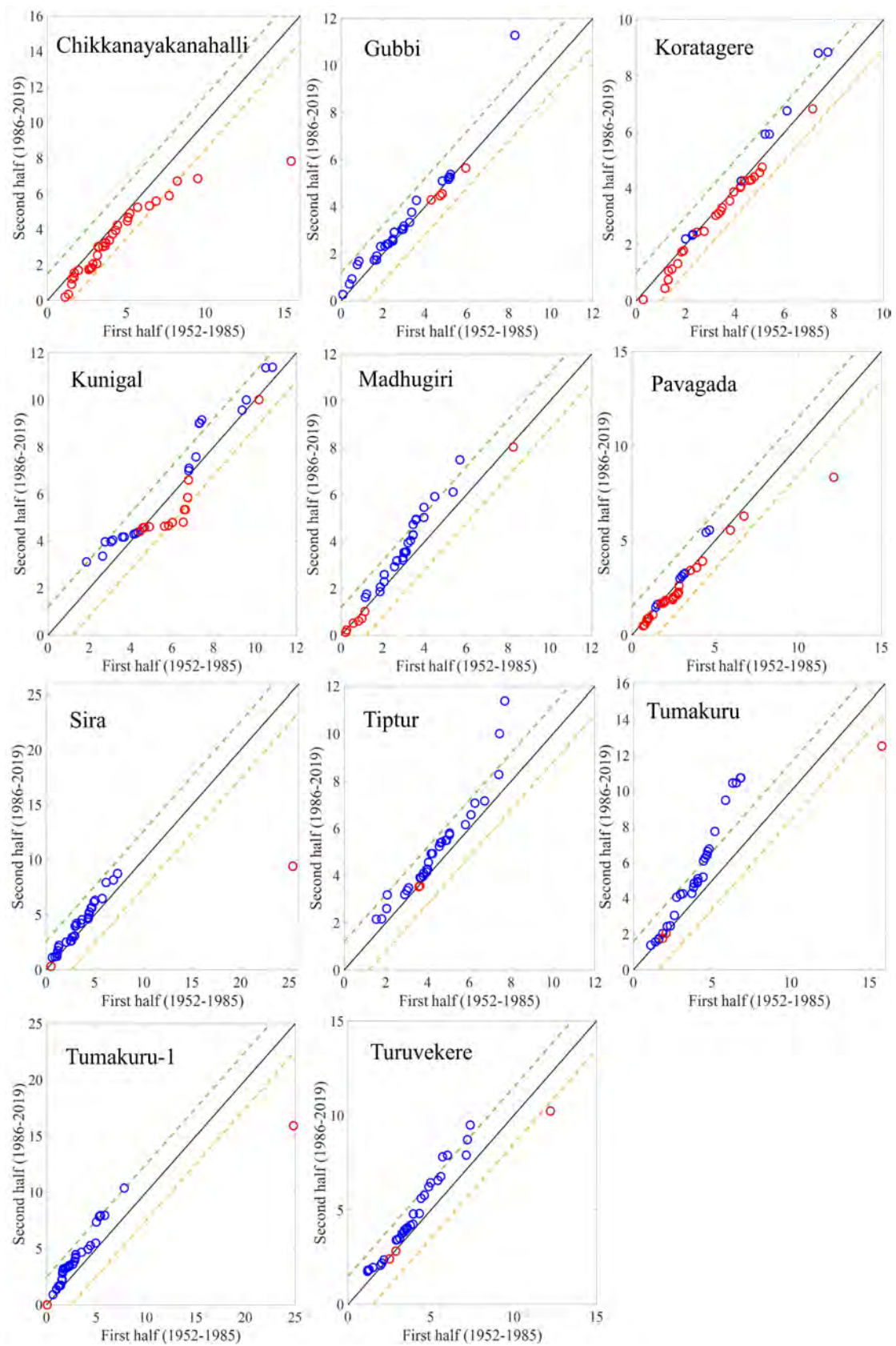


**Figure 17:** Graphical representation of pre-monsoon ITA

The station CN Halli has only shown a non-significant negative trend, whereas the remaining seven grid stations have shown non-significant positive trends. However, ITA values indicate eight grid stations with a non-significant increasing trend and three grid stations with a non-significant negative trend. The spatial differences in trend results are presented in Figure 19, whereas, Figure 17 depicts the ITA graphical trend movements for individual grid stations. The presented results Table 9 have disseminated the credibility and reliability of ITA over MK by identifying some invisible trend in the data, while this decreasing trend has not been detected in MK. Likewise, the ITA result reveals that only CN Halli (-0.84 mm), Koratagere (-0.06 mm), and Pavagada (-0.26 mm) reported a non-significant decreasing trend.

**Table 9:** Description of the Seasonal rainfall variation result for 11 grid stations of Z statistics, ITA slope and Sen's slope with the positive and negative ITA trend during 1952-2019. (The trend at (P<0.05) Significant level is indicated in bold character)

Stations	Pre-monsoon				Southwest				Northeast			
	Z	ITA	Trend	SS	Z	ITA	Trend	SS	Z	ITA	Trend	SS
CN Halli	-0.47	-0.84	-	-0.16	0.56	-1.27	-	0.45	-1.05	-0.92	-	-0.65
Gubbi	1.45	0.24	+	0.36	<b>2.41</b>	1.72	+	<b>2.08</b>	0.89	0.39	+	0.40
Koratagere	0.87	-0.06	-	0.36	0.06	-0.71	-	0.05	-1.40	-0.90	-	-0.82
Kunigal	0.79	0.16	+	0.34	0.04	-1.59	-	0.03	-0.98	-0.78	-	-0.51
Madhugiri	1.79	0.36	+	0.61	<b>2.13</b>	1.85	+	1.43	0.64	0.84	+	0.43
Pavagada	0.21	-0.26	-	0.07	0.75	-1.19	-	0.55	-1.30	-0.70	-	-0.66
Sira	1.32	0.11	+	0.58	<b>2.39</b>	<b>2.49</b>	+	<b>2.11</b>	0.80	0.79	+	0.49
Tiptur	<b>2.41</b>	0.55	+	0.70	<b>3.74</b>	<b>3.07</b>	+	<b>3.34</b>	0.80	0.18	+	0.51
Tumakuru	<b>3.31</b>	1.09	+	1.34	<b>1.97</b>	0.52	+	1.83	0.44	0.99	+	0.26
Tumakuru-1	<b>2.61</b>	0.74	+	0.87	1.83	1.94	+	1.74	-0.09	0.19	+	-0.03
Turuvekere	1.86	0.60	+	0.77	<b>2.49</b>	<b>2.47</b>	+	<b>2.10</b>	0.96	0.67	+	0.66

#### 4.3.2. Southwest Monsoon

The SS result reported the lowest slope rate in Kunigal with 0.03 mm/year, whereas the highest slope is found at Tiptur station with 3.34 mm/year (Figure 18). Figure 19 depicts the spatial distribution of MK, ITA, and SS magnitude, where a major decreasing trend spread across the eastern side of the study, except for one station (CN Halli) on the western side of the study area which has shown the decreasing trend. Yet, these stations including CN Halli, Koratagere, Kunigal, and Pavagada have recorded a non-significant negative trend in ITA over the MK method with the trend values of -1.27, -0.71, -1.59, and -1.19 in ITA and 0.56, 0.06, 0.04, and 0.75 value in MK respectively (Table 9). Therefore, by finding these invisible negative trends in the data series, ITA has dominated its consistency over other methods such as MK and SS. The graphical ITA trend movements for eleven grid stations are shown in Figure 20, where the positive trends of the data series are identified in stations such as Gubbi, Madhugiri, and Sira.

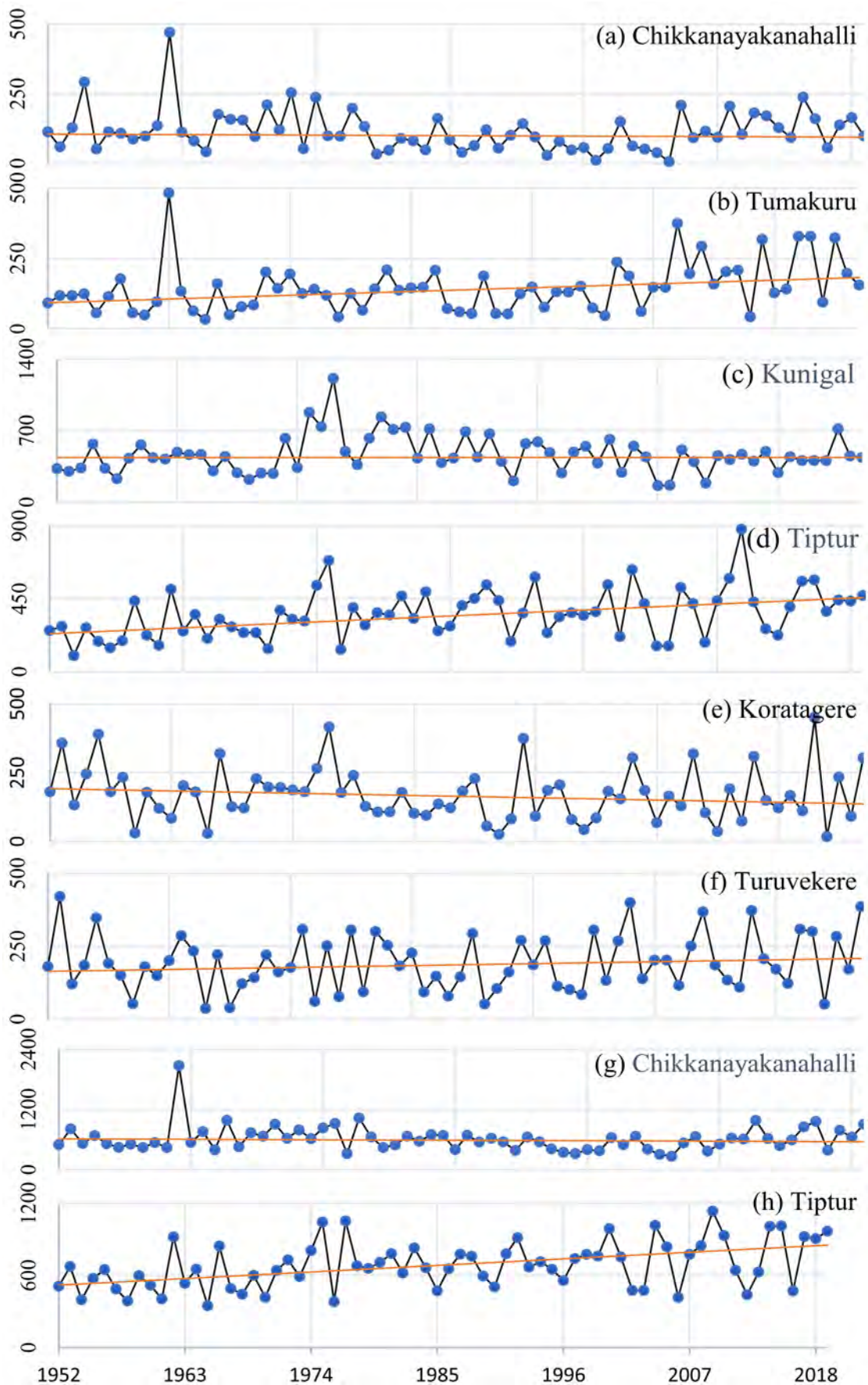


**Figure 18:** Minimum and maximum magnitude of trend of time series rainfall in the pre-monsoon (a & b), SW monsoon (c & d), NE monsoon (e & f) and annual (g & h)

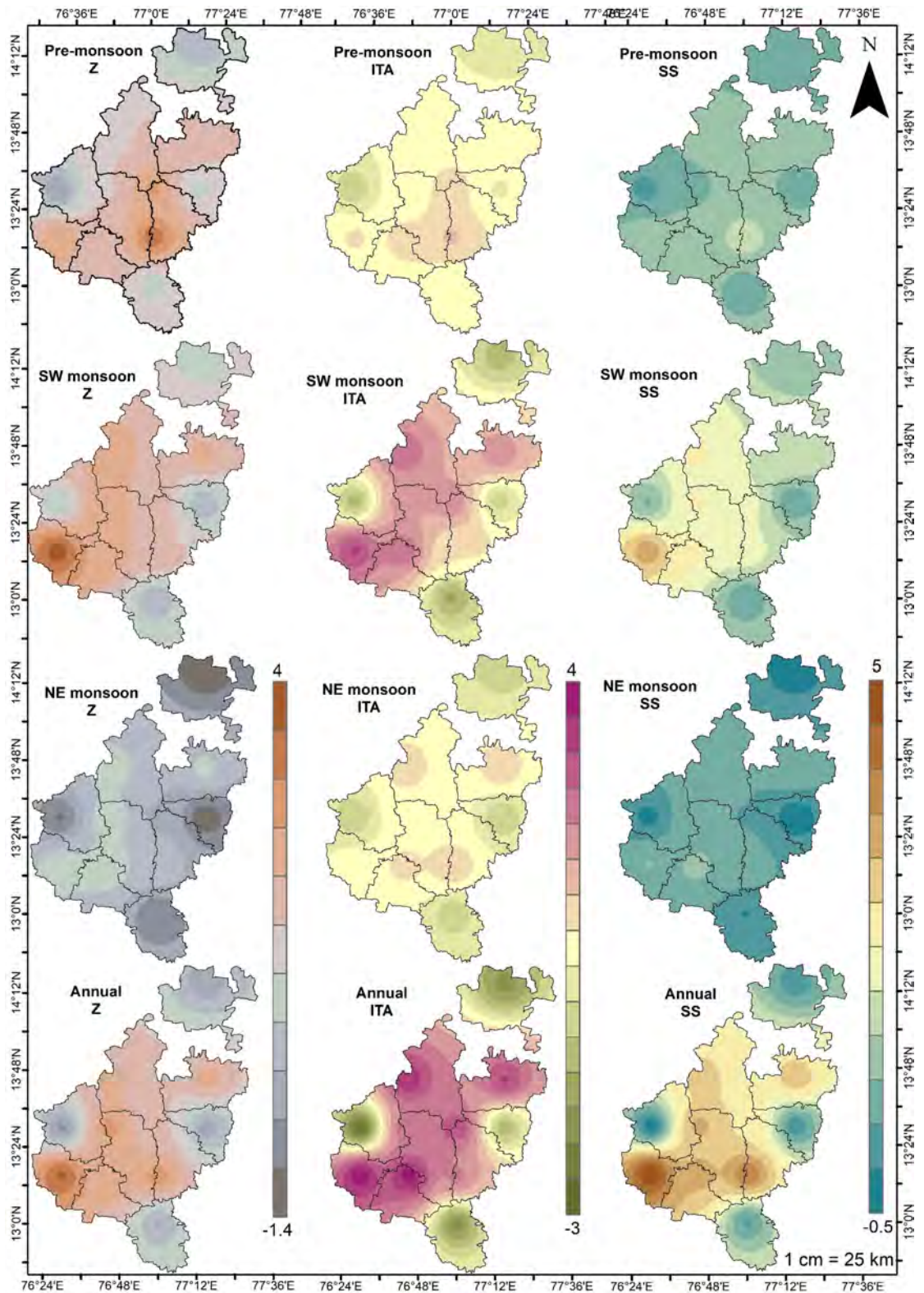


**Figure 19:** Seasonal and annual spatial dispersion of Z, ITA slope and Sen slope

Nevertheless, stations specifically Tiptur and Turuvekere are representing the monotonic positive trend. A negative trend was observed in stations Koratagere and Kunigal, and the remaining nine stations showed a positive trend.

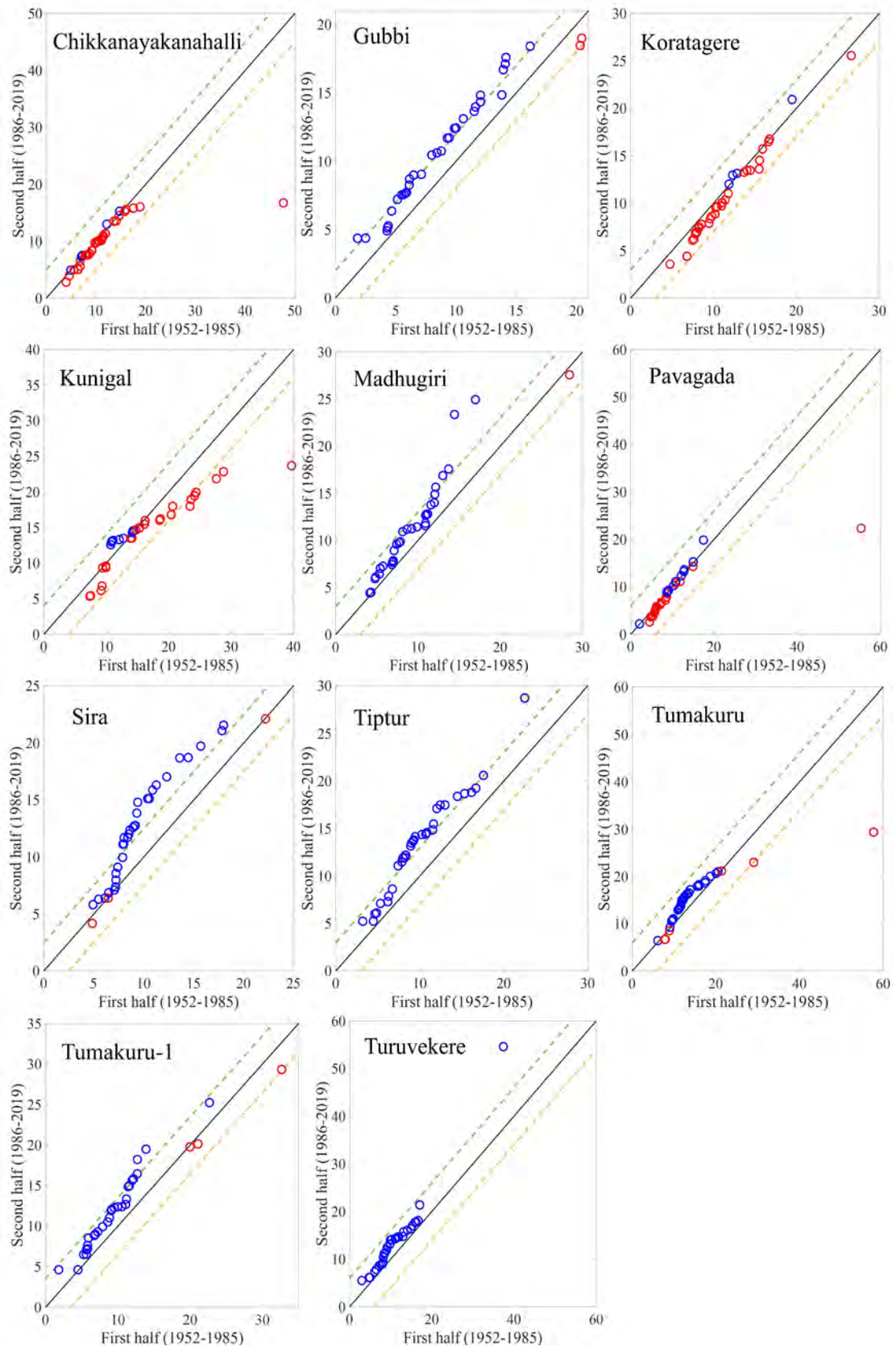


**Figure 20:** Graphical representation of SW monsoon ITA



#### 4.3.3. Northeast Monsoon

The Koratagere and Turuvekere stations observed minimum and maximum magnitude of rainfall trends in the northeast monsoon season respectively (Figure 18). The Z statistics and Sen's slope gives an almost similar trend either towards the increasing (54%) or decreasing (45%) tendency of rainfall in eleven grid stations in the study region (Table 9) while the ITA result has shown a dissimilar spatial pattern in the northeast monsoon season. Although the non-significant increasing trend of MK results exists mainly in the middle part of the district, 63% of stations are indicating a non-significant increasing trend in ITA at Gubbi, Madhugiri, Sira, Tiptur, Tumakuru, Tumakuru-1, and Turuvekere at 95% confidence level and none of the stations reported a significantly increasing trend Figure (19). The majority of decreasing trend is recognized in the southern part particularly CN Halli (-0.92), Koratagere (-0.90), and Kunigal (-0.78) respectively. Consequences of such decreasing pattern in rainfall influence the crop yield, hydrometeorological conditions, and the groundwater level in the region. Figure 22 illustrates the station-wise ITA trend result of the northeast monsoon, where the non-monotonic trend has been identified in all stations except Tumakuru station which shows a monotonic trend. The maximum increasing trend of ITA has been recorded in Tumakuru station with 0.99 mm per year, and the highest negative trend in CN Halli with -0.92 mm per year respectively.

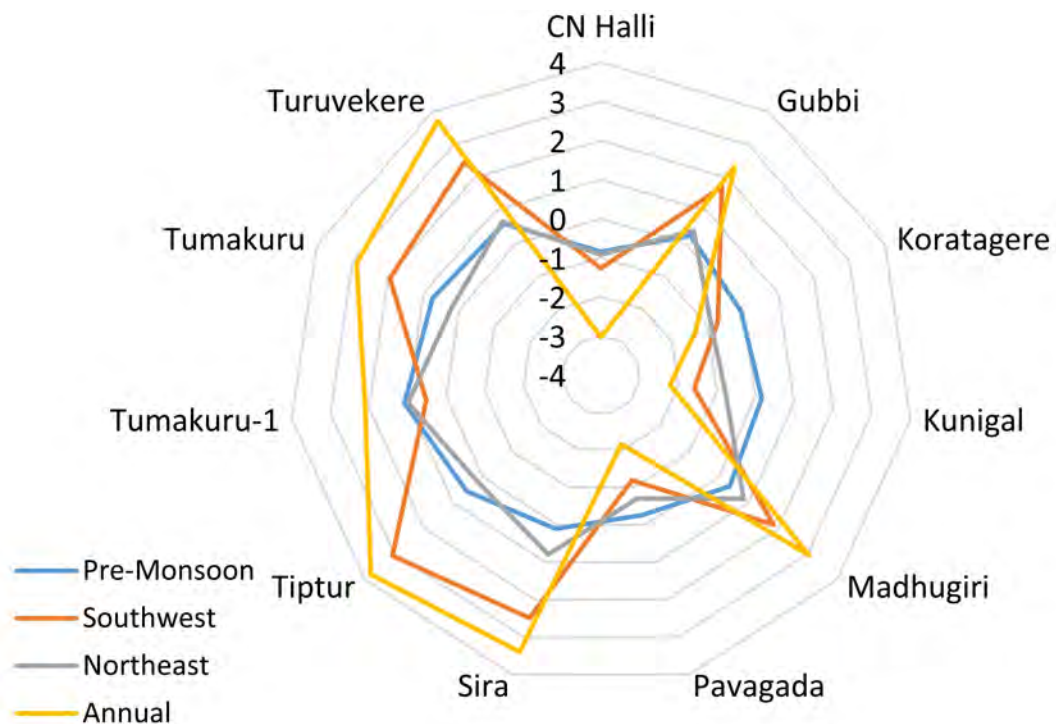


**Figure 21:** Trend comparison of the seasonal and annual ITA

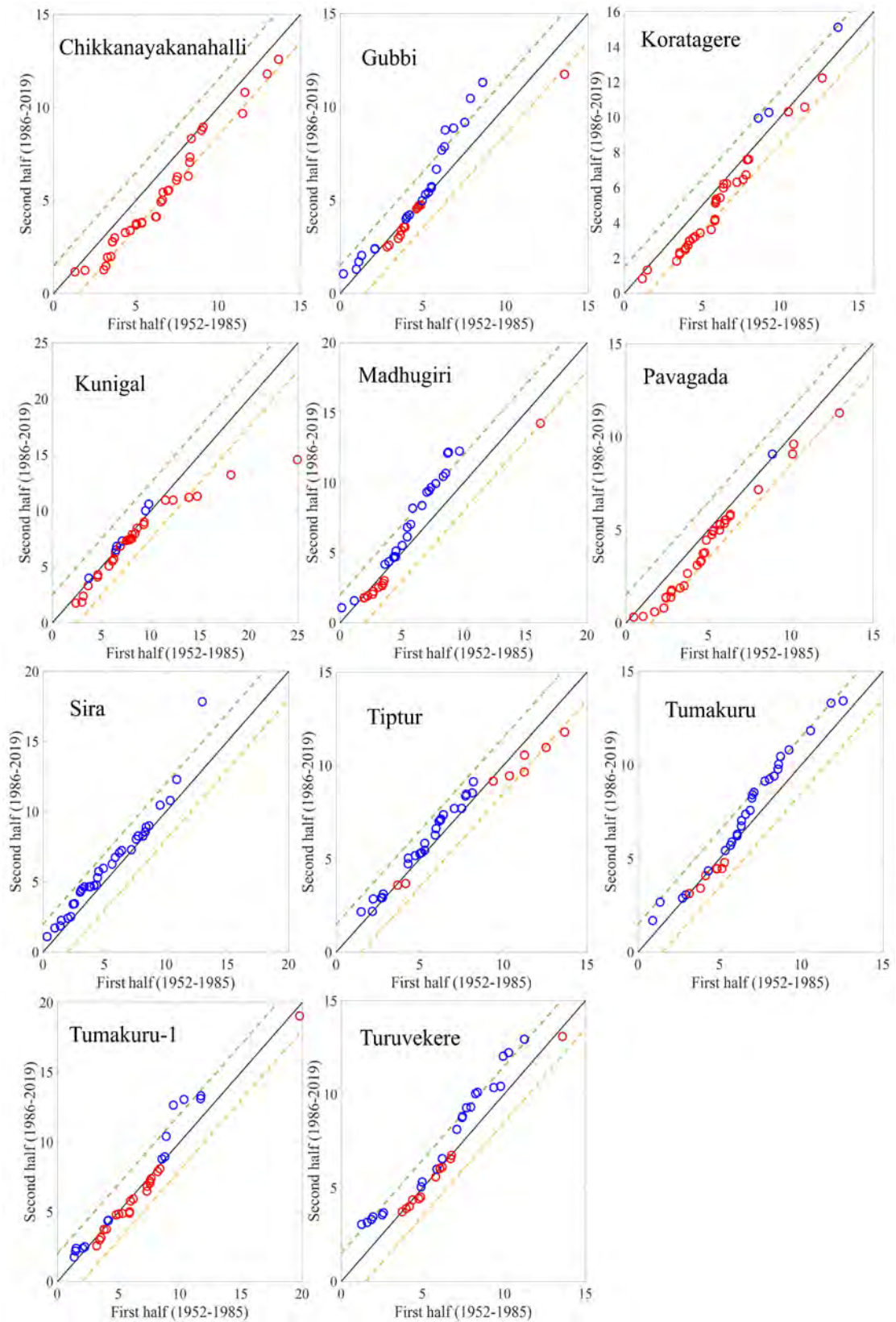


**Figure 22:** Graphical representation of NE monsoon ITA

4.3.4. Annual

Figure 18 illustrates the highest decreasing (-0.81) and increasing (4.97) magnitude (mm/year) at CN Halli and Tiptur stations respectively.

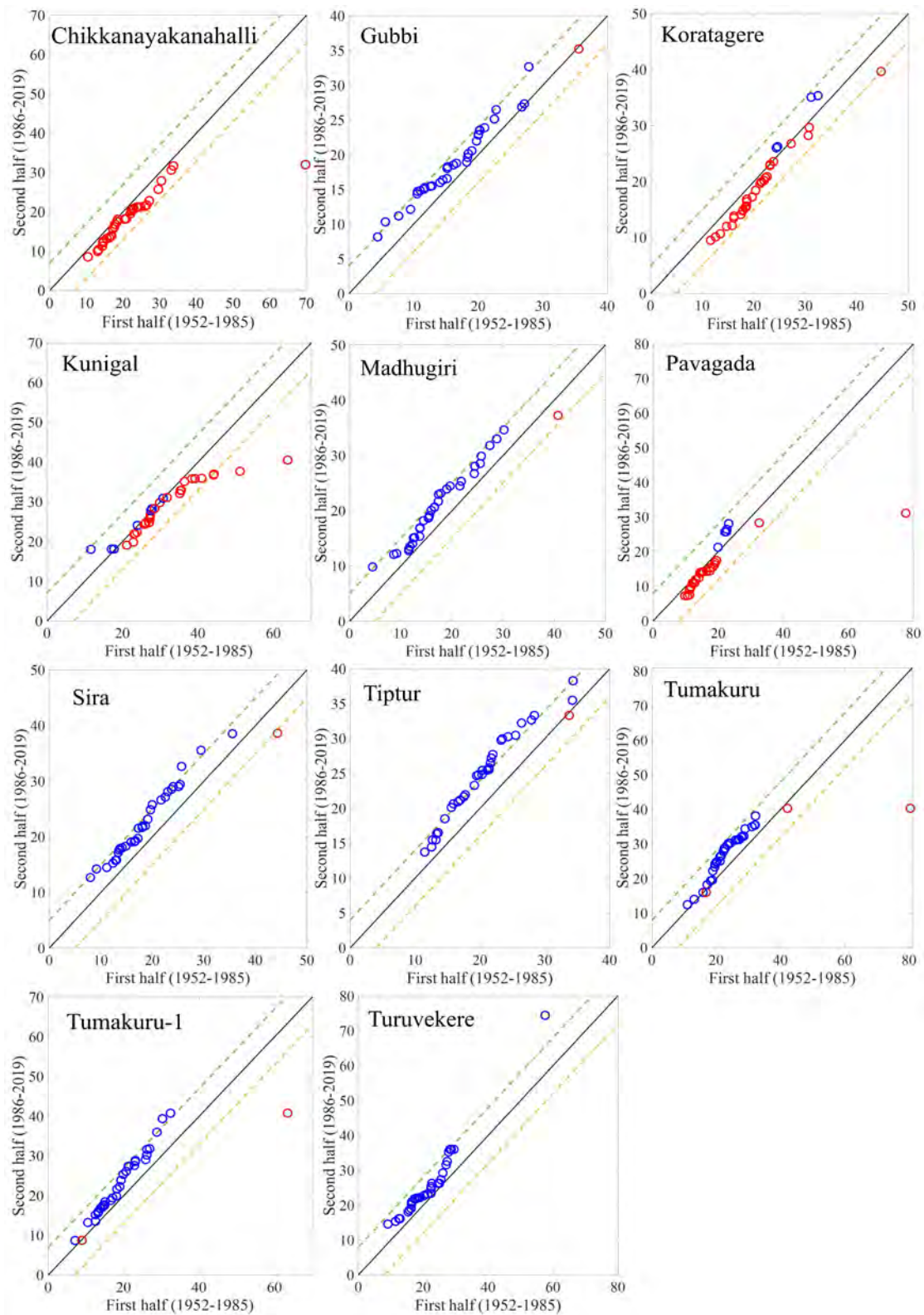


**Figure 23:** Graphical representation of annual ITA

Table 10 represents the annual statistical summary of Sen's slope, MK, ITA, and p-value for eleven grid stations, where six grid stations reported an increasing trend while five stations showed a decreasing trend in p-value. The Z statistics and ITA values of Tiptur station have recorded a maximum increasing trend with 3.55 mm/year and 3.80 mm/year respectively, showing a significant increase in the annual rainfall trend, which justifies the influences of geographical and topographical conditions such as maximum elevation compared to the other stations (Figure 19). Figure 23 highlights the annual monotonic or non-monotonic trend of ITA result, where CN Halli has only shown the negative, whereas Tiptur recorded a positive trend. The overall ITA statistics of eleven grid stations in the Tumakuru district including all three seasons as well as annual time series trends are shown in the radar chart (Figure 21), which specifies CN Halli, Koratagere, and Pavagada with negative trend patterns, while Kunigal station has reported diminishing trend except in the pre-monsoon season. The rest of the stations have shown an increasing trend over the season and annual time scale.

**Table 10:** Summary of the statistical test result for Annual rainfall from 1952-2019

Stations	Sen's Slope	p-value	Z Statistics	ITA Slope	ITA Trend
CN Halli	-0.81	0.564	-0.58	-3.03	↓
Gubbi	3.15	0.007	2.69	2.35	↑
Koratagere	-0.36	0.779	-0.28	-1.34	↓
Kunigal	-0.06	0.966	-0.04	-2.21	↓
Madhugiri	2.83	0.032	2.14	3.05	↑
Pavagada	-0.20	0.832	-0.21	-2.15	↓
Sira	2.70	0.034	2.12	3.39	↑
Tiptur	4.97	0.000	3.55	3.80	↑
Tumakuru	3.98	0.007	2.72	2.10	↑
Tumakuru-1	2.46	0.117	1.57	2.88	↑
Turuvekere	3.21	0.014	2.46	3.73	↑

#### 4.3.5. Modified Mann Kendall test

MMK test was performed on the rainfall dataset at a chosen significance level in this research of 0.05. This leaves us with positive z values indicating an increasing trend while values greater than 1.96 indicate a significant increase and at the same time, negative values indicate a decreasing trend with a z value less than -1.96 showing a significant decrease in trend. The trend is defined at different time scales based on the z value for all the stations. In the pre-monsoon season, stations such as Madhugiri, Tiptur, Tumakuru, and Tumakuru-1 showed a significant increase in the trend with values of 2.02, 3.3, 3.33, and 3.72 respectively while the rest of the stations showed an increasing trend (Table 11). The only exception is Chikkanayakanahalli having a decreasing trend at -0.37. For the southwest monsoon, only an increasing trend is noted for all the stations with Gubbi, Sira,

Tiptur, Tumakuru-1, and Turuvekere holding a significant increasing trend with z values of 2.37, 2.05, 3.17, 2.2, and 3.64 respectively.

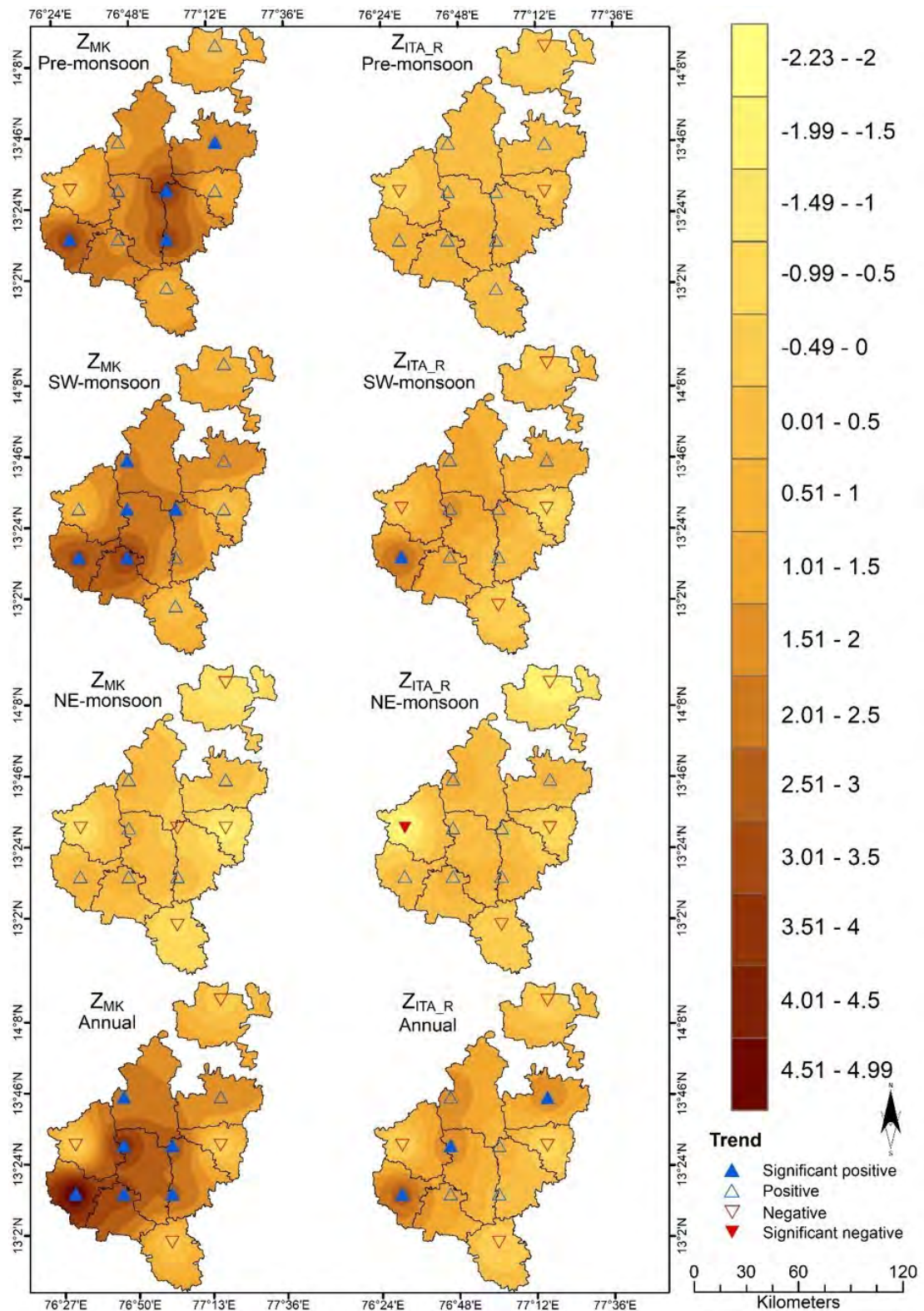


**Figure 24:** Spatial variability of MMK and ITA with trend indicators

**Table 11:** Z and slope value of MMK and ITA\_R

Station	Season	MMK				ITA	
		Z	p	Tau	Sen Slope	ITA Slope	Z ITA_R
<i>CN Halli</i>	Pre-monsoon	-0.37	0.71	-0.04	-0.01	-0.027	-0.72
	SW Monsoon	0.4	0.69	0.04	0.01	-0.042	-0.27
	NE Monsoon	-1.33	0.18	-0.11	-0.03	-0.035	-2.23
	Annual	-0.62	0.54	-0.06	-0.03	-0.104	-0.58
<i>Gubbi</i>	Pre-monsoon	1.71	0.09	0.12	0.01	0.008	0.51
	SW Monsoon	2.37	0.02	0.2	0.07	0.056	1.76
	NE Monsoon	0.88	0.38	0.06	0.01	0.012	0.41
	Annual	3.85	0	0.22	0.1	0.076	2.07
<i>Koratagere</i>	Pre-monsoon	0.87	0.39	0.08	0.01	-0.001	-0.11
	SW Monsoon	0.09	0.93	0.01	0	-0.024	-1.11
	NE Monsoon	-1.78	0.07	-0.15	-0.03	-0.022	-0.93
	Annual	-0.43	0.67	-0.04	-0.02	-0.047	-0.86
<i>Kunigal</i>	Pre-monsoon	0.85	0.39	0.07	0.01	0.006	0.21
	SW Monsoon	0.03	0.98	0	0	-0.052	-0.52
	NE Monsoon	-1.12	0.26	-0.1	-0.02	-0.027	-0.46
	Annual	-0.2	0.84	-0.02	-0.01	-0.074	-0.52
<i>Madhugiri</i>	Pre-monsoon	2.02	0.04	0.15	0.02	0.012	0.43
	SW Monsoon	1.87	0.06	0.18	0.05	0.06	1.06
	NE Monsoon	0.47	0.64	0.04	0.01	0.024	0.62
	Annual	1.95	0.05	0.16	0.09	0.096	1.98
<i>Pavagada</i>	Pre-monsoon	0.28	0.78	0.02	0	-0.008	-0.37
	SW Monsoon	0.61	0.54	0.06	0.02	-0.039	-0.24
	NE Monsoon	-1.45	0.15	-0.11	-0.02	-0.024	-1.91
	Annual	-0.21	0.84	-0.02	-0.01	-0.071	-0.3
<i>Sira</i>	Pre-monsoon	1.39	0.17	0.12	0.02	0.004	0.05
	SW Monsoon	2.05	0.04	0.2	0.07	0.081	1.47
	NE Monsoon	0.78	0.44	0.07	0.02	0.026	1.1
	Annual	2.12	0.03	0.18	0.09	0.111	1.9
<i>Tiptur</i>	Pre-monsoon	3.3	0	0.2	0.02	0.019	0.89
	SW Monsoon	3.17	0	0.3	0.11	0.1	2.63
	NE Monsoon	0.78	0.44	0.07	0.01	0.005	0.23
	Annual	4.99	0	0.29	0.16	0.123	2.81
<i>Tumakuru</i>	Pre-monsoon	3.33	0	0.28	0.04	0.036	0.82
	SW Monsoon	1.71	0.09	0.16	0.06	0.018	0.11
	NE Monsoon	0.4	0.69	0.03	0.01	0.018	0.86
	Annual	2.62	0.01	0.23	0.13	0.072	0.31
<i>Tumakuru-1</i>	Pre-monsoon	3.72	0	0.22	0.03	0.025	0.46
	SW Monsoon	2.2	0.03	0.15	0.06	0.063	1.3
	NE Monsoon	-0.37	0.71	-0.02	0	0.005	0.17
	Annual	2.84	0	0.14	0.08	0.093	0.63
<i>Turuvekere</i>	Pre-monsoon	1.91	0.06	0.16	0.03	0.02	0.91
	SW Monsoon	3.64	0	0.2	0.07	0.081	1.01
	NE Monsoon	0.84	0.4	0.07	0.02	0.022	0.89
	Annual	3.22	0	0.2	0.11	0.122	1.48

In the northeast monsoon, we observe that there is a lack of significant increase or significant decrease in the rainfall trend. Chikkanayakanahalli, Koratagere, Kunigal, Pavagada, and Tumakuru-1 displayed a negative trend and rest of the stations of Gubbi, Madhugiri, Sira, Tiptur, Tumakuru, and Turuvekere had a positive trend. At the annual timescale, Madhugiri shows an increasing trend while Gubbi, Sira, Tiptur, Tumakuru, Tumakuru-1, and Turuvekere witness a significant increase with z values of 3.85, 2.12, 4.99, 2.62, 2.84, and 3.22 respectively. The rest of the stations recorded a negative trend on the annual scale. From Figure 24, it is evident that in all the timescales, Chikkanayakanahalli, Koratagere, Kunigal, and Pavagada have low values for z but not to the extent of any significance. Mostly the central and western part of the area has higher values for z in all the timescales. A p-value less than 0.05 indicates a monotonic trend which is seen majorly in the annual timescale while a value greater than 0.05 indicates a non-monotonic trend. A positive or negative Tau similar to Sen's slope is seen in the result.

#### 4.3.6. Innovative trend analysis with type-I error removed

ITA was conducted at a confidence level of 95% for the study region and the trend is shown as increasing or decreasing for positive and negative z values respectively. The significance of the trend is defined for values beyond  $\pm 1.96$ . The trend is described on the ITA z value for the 11 grid stations at the annual and seasonal timescale. In the pre-monsoon season, Chikkanayakanahalli, Koratagere, and Pavagada show decreasing trend while all other stations showed an increasing trend (Figure 17). Tiptur displayed a significant increase in the trend with a z value of 2.63 at the southwest monsoon scale (Figure 20). All the stations experienced an increase in the trend except for Chikkanayakanahalli, Koratagere, Pavagada, and Kunigal which have a decrease in the trend. For the northeast monsoon, Chikkanayakanahalli only showed a significant decreasing trend with a -2.23 z value while Pavagada, Koratagere, and Kunigal had a decreasing trend (Figure 22). The remaining stations portrayed an increasing trend. Tiptur, Gubbi, and Madhugiri showed a significant increasing trend with values of 2.81, 2.07, and 1.98 respectively defined for the annual rainfall (Figure 23). Chikkanayakanahalli, Koratagere, Pavagada, and Kunigal had a decreasing trend and the rest showed an increasing trend (Table 11). There is consistency in the spatial distribution of the trend throughout all the timescales where the central and southwestern parts have increasing trends while the rest of the region mostly experiences a decreasing trend. Chikkanayakanahalli and Sira have a monotonic decreasing and increasing trend respectively in all the timescales. Kunigal has a non-monotonic trend throughout with an increase in pre-monsoon while the rest of the seasons have a decrease in trend. Pavagada has a consistent decreasing trend where it is monotonic only in the northeast monsoon. Koratagere displayed a non-monotonic decrease.

#### 4.4. Discussion and Conclusion

The present research has analysed the long-term rainfall trend pattern from 1952 to 2019 by implementing the Innovative Trend Analysis and Mann-Kendall test methods. The seasonal and annual time series rainfall trend has been computed using ITA for eleven grid stations across the Tumakuru district by categorising long-term time series rainfall into two sub-series as first (1952-1985) and the second half (1986-2019). The well-known traditional method such as MK and SS was also utilized to check the consequences of the ITA in the long-term rainfall trend, where each method has projected different results. The annual rainfall pattern governs the agrometeorology of any region, and any unpredicted changes in the rainfall or any extreme dynamic fluctuation will impact the socio-economic activities. Certainly, in the semiarid regions, where major crop cultivation is characterised by rainfed farming, changes in the rainfall trend will cause the rainfed crops to decimate, which directly affects the crop yield. The ITA test result shows that 63% of stations observed a significant positive trend in the annual rainfall, such as Gubbi, Madhugiri, Sira, Tiptur, Tumakuru, and Turuvekere. Though, the Tumakuru-1 station shows a significant upward trend according to the ITA result, the MK test shows a non-significant trend. Nevertheless, a similar opposite trend in the annual rainfall showed a significant decreasing trend in the ITA for stations such as CN Halli, Kunigal, and Pavagada. MK and Sen's slope methods prominently detected a non-significant diminishing trend in these stations. The long-term annual rainfall trend indicates the advantages of ITA over the MK test.

At the seasonal level, a significant increasing trend was observed in the southwest monsoon season for six stations (54%), while pre-monsoon and northeast monsoon revealed a non-significant increasing trend for eight and seven stations respectively. Maximum rainfall in southwest monsoon showed an increasing rainfall pattern at all stations as well as the lowest rainfall in pre-monsoon and northeast season displayed the negative trend at some of the stations, where it influenced the agriculture and meteorological drought in the study area. The present research on ITA over MK method reveals that ITA is reliable for accurate rainfall trend identification and it has the capability for finding the hidden variation in rainfall. Similarly, it gives a visual-graphical representation of upward and downward trends which assists with extreme flood and drought conditions. Henceforth, this study on precise rainfall trend observation is informative and advantageous for administrators and concerned authorities who are responsible to develop and implement the policy for the affected circumstances of climate change. The potential drivers of the achieved variation in seasonal as well as annual time series rainfall in the district are climatic change and urbanization which needs more



futuristic research and exploration.

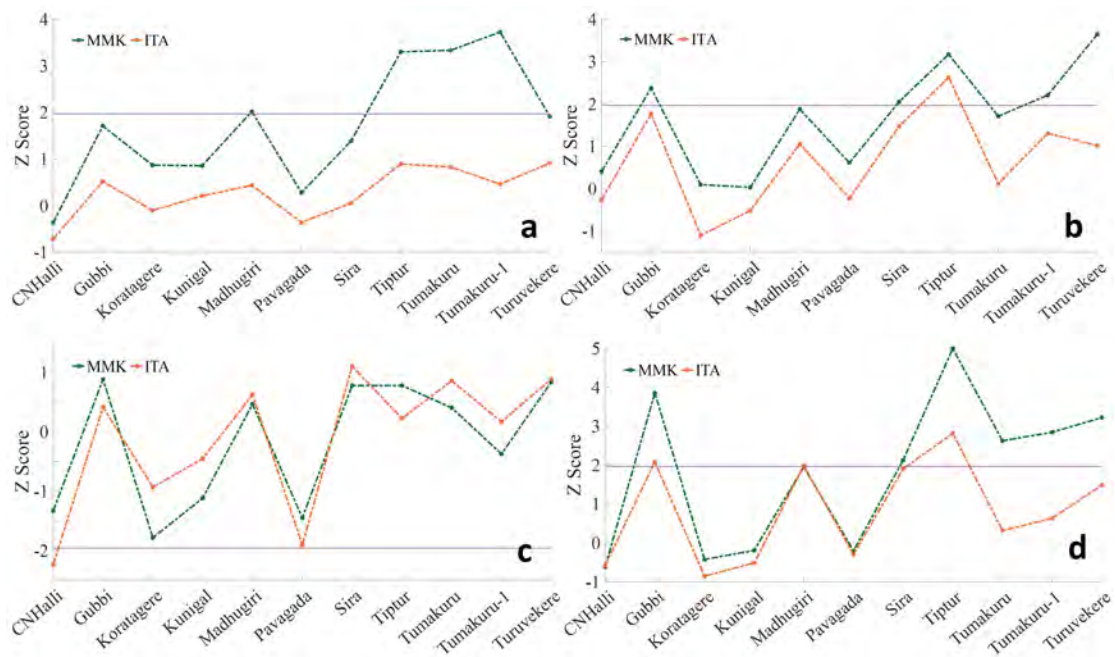


**Figure 25:** Comparison of Z value of MMK and ITA\_R with significance threshold

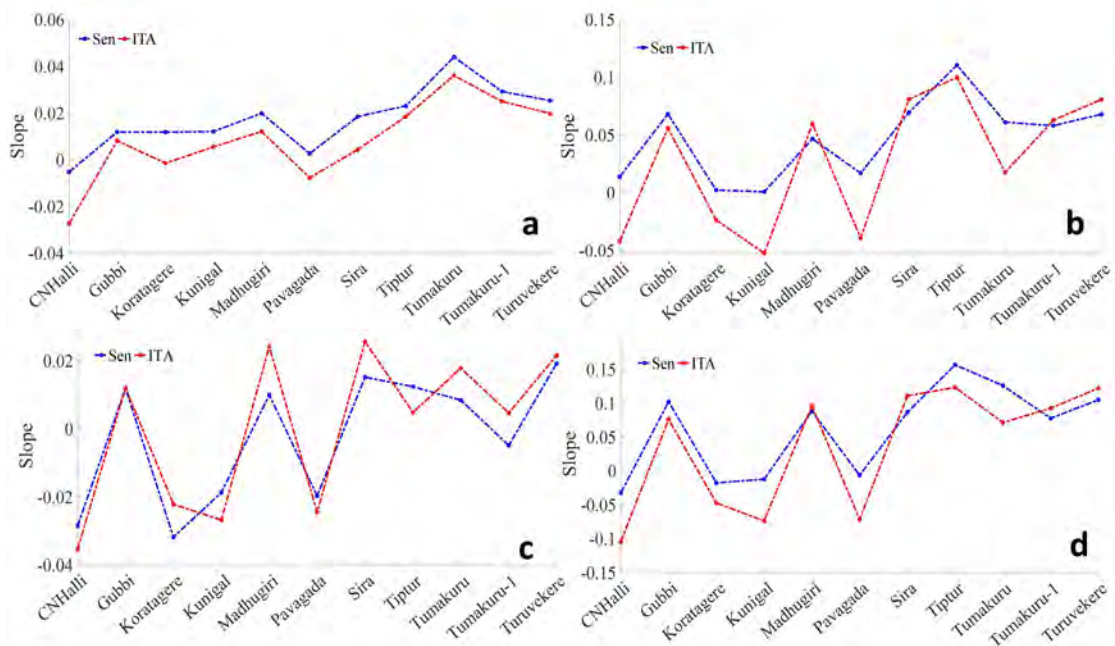


**Figure 26:** Comparison of MMK Sen slope and ITA\_R slope

MMK result showed a greater occurrence of a significantly increasing trend in comparison to the ITA result in both annual and seasonal timescales. Tiptur and Pavagada stations have the lowest and the highest values for variance, standard deviation, skewness, and kurtosis. The plot of the z score for MMK and ITA shows a greater correlation wherein the station wise fluctuation is consistent. Pre-monsoon, southwest monsoon, and Annual timescale have values exceeding the threshold of

positive significance.

Northeast monsoon has a significant decreasing value of the threshold and in this season we see the best correlation of both the MMK and ITA values. The annual value of Z also agrees well for all the stations. Although pre-monsoon and southwest monsoon follow a similar fluctuation for each station, there is a difference in the z value which seems to be consistency to an extent (Figure 25). The plot of the slope shows a similar result with the exception of the southwest monsoon (Figure 26). There is a larger gap between the two slopes of Kunigal and Pavagada seen. The trend of rainfall is similar when we compare both the MMK and ITA result for all the stations. In both cases, for all the seasons, Tiptur, Turuvekere, and Gubbi tend to show higher z values while Chikkanayakanahalli, Koratagere, and Pavagada hold very low values for z in comparison to other stations.

## 5. Change Point Detection and Rainfall Forecast

### 5.1. Introduction

Climate change threatens the basic components of survival such as drinking water, clean air, food availability, and shelter while at the same time can destroy a decade worth of progress achieved by mankind. The precipitation pattern of the Indian sub-continent is subjected to the highly seasonal Indian monsoon which makes up for almost 70-90% of the total annual rainfall received<sup>111</sup>. The economy of the country stands on a balance mainly dependent on the rain-fed agricultural outcome which is subjected to extreme fluctuations due to the unreliable pattern of the rainfall causing a major disturbance in the socio-economic condition of the country. With the increase in the frequency of extreme weather events as a direct impact of climate change, there is a growing concern over the anthropogenic factors contributing to it. One of the major components of the Earth's climate system is the hydrological cycle and any fluctuation will result in a disturbance in the water resources, and food security and induce events of drought and floods<sup>125</sup>. This further puts into focus the need to devise better prediction models for better monitoring of the rainfall pattern. It is important to have a complete grasp on the mechanism of the rainfall process as it forms a key factor in addressing the difficulties posed by the drastic modification in the spatio-temporal pattern of rainfall<sup>126</sup>. The Sixth Assessment Report of IPCC strongly suggests that the temperature rise will increase the chances of drought conditions in Central, West, and South Asia, and floods in monsoon regions of South Asia. There is a high probability of heat waves across Asia which could mean a 5-20% increment in the drought condition in the following decades as a result of global warming. Asia is prone to climate change induced diseases from events such as heatwaves, floods, drought, and others which in turn will hurt food prices and availability<sup>127</sup>. Over the past decade, there is a greater focus on trend analysis in the field of climatology and hydrology<sup>128</sup>. Evolving technologies have allowed us to access both satellite data and ground based data for the study of rainfall anomalies<sup>129</sup>. Methods of non-parametrical statistical techniques like MK test and Sen's Innovative trend analysis were used for trend analysis and machine learning using ANN-Multilayer Perceptron in forecasting was mainly employed. Ref.<sup>126</sup> addressed the concern of the implication of climate on rainfall patterns in northeastern Ghana. The trend and forecasting were achieved by utilizing ARIMA and simple seasonal exponential smoothing models. Ref.<sup>130</sup> analyzed the daily rainfall data in Ningxia, China to arrive at the seasonal and annual precipitation trend using the ITA method.

## 5.2. Methodology

**Change Point Detection:** The abrupt change in the precipitation time series data is detected using the Pettitt test, SNHT, test, and Buishand test.

### 5.2.1. Pettitt Test

The Pettitt test is a popular non-parametric method for change detection in the mean of the rainfall time series dataset<sup>131</sup>. The method is effective when it comes to pointing out the change in hydro-climatological data series.

$$U_{t,m} = \sum_{i=1}^m \sum_{j=t+1}^t \text{sgn}(A_i - A_j) \quad (33)$$

Where  $m$  is the years in which shift takes place, and  $t$  represents the length of the series, the index of the Pettitt test is given by  $U_{t,m}$ . The two samples of Mann-Whitney statistics are defined as  $a_1 \dots a_r$ , and  $a_{r+1} \dots a_n$  from the rainfall series data, and the  $\text{sgn}$  is defined as

$$\text{sgn}(A_i - A_j) = \begin{cases} 1 & \text{if}(A_i - A_j) > 1 \\ 0 & \text{if}(A_i - A_j) = 0 \\ -1 & \text{if}(A_i - A_j) < 1 \end{cases} \quad (34)$$

Two statistics are calculated for finding the time at which the greatest absolute value of  $U$  is present.

$$Z_T = \text{Max}_{1 \leq t \leq m} |U_{t,m}| \quad (35)$$

$$P = 1 - \exp\left(\frac{-6Z_T^2}{K^2 + K^3}\right) \quad (36)$$

### 5.2.2. Standard Normal Homogeneity Test (SNHT)

The SNHT is applied for the detection of point of change in a time series data such as rainfall dataset. Where the sudden shift is highlighted. The test is fulfilled by the formula given below.

$$H_s = \text{max} H_n, 1 \leq n \leq m \quad (37)$$

The change point is realized when  $H_s$  reaches the maximum value in the data series.  $H_m$  is calculated as

$$H_m = \bar{n}z_1 + (m - n)\bar{z}_1, n = 1, 2, \dots, m \quad (38)$$

Where

$$\bar{z}_1 = \frac{1}{n} \sum_{i=1}^m \frac{(M_i - \bar{M})}{s} \quad (39)$$

$\bar{n}$  represents the mean and the standard deviation is given by  $s$ .

### 5.2.3. Buishand Test

It is calculated based on the cumulative deviation from the mean or the adjusted biased sums and is hence also called as Cumulative Deviation test<sup>132</sup>. The following

$$B_0^* = 0 \text{ and } B_m^* = \sum_{t=1}^m R_t - R_{mean} \quad (40)$$

Where,  $m = 1, 2, \dots, n$

$$B_m^{**} = B_m^* / \sigma \quad (41)$$

$$S = \text{Max}|B_m^{**}| - \text{Min}|B_m^{**}|, 0 \leq m \leq n \quad (42)$$

The value of  $S/\sqrt{\bar{n}}$  is then calculated using the Buishand critical value.

## Rainfall Forecast

### 5.2.4. Autoregressive Integrated Moving Average (ARIMA)

The autoregressive model for hydrological data has been explored by many researchers<sup>133</sup>. ARIMA models help to determine the future rainfall based on the historical rainfall data<sup>134</sup>. The ARIMA  $(p, d, q)$  expression corresponding to the autoregressive (AR), integrated, and moving average (MA) corresponding to  $p$ ,  $d$ , and  $q$  is calculated as

$$y'_t = d + \phi_1 y'_{t-1} + \dots + \phi_p y'_{t-p} + \theta_1 \epsilon_{t-1} + \dots + \theta_q \epsilon_{t-q} + \epsilon_t \quad (43)$$

where,  $d$  is a constant,  $\phi_1 y'_{t-1} + \dots + \phi_p y'_{t-p}$  is the autoregressive term with  $\phi_1$  to  $\phi_p$  is the coefficient at the  $p$  order.  $\theta_1 \epsilon_{t-1} + \dots + \theta_q \epsilon_{t-q}$  is the moving average term with  $\theta_1$  to  $\theta_p$  being the coefficient in  $q$  order.  $\epsilon_t$  is the error term for background noise at time  $t$ .

## 5.3. Result

The rainfall data analysis was carried out for the Tumakuru district from 1952 to 2019. The result shows the analysis of the time series precipitation data and the trend for each of the 11 grid stations present in the study area. The change point for all the stations was analyzed and furthermore, the ARIMA model was run to depict the temporal and spatial changes in the precipitation from 2019 to 2029.

### 5.3.1. Rainfall time series analysis

The rainfall time series analysis discovered that the rainfall was nearly evenly distributed. With the elevation varying between 406 m to 1193 m, the topography of the region is nearly plain with very little undulation, there is not much variation in rainfall with elevation changes.

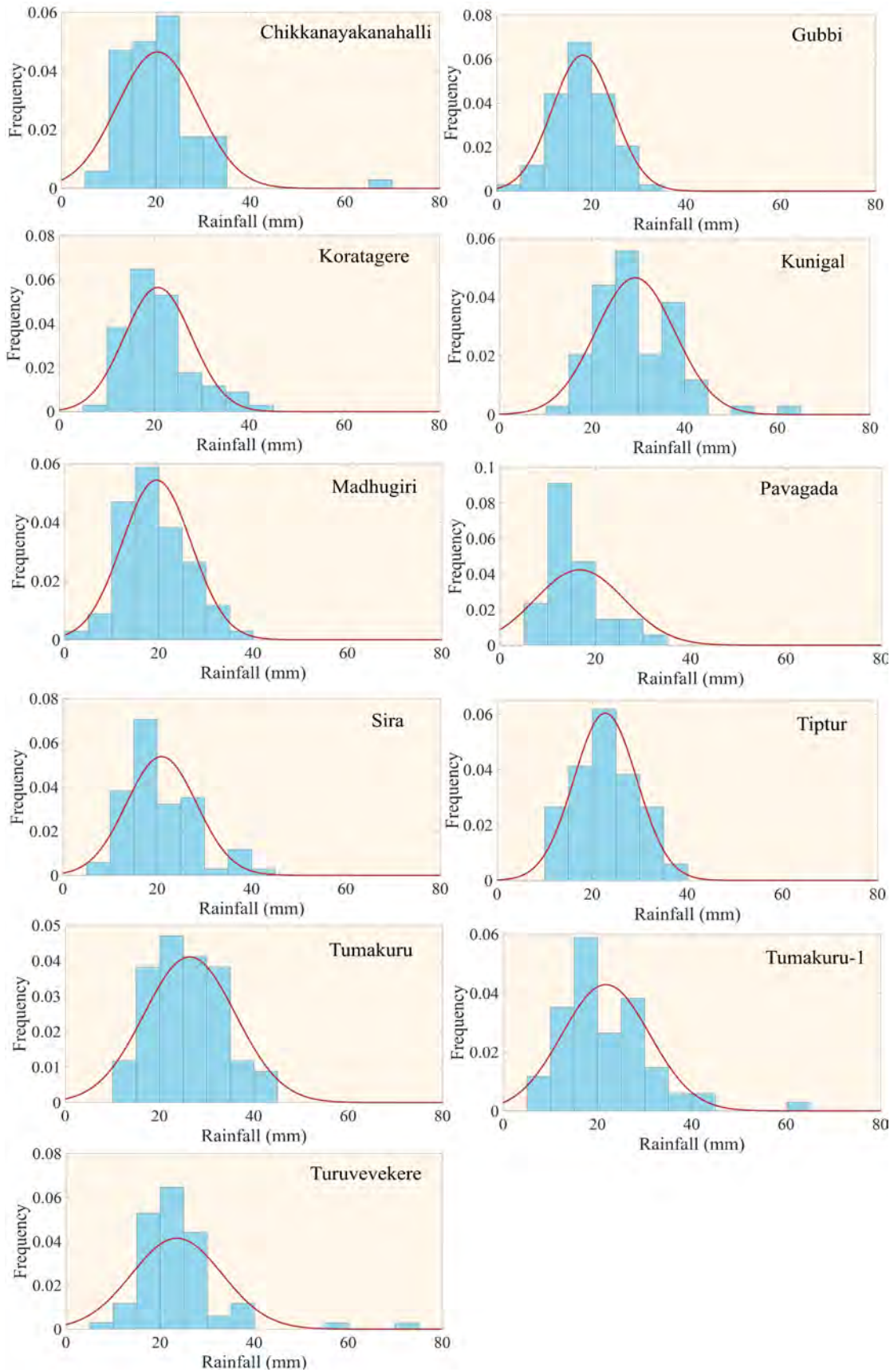


**Figure 27:** Histogram of time series analysis of rainfall with the normal distribution curve

The initial analysis of the data revealed that the region received an average of 658.9 mm of rainfall annually. The highest rainfall receiving station is Kunigal in the southern region with an average of 29.9 mm and the least is at Pavagada in the northern region with 16.7 mm. The standard deviation varies from 6.4 and 9.6. Skewness value is found between 0.28 and 0.55 with Pavagada and Tiptur holding the highest and the lowest value respectively. The kurtosis of the rainfall histogram ranges from -0.69 to 24.13. Tiptur is the only station with a negative kurtosis while most of the stations have values below 5. Chikkanayakanahalli, Pavagada, Tumakuru, and Turuvekere have higher values with 14.2, 24.13, 12.2, and 11.58 respectively. Figure 27 shows a histogram of the rainfall series at the different stations in the study area. The range of precipitation values is from 0 mm to 80 mm. While most of the stations hold values from 0 mm to about 40 mm as defined by the normal distribution curve, Kunigal, Tumakuru-1, and Turuvekere boast a higher value of rainfall. The normal curve for most of the stations has the mode at around 20 mm slightly varying for each station.

### 5.3.2. Homogeneity test

The homogeneity test was conducted for the precipitation data for the 11 grid stations at a confidence level of 95%. These tests are sensitive to shifts in the homogeneous series. The p-value for the tests varies for the stations with only Tiptur carrying a common value of 0.01. For the Turuvekere station, only Buishand shows a statistically significant value of 0.02 while Pettitt and SNHT showed 0.08 and 11 respectively (Table 12).

**Table 12:** Result of homogeneity test

Station	Annual								
	Pettitt			SNHT			Buishand		
	K	t	p	T0	t	p	Q	t	p
<i>CN Halli</i>	309	1984	0.5	4.14	1978	0.4	8.27	1978	0.2
<i>Gubbi</i>	485	1972	0	10.5	2006	0	10.6	2006	0.1
<i>Koratagere</i>	291	1988	0.7	4.16	2014	0.5	5.96	2007	0.6
<i>Kunigal</i>	304	1969	0.6	4.98	1970	0.3	8.32	1970	0.2
<i>Madhugiri</i>	486	1971	0	10.5	1971	0	12.3	1971	0
<i>Pavagada</i>	348	2009	0.3	3.77	2009	0.4	6.32	1964	0.5
<i>Sira</i>	385	1986	0.2	5.66	1997	0.3	9.24	1997	0.1
<i>Tiptur</i>	552	1973	0	12.6	1971	0	13.7	1973	0
<i>Tumakuru</i>	419	1978	0.1	3.46	2003	0.5	6.56	2003	0.5
<i>Tumakuru-1</i>	364	1987	0.2	3.13	1961	0.6	7.09	1987	0.4
<i>Turuvekere</i>	438	2003	0.1	10	2004	0.1	11	2003	0

**Pettitt test:** The Pettitt test reveals a normal distribution for all the stations except a few. The test has detected a change in the stations Gubbi, Madhugiri, and Tiptur. Gubbi showed a change in normal from 15 to 19.5 in the year 1972, Madhugiri shifted from 15.16 to 21.32 in 1971, and Tiptur shifted from 18.83 to 24.6 in 1973 (Figure 28).

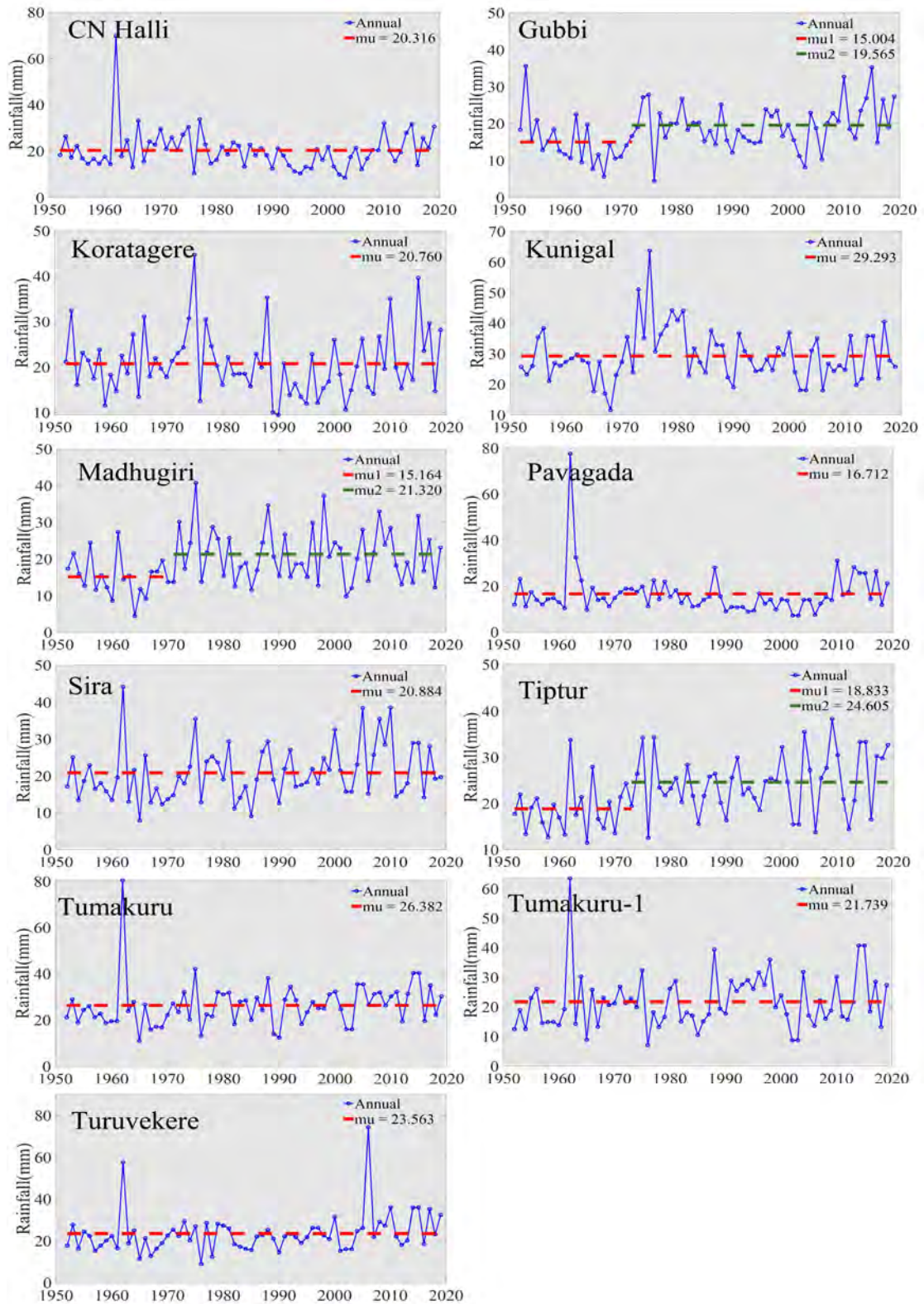


**Figure 28:** Change point in rainfall series from Pettitt test



**SNHT:** This test compares the observation from a certain station with the average of all the stations which are then standardized. SNHT revealed change at Gubbi in 2007 from 16.97 to 23.65, at Madhugiri in 1971 from 15.16 to 21.32, and at Tiptur from 24.49 to 18.52 in the year 1971 (Figure 29).

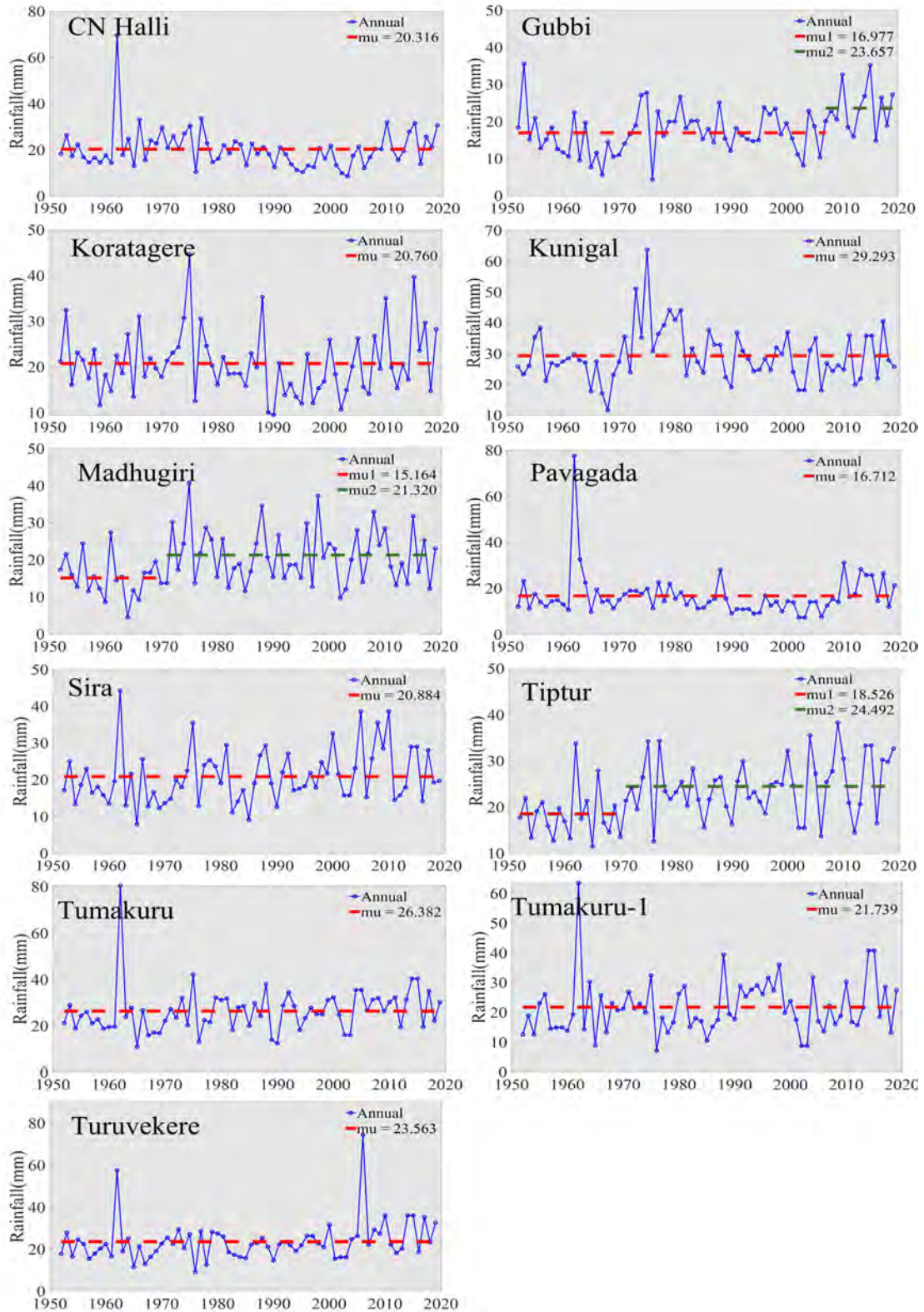


**Figure 29:** Change point in rainfall series from SNHT

**Buishand:** Buishand test has the advantage of operating over any type of distribution. Here the test disclosed a change point in three of the stations. Madhugiri changed from 15.16 to 21.32 in the year 1971, Tiptur in 1973 shifted from 18.83 to 24.605, and in 2003 from 21.54 to 30.13 in Turuvekere (Figure 30).

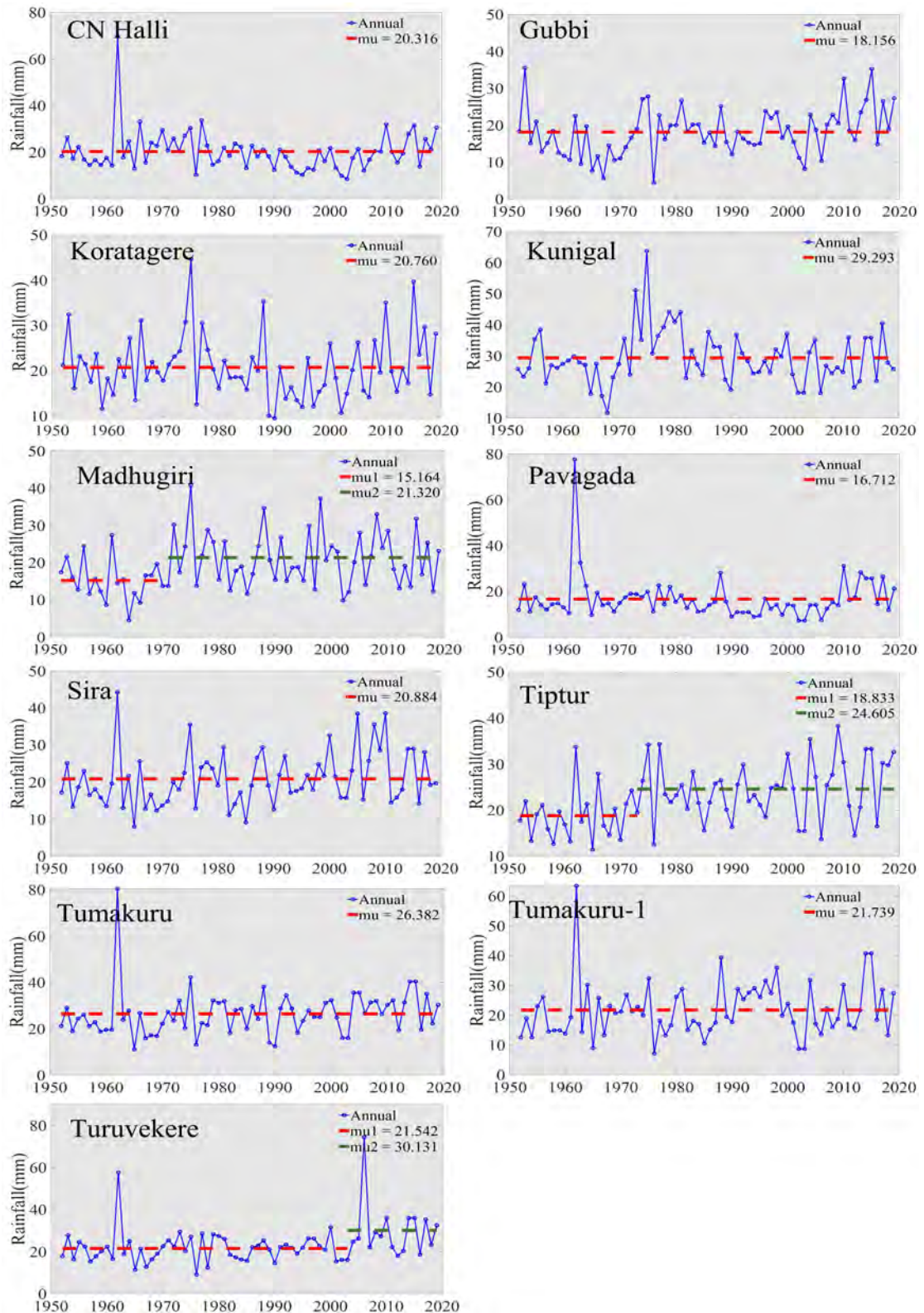


**Figure 30:** Change point in rainfall series from Buishand test

### 5.3.3. ARIMA

ARIMA model looks into how the rainfall could fluctuate in 10 years from 2019 to 2029. From the graph, it is apparent that all the stations see a downward trend as the ARIMA model shows decreasing value of rainfall amount through the years. The spatial distribution of ARIMA shows that along with the rainfall fluctuation, the ARIMA model also fluctuates correspondingly. The Pavagada station has the least rainfall both in 2025 and 2029 while the maximum is at Tiptur station (Figure 31). At Chikkanayakanahalli station, the RMSE is 11.85 and the error for the auto-regression parameter value of 0.847 is 0.064. Gubbi recorded an RMSE of 8.28 while the AR is 0.908 with an error of 0.049. The RMSE for Koratagere is 9.97 and AR is 0.894 with an error of 0.053. Kunigal recorded an RMSE of 10.44 while the AR was 0.936 with an error of 0.038. Madhugiri has an RMSE of 10.1 with AR being 0.874 and an error of 0.057. Pavagada witnessed an RMSE of 11.37 and an error of 0.071 for the AR of 0.802. Sira is known to have an RMSE of 10.18 with an AR value of 0.884 and an error of 0.053. Tiptur had an RMSE of 8.73 an AR of 0.932 and an error of 0.041. Tumakuru station showed an RMSE of 13.64 and AR of 0.872 with an error of 0.057. Tumakuru-1 displayed an RMSE of 12.6 and AR of 0.844 with a 0.063 error. Turuvekere showed an AR value of 0.855 and an error of 0.061 while the RMSE is 13.22 (Figure 32).

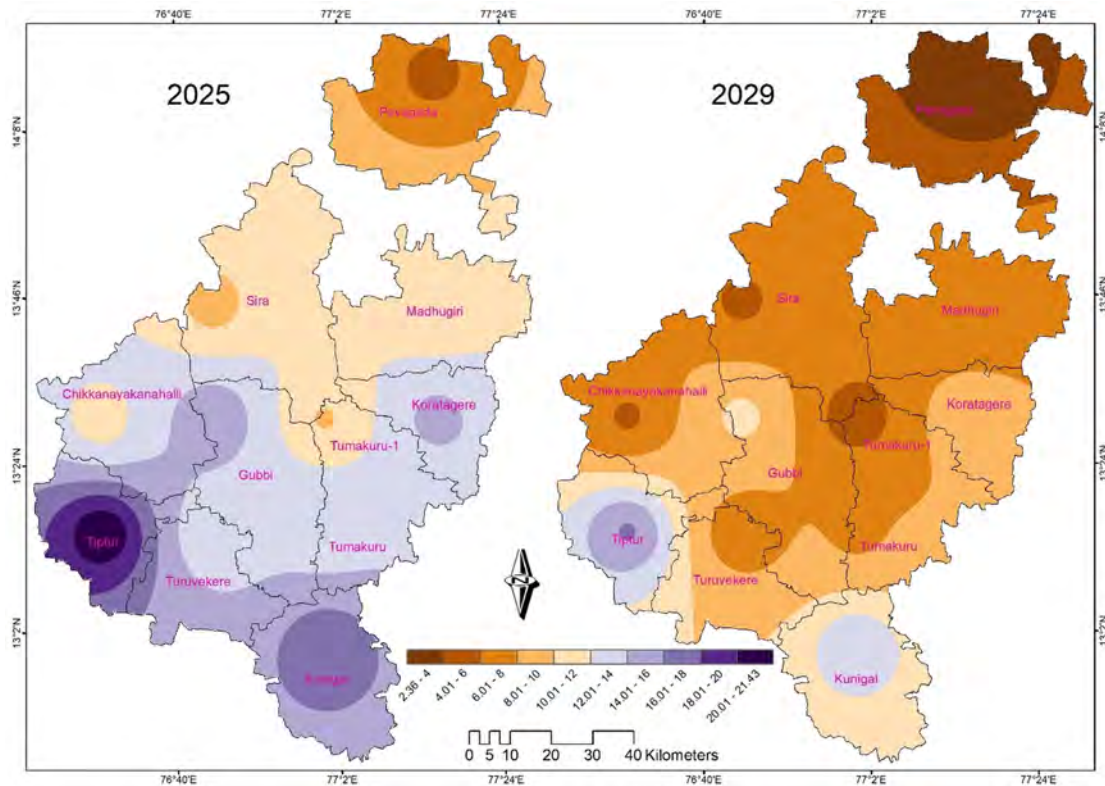


**Figure 31:** Prediction of spatial rainfall for 2025 and 2029

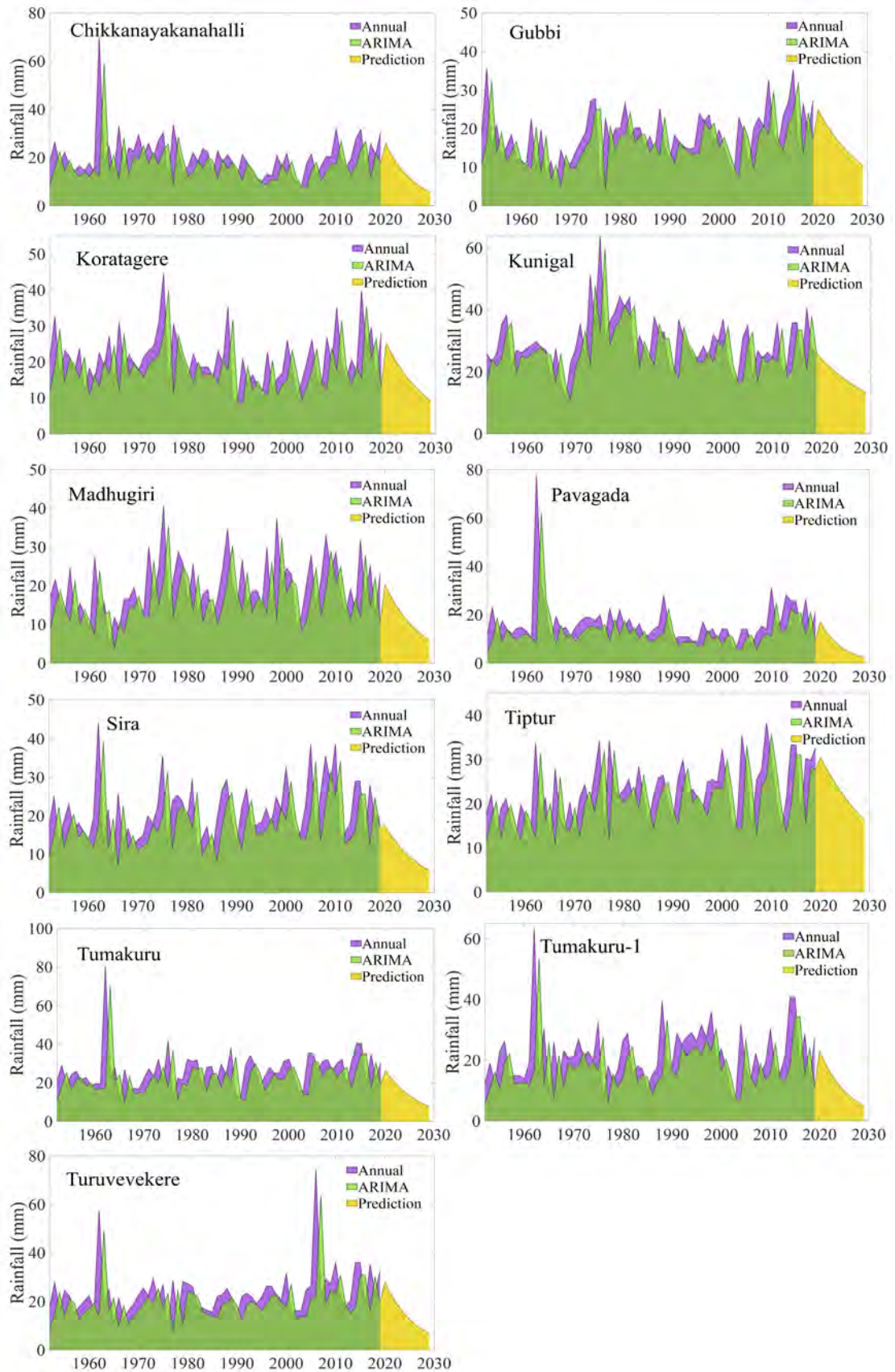


**Figure 32:** Actual rainfall, ARIMA, and predicted rainfall

#### **5.4. Discussion and Conclusion**

There is a greater similarity between the Pettitt and Buishand test wherein five of the stations show the same value of change point. Three stations have the same value for SNHT and Buishand test whereas only Kunigal and Madhugiri hold the same change year for all three tests. All three homogeneity tests detected change in the station Madhugiri in 1971. Although the tests showed a shift in Tiptur also, the year of change varied at 1973 for Pettitt and Buishand while SNHT showed a shift in 1971. Further, Pettitt and SNHT identified changes in Gubbi in the years 1972 and 2007 respectively. Turuvekere was noticed only in the Buishand test with change occurring in 2003. Despite the slight variation in the year of shift, Pettitt and SNHT showed a similar result with change in Gubbi, Madhugiri, and Tiptur. Buishand slightly varies from the other tests by detecting change points in Madhugiri, Tiptur, Tumakuru-1, and Turuvekere. The p-value was in favour of the alternative hypothesis of a lack of homogeneity for stations Gubbi, Madhugiri, and Tiptur for all three tests. The above statement sits well with the change point graphs obtained for the same stations.

ARIMA is utilized to plot the rainfall values for 10 years. The result shows that there is a consistent decrease in the rainfall values with progression in time. At the same time, the northern region of the study has low values while the south and the south western region have the highest values for rainfall. The central and eastern regions have intermediate values.

- Kunigal and Madhugiri are the only stations that show similar change points in all three tests. Pettitt and Buishand test is found to carry higher similarities.
- ARIMA model shows a declining trend of rainfall for all the stations with an average RMSE of 10.94. The average autoregressive value is 0.877.

## 6. Validation of IMD and TRMM data for drought analysis

### 6.1. Introduction

Climate change is continually adding pressure on the water system of the world drawing an even bigger focus on the study of the extreme events. Dealing with such disasters on a global scale is crucial not only for the sustenance of the planet but also for the socio-economic scenario of the world due to the extreme events that we are witnessing with increasing frequency. Over the past couple of decades, there is an acute shortage of drinking water as a direct result of the prolonged periods of abnormally dry weather. There is an acceleration in the rate of drying up of freshwater resources along with a downward trend in the precipitation amount resulting in drought. Drought is a complex phenomenon impacted by various natural and human factors and at the same time is very poorly understood. This draws our attention to the urgency in the need for evaluating and understanding the drought condition to escape from the trail of the havoc caused by drought. Quantifying the characteristic features of dry events is an important step in the study of drought. For this purpose, various drought indices are developed to analyze the magnitude, intensity, duration, and distribution of drought such as the Rainfall Anomaly Index (RAI)<sup>3</sup>, Standardized Precipitation Index (SPI)<sup>1</sup>, Modified China Z Index (MCZI)<sup>4</sup>, Palmer Drought Severity Index (PDSI)<sup>135</sup>, Decile Index (DI)<sup>5</sup>, Standardized Precipitation Evapotranspiration Index (SPEI)<sup>2</sup>, Percent of Normal Index (PN)<sup>6</sup> and Standardized Runoff Index (SRI)<sup>72</sup>.

Drought indices are a crucial tool that facilitates studying drought and also the decision-making process. The selection of suitable and accurate data is crucial not only for the study of rainfall irregularities but also to arrive at appropriate mitigation methods and prediction models to deal with the anomalies. The importance of meteorological parameters especially precipitation in climate, hydrological and agricultural studies is immense. In order to fulfill the requirements of various fields of research, different rainfall data products have been proved successful. Large scale data sets are used to study the precipitation extreme at different temporal and spatial scales<sup>136</sup>. To identify early warning signs of drought and develop a system for continuous monitoring in time and space, indices play a crucial role. Satellite data provide valuable information with better temporal resolution facilitating better monitoring but lacks long-term data availability. Many studies have emerged in recent years concerning the comparison of climate datasets. The comparative study of rainfall data from multiple data sources has been gaining popularity and a few are mentioned here. In the semi-arid region of Iran, rain gauge and TRMM rainfall data were used to compare the precipitation extremes by ref.<sup>137</sup>. It was concluded that a method to solve the issue could not be arrived at. Ref.<sup>138</sup> worked on how

applying bias correction methods to the TRMM data could enhance the dependability of the data and find wide application in the Himalayan region. Ref.<sup>139</sup> aimed at figuring out the possibility of using TRMM-3B42V6 and the point gauge data over the Ganga, Brahmaputra, and Meghna river basin in forecasting flood and predicting the changes in climate. Ref.<sup>140</sup> compared the reliability of the global satellite based rainfall datasets such as CHIRPS, SM2RAIN-ASCAT, and TRMM in comparison to ground based gauge rainfall (IMD) data in India. The result found that the TRMM product was the closest to the IMD in comparison while intensity based indices showed that TRMM and CHIRPS were close to IMD data. During the southwest monsoon over the Indian land mass, the study by ref.<sup>141</sup> compared the IMERG product with the IMD gridded data. The IMERG adequately reflected the gauge data for very light and very heavy rain but proved unsatisfactory for depicting extreme heavy rain events.

Ref.<sup>142</sup> assessed the GPM estimates over the Indian subcontinent where the study revealed that the performance of IMERG was better than TRMM even though both the products fell short of the ground based measurements. Monthly TRMM data has a better linear correlation with the rain gauge precipitation data over the daily TRMM dataset which show a poor description of the occurrence and accuracy of precipitation in Poyang Lake Basin, China<sup>143</sup>. Ref.<sup>144</sup> evaluated the gauge data along with the satellite rainfall product in the Congo basin and concluded that gauge data provide greater reliability to estimate rainfall. In comparison to the TRMM 3B42 and CMORPH, the former had greater compatibility with the rain gauge data than the latter in the Amazon region as analyzed by ref.<sup>145</sup>. The study carried out by ref.<sup>146</sup> in China brings to light the incapability of 3B42 product to capturing extreme wet events, all the while as its accuracy falls with rising intensity of rainfall. The correlation of TRMM-3B42V7 with other products as mentioned by ref.<sup>147</sup> was higher at monthly scale rather than weekly or daily time period in Ecuador and Peru region. Satellite products when infused with gauge correction shows a significant enhancement in the reliability of data by bringing down the bias in the prediction of hydrological parameters especially in the mountainous areas as analysed by ref.<sup>148</sup>. Ref.<sup>149</sup> deduced that between the rain gauge data and the 3B42 and 3B43, the correlation was better in the dry season while the level of statistical error was much better during the wet season over the Bali Island. In Thailand, the difference between the gauge and TRMM-3B42 and TRMM-3B43 were analyzed by ref.<sup>150</sup> resulting in the 3B43 having less bias than 3B42 concerning gauge data along with apparent seasonal and regional differences.

Tumakuru District in Karnataka being a semi-arid region is often prone to drought which in turn has caused the huge agricultural loss. Over the past decade, farmer

suicides have persisted in being the reason of major concern. One of the ways to turn the tables on the situation is to build a better prediction model along with devising mitigation methods. To fulfill this objective, 1) this study aims at validating ground and satellite-based rainfall products in the analysis of meteorological drought. 2) The rain gauge data from IMD along with TRMM-3B43 monthly precipitation data is utilized to derive various drought indices such as DI, PN, MCZI, and RAI. 3) In addition to this, statistical methods like correlation, t-test, and RMSE are employed to evaluate the variations in the output from both datasets.

## 6.2. Methodology

The flow of workings of this study follows in Figure 33 detailing the data, methods used, and the analysis. The range of drought/wet categories for the indices is mentioned in Table 13. Matlab, R Studio, and SPSS software were used to obtain the indices and plot the data.

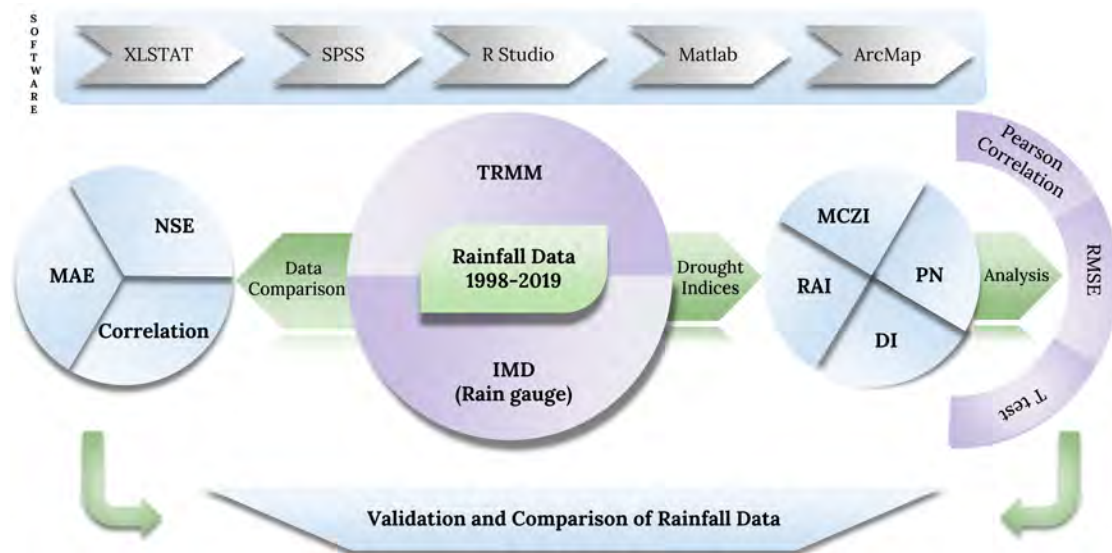


**Figure 33:** Methodology used in the study

### Error Calculation

#### 6.2.1. Mean Absolute Error

Mean absolute error is a way to express the error between the paired datasets indicating the same phenomenon which in this case is precipitation. The value of the MAE is an indication of the average difference between the two datasets when any instance of data is chosen. It portrays how far the data is going to be in comparison to the other.

#### 6.2.2. Nash Sutcliffe Efficiency coefficient

The Nash Sutcliffe model Efficiency coefficient particularly determines the predictive skill of the hydrological models. It assesses the relative magnitude of the ratio with



the denominator being measured data variance and the numerator being residual variance and is represented as normalized statistics.

### Drought Indices

#### 6.2.3. Rainfall Anomaly Index (RAI)

RAI defines a system to indicate the deficit or surplus of rainfall in the range of -4 to +4. The index helps recognize the magnitude of deviation in rainfall. It categorizes the positive and negative anomalies of the rainfall extremes<sup>3</sup>. For a positive anomaly when  $P > \bar{P}$ ,

$$RAI = 3 \left[ \frac{P - \bar{P}}{\bar{M} - \bar{P}} \right] \quad (44)$$

For a negative anomaly when  $P < \bar{P}$ ,

$$RAI = -3 \left[ \frac{P - \bar{P}}{\bar{X} - \bar{P}} \right] \quad (45)$$

The terms of the equations are defined as;  $P$  is the present monthly rainfall,  $\bar{P}$  shows the average of the historical monthly rainfall data,  $\bar{M}$  indicates the mean of 10 of the maximum monthly rainfall values and  $\bar{X}$  denotes the mean of 10 of the minimum monthly rainfall values.

#### 6.2.4. Modified China Z Index (MCZI)

Wilson-Hilferty cube root transformation forms the basis for the China Z index<sup>4</sup>. MCZI serves as a good alternative to SPI when mean precipitation follows the Pearson type III distribution. The China Z index follows the equation:

$$CZ_k = \frac{6}{C_s} \left( \frac{C_s}{2} \varphi_k + 1 \right)^{\frac{1}{3}} - \left( \frac{6}{C_s} \right) + \left( \frac{C_s}{6} \right) \quad (46)$$

$$C_s = \frac{\sum_{k=1}^n (x_k - \bar{x})^3}{n\sigma^3} \quad (47)$$

$$\varphi_k = \frac{x_k - \bar{x}}{\sigma} \quad (48)$$

Where,  $C_s$  represents the coefficient of skewness.  $\varphi_k$  is the value of the standardized variate which is also referred to as the  $Z$  score. The precipitation in the period  $k$  is  $x_k$  and standard deviation for the  $n$  number of months is  $\sigma$ . To compute MCZI the mean is replaced by the median value in the CZI equation.

#### 6.2.5. Percent of Normal Index (PN)

Percent of normal<sup>6</sup> is a simple method to indicate drought which shows the percentage of the precipitation that occurred, in comparison to the long-term mean rainfall. The index is obtained by multiplying 100 with the ratio of actual rainfall ( $P_i$ ) to the normal rainfall ( $\bar{P}$ ). ( $\bar{P}$ ) is typically calculated using long term rainfall data.

$$PN = \left( \frac{P_i}{\bar{P}} \right) .100 \quad (49)$$

### 6.2.6. Deciles Index (DI)

Deciles index is a method for analyzing meteorological drought. To attain the most accurate result, long-term precipitation data is required for the estimation of the index. For the available historical data set of rainfall, the decile index defines the ranking of precipitation at a particular time. The monthly rainfall data is rearranged from highest to the lowest rainfall which is divided into 10% parts termed deciles. The lowest and highest deciles represent the precipitation extremes indicating drought and flood respectively<sup>5</sup>. Deciles help provide useful knowledge about the deviation of the rainfall value from the normal.

**Table 13:** Dry and wet categories of the indices used<sup>3-6</sup>

Category	RAI	MCZI	PN	DI
Extreme wet	$\geq 4$	$\geq 2.0$	>115	9 to 10
Severe wet	2 to 4	1.5 to 1.99	110 to 115	8
Moderate wet	0 to 2	1.0 to 1.49	80 to 110	7
Near Normal	-	-0.99 to 0.99	70 to 80	5 to 6
Moderate dry	-2 to 0	-1.49 to -1.0	55 to 70	4
Severe dry	-4 to -2	-1.99 to -1.5	40 to 55	3
Extreme dry	$\leq -4$	$\leq -2.0$	<40	1 to 2

## Correlation Analysis

### 6.2.7. Root Mean Square Error (RMSE)

RMSE helps us arrive at an average magnitude of the error to assess the dependability of the data available.

$$RMSE = \sqrt{\frac{\sum_{i=1}^N (x_i - \hat{x}_i)^2}{N}} \quad (50)$$

### 6.2.8. t-Test

This is a statistical method to figure out if the average between the two sets of data results in a zero<sup>151</sup>. It is predominantly used to compare two sets of data by paring the observation in one data set to the corresponding one in the other data set.

$$t = \frac{\bar{X}_1 - \bar{X}_2}{s_p \sqrt{\frac{2}{n}}} \quad (51)$$

$$s_p = \sqrt{\frac{s_{X_1}^2 + s_{X_2}^2}{2}} \quad (52)$$

Where  $t$  is the statistical result.  $s_p$  is the standard deviation for  $n$  number of samples.

### 6.2.9. Pearson Correlation

Pearson correlation coefficient is calculated to draw a linear correlation between the rain gauge and the TRMM data. The value is calculated as a ratio of their covariance and the multiplicative result of standard deviations<sup>152</sup>.

$$r = \frac{\sum(x_i - \bar{x})(y_i - \bar{y})}{\sqrt{\sum(x_i - \bar{x})^2 \sum(y_i - \bar{y})^2}} \quad (53)$$

Where  $r$  is the correlation coefficient,  $x_i$  refers to the rain gauge values,  $\bar{x}$  denotes the mean of the rain gauge values.  $y_i$  is the TRMM values and  $\bar{y}$  is the mean of the TRMM values.

## 6.3. Result and discussion

TRMM and rain gauge although representing the same data tend to show variations in their values. Drought indices are chosen to know the deviations of one data set from the other. The study solely relies on precipitation data set and hence only meteorological drought is established from the results. The study region is mostly covered with plains and there are barely any variations in the topography. The fluctuation in data is assumed to be uniform throughout. The precipitation obtained from TRMM and ground based IMD rain gauge data are compared against each other to evaluate the scenario of error present between the datasets. To study the compatibility of the TRMM and the rain gauge data for drought analysis, statistical methods were employed. Pearson correlation coefficient draws a detailed correlation between the two datasets whereas the homogeneity is described by the two-sample t-test. RMSE is also calculated to denote the deviation of the rainfall values.

### 6.3.1. Mean Absolute Error

The average MAE for our datasets for the annual time period is about 1.86. The MAE is lower than 0.3 for December to March. April and November carry an error of about 1.19 and 1.64 respectively while the months from May to October are where we see a higher error. May to July carry an error of about 2.05 and September and October is about 4.2. The seasonal change is clearly visible with the MAE value but the spatial fluctuation is mostly uniform as seen in Figure 34.

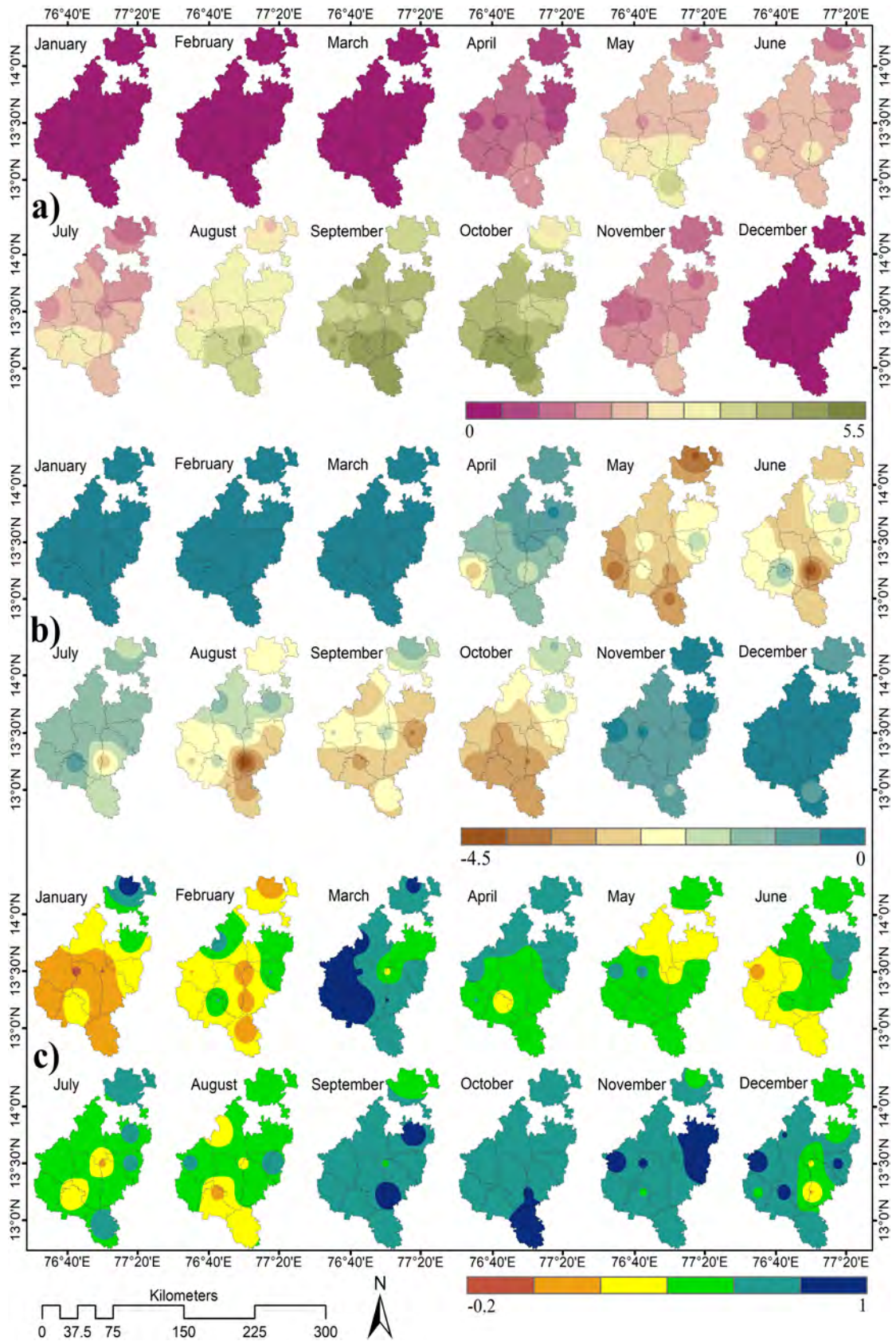


**Figure 34:** Spatial distribution of MAE(a), NSE(b), and Pearson Correlation(c)

### 6.3.2. Nash Sutcliffe Efficiency coefficient

The Nash Sutcliffe Efficiency coefficient is calculated for the IMD and TRMM precipitation datasets. It compares the plot of the IMD and TRMM datasets with the 1:1 line. An NSE of 1 says that both datasets are a perfect match. NSE of 0 represents that the plot is a good representation of the mean of the observed data and the negative value of NSE shows that the observed value (IMD) is a better fit than the measured value (TRMM). An average value of -1.41 was obtained for the entire duration of the study (Figure 34).

### 6.3.3. Pearson Correlation

It assumes a value in the range of -1 to +1. The absence of correlation is denoted by 0, and a completely positive and negative correlation is denoted by +1 and -1 respectively. A positive correlation implies that both variables fluctuate in the same direction, while a negative correlation implies that the variables fluctuate in the opposite direction. The average value of the Pearson correlation coefficient is 0.55 for the data from 1981 to 2019 (Figure 34). The range of the coefficient values in the study area ranges from -0.03 to 0.94. Maximum correlation is found in the months of September to December and March where the coefficient is greater than 0.7. In March, all the stations show a good correlation greater than 0.8 while Madhugiri and Tumakuru-1 correlate less than 0.4. The months from April to August show a correlation between 0.4 and 0.55. The least correlation is found in January and February with values of 0.25 and 0.33 respectively. Pavagada in January exhibits a very high correlation of 0.88 in contrast to all other stations in the same month. The only negative correlation is found in January at the Gubbi station with -0.03 while all other correlations are positive while Tumakuru-1 station shows no correlation.

### 6.3.4. Rainfall Anomaly Index

The Rainfall Anomaly Index is prominently used to assess the deviation of rainfall. The index has an average rmse of 4 with the error reaching a maximum of more than 10 in January while the lowest error is seen across June and July as shown in Figure 35. The t-test bears the value of mostly negative values showing some correlation, especially in January and February for all stations. The positive t-test result is seen predominantly in June and December. A positive correlation coefficient is seen in all the stations in March, September, October, November, and December. The least similarity is seen in January and February where the coefficient value is closer to zero (Figure 36). The index obtained for the rain gauge and TRMM data go well beyond the range of +4 and -4 for a good portion of data. While comparing the total number of months for the categories of the index, Tiptur station showed very good matching with a difference of not more than 2 months. At the same time for Kunigal, the same difference was up to 5 months. Figure 37 shows the month-wise variation in data

between TRMM and rain gauge from 1998 to 2019.

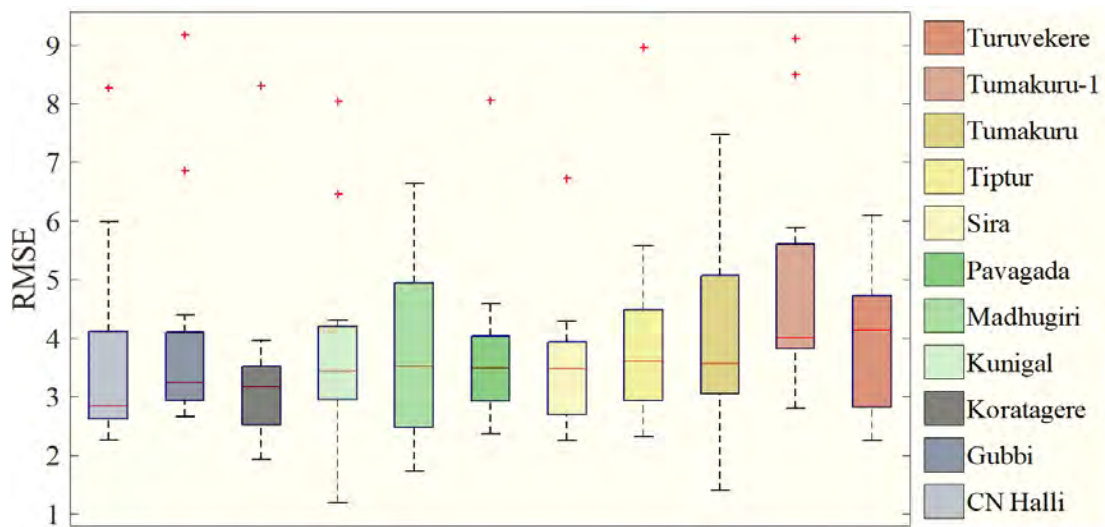


**Figure 35:** RMSE of 3B43 and rain gauge dataset for RAI from 1998 to 2019

Chikkanayakanahalli shows the maximum correlation of 30.68% on the whole while moderate, severe, and extreme dry events hold 3.41%, 28.41%, and 2.65% respectively. Gubbi shows a total of 27.65% similarity and 4.55%, 26.89%, and 3.03% for moderate, severe, and extreme droughts. Koratagere station has a 26.52% match while moderate, severe, and extreme dry events are at 5.30%, 23.48%, and 3.79% respectively. 22.73% harmony is defined for Kunigal station and moderate, severe, and extreme dry events show 4.17%, 22.73%, and 1.14% respectively. Madhugiri has an overall 30.30% of equivalence at the same time, moderate, severe, and extreme dry spells are at 5.30%, 27.65%, and 3.03% respectively. Pavagada has moderate, severe, and extreme dry events with a similarity of 3.41%, 24.62%, and 2.65% respectively with 23.11% being the total match. Sira with a total of 28.03% shows moderate, severe, and extreme spells at 4.55%, 27.65%, and 1.89% respectively. Tiptur has an overall 26.52% harmony while 5.3%, 25%, and 1.14% are the similarity for moderate, severe, and extreme droughts. Tumakuru has 27.27% in the entirety while moderate, severe, and extreme dry are defined with 7.2%, 23.48%, and 2.27% respectively. Tumakuru-1 hold a total of 28.79% commonality all the while with the moderate, severe, and extreme dry event being 6.82%, 22.73%, and 1.52% respectively. Turuvekere displays 26.89% for all categories with 5.30%, 24.62%, and 1.14% for moderate, severe, and extreme dry extremes respectively. The data concerning the detailed statistical analysis is attached in the supplementary material. The correlation of the datasets for wetness indicated by the index can be understood by looking at the stations individually. Kunigal shows a very low match for severe at 0.38% while extreme and moderate wet conditions are at 5.68% and 4.92% respectively. The extreme, severe, and moderate event of Tiptur

shows a similarity of 5.68%, 2.65%, and 1.89% respectively. It is necessary to talk about the disparity or the similarity expressed in the data to draw further analysis. For the RAI, with a range of -4 to +4, the result obtained fluctuates from -10 to +10, and a few scattered data beyond this range. The data results carry a fairly similar correlation as we see an average of 4 rmse throughout the year. In comparison of each month for the severe dry condition, both rain gauge and TRMM data show about 25% of similarity in drought months while all other categories are below 5%.

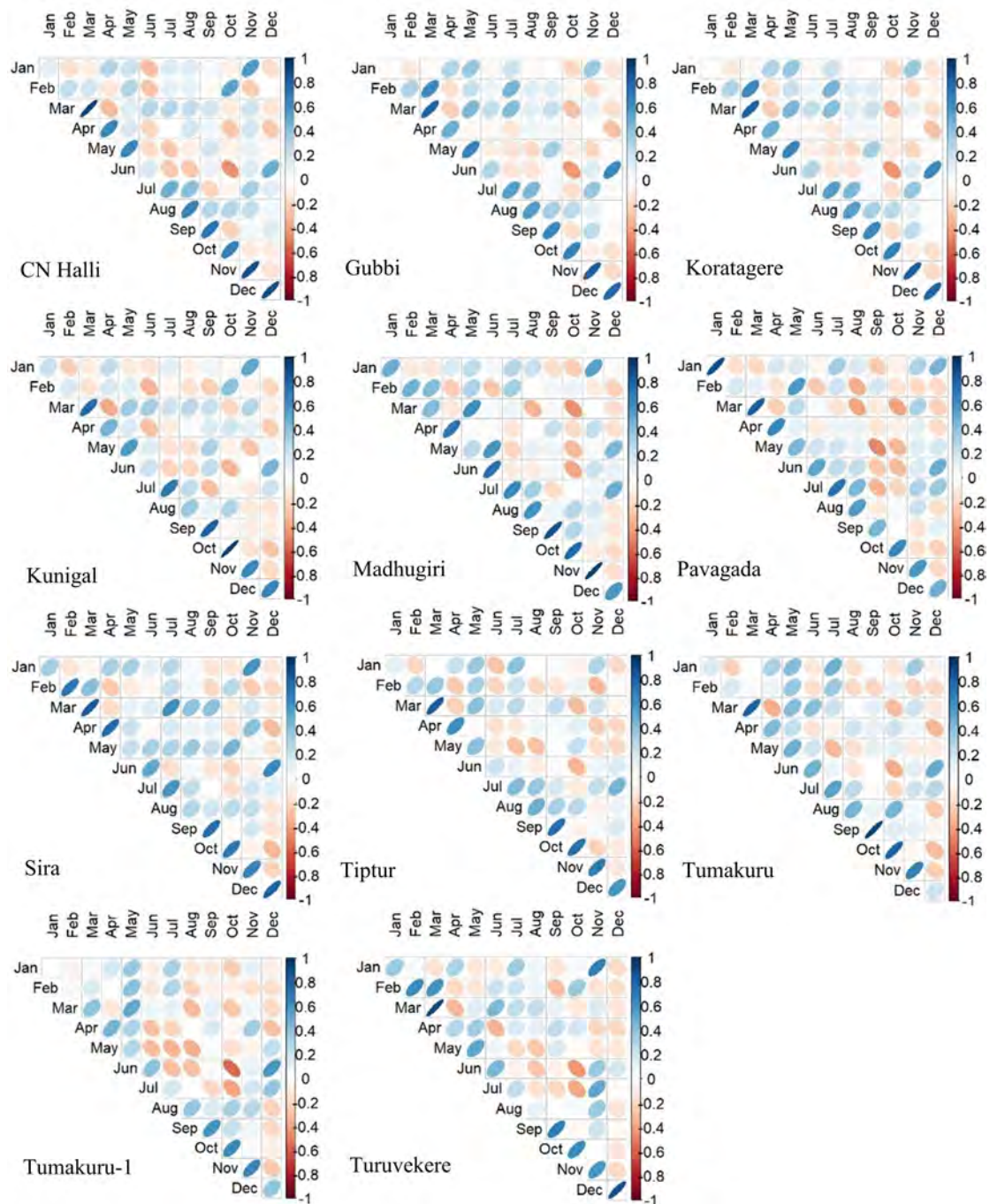


**Figure 36:** Pearson correlation of rain gauge and TRMM 3B43 for RAI

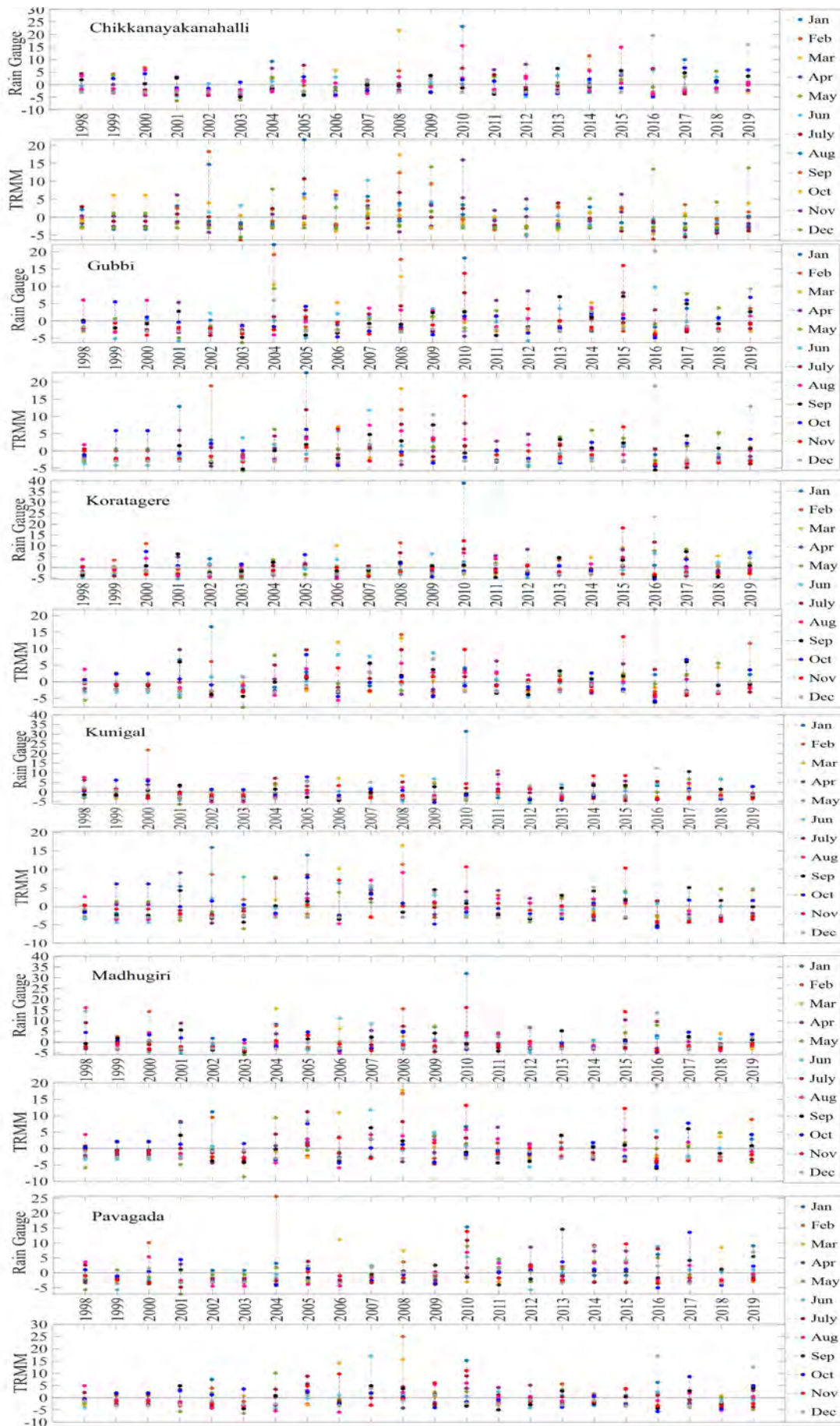


**Figure 37:** RAI plot for rain gauge versus TRMM from 1998 to 2019



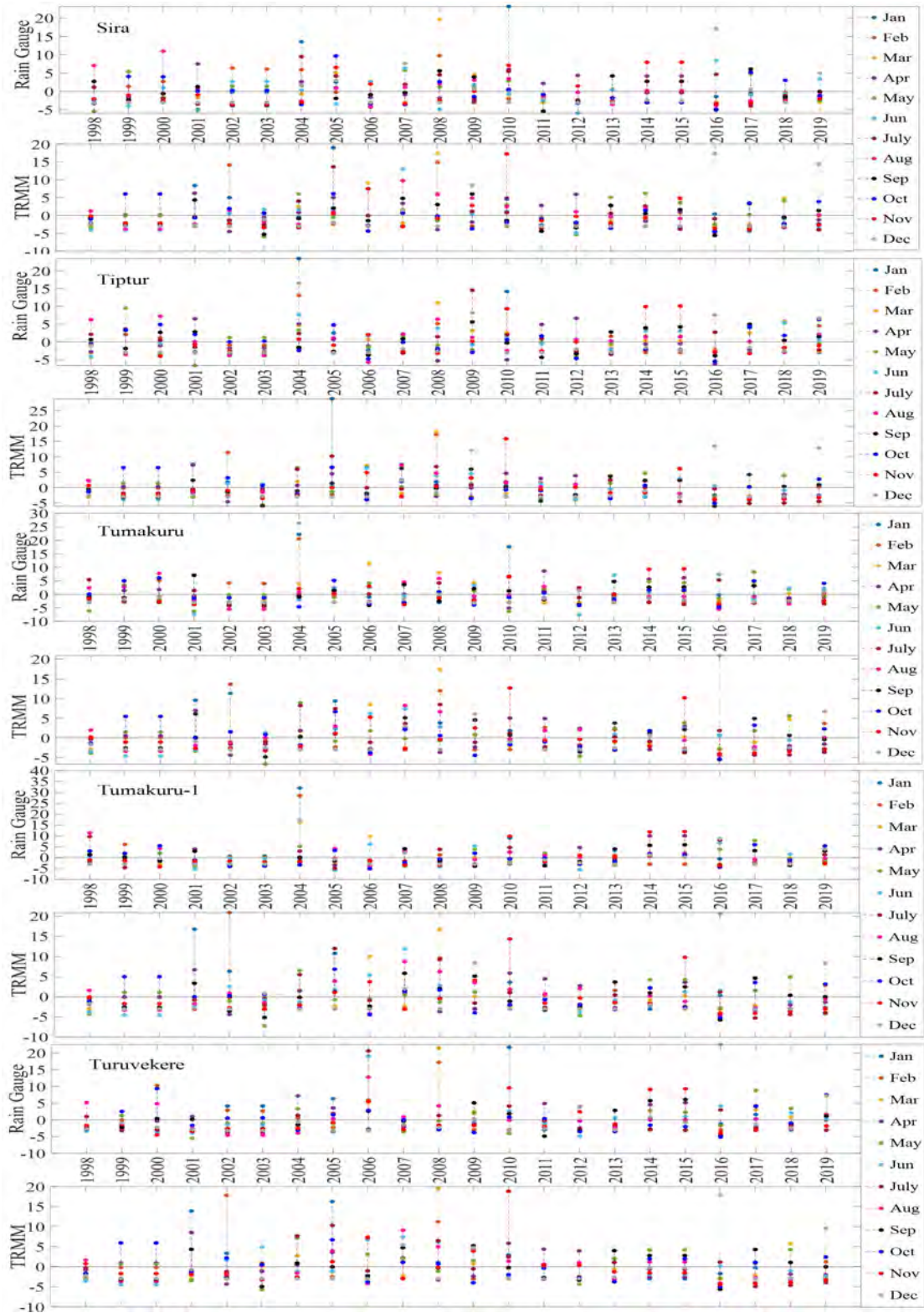
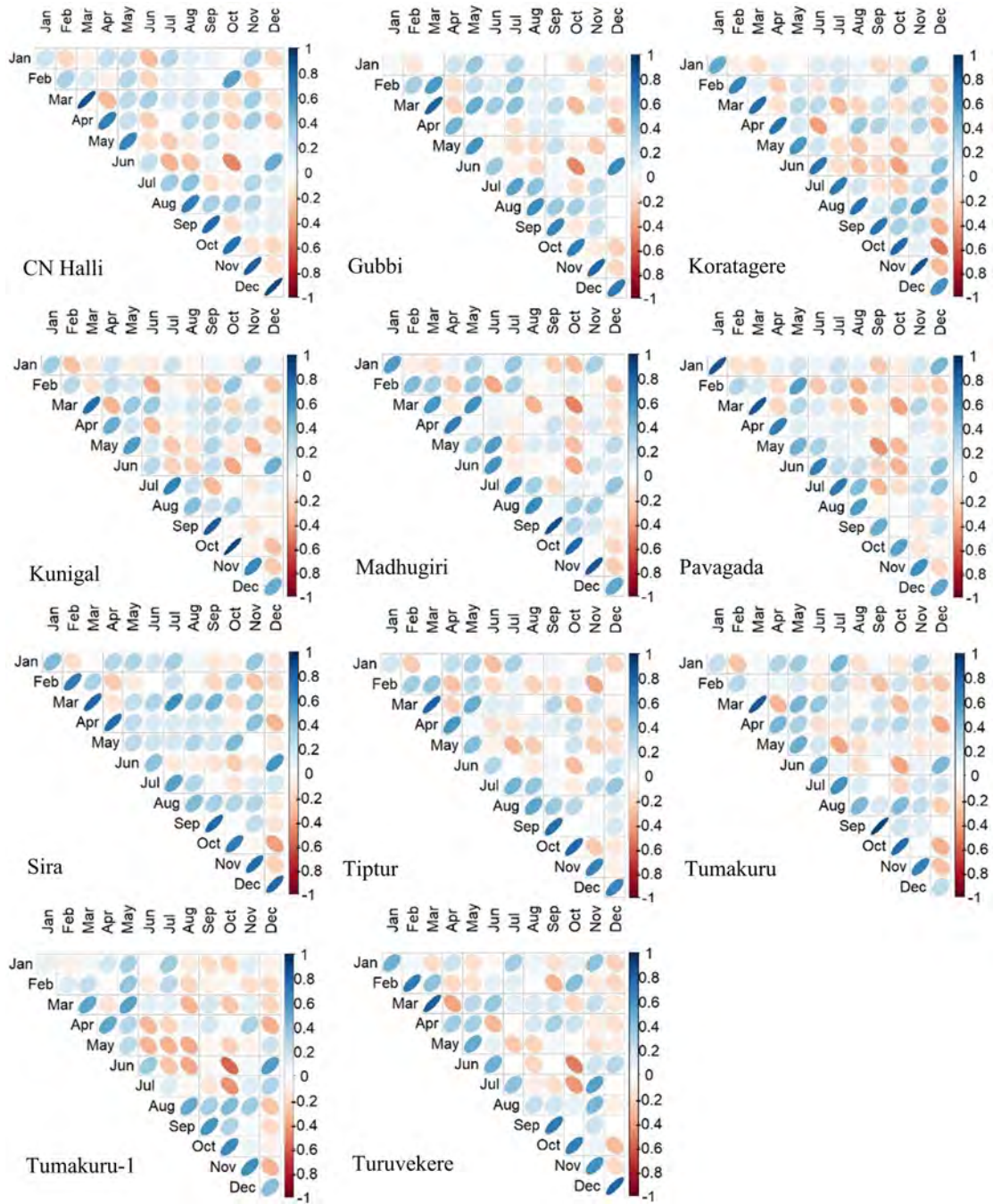


Figure 37: continued

6.3.5. Modified China Z Index

The result of the index varies only slightly beyond the limit of the -2 and +2 defined. Under normal conditions, the index shows about 61% of a match between the data sets. Koratagere and Pavagada are chosen as the two representative stations to

describe the index from Figure 40.



**Figure 38:** Pearson correlation of rain gauge and TRMM 3B43 for MCZI

August to September of 2016 experienced extreme drought conditions according to both the datasets in Koratagere station apparent from the figure and the rest of the data also finds similarities to a certain extent. While Pavagada shows contradictory conditions between the datasets. For example, May 2003 had the wet condition as seen from rain gauge data while TRMM shows drought. As expressed in Figure 39, the average rmse is about 0.68 with the months from April to October carrying higher values compared to the other months in all the stations. Tiptur in August

(-2.71) and Pavagada in December (-3.16) are the only stand-out values among all the stations while all other t-test values are closer to zero. From Figure 38, we find that the coefficient values are only positive with March holding the largest values. Chikkanayakanahalli shows an overall match of only 10.61% while there is a correlation of 0% for extreme drought, severe and moderately dry conditions account for 0.76% and 0.38% respectively. Gubbi holds an overall match of 19.32% while moderate and severe drought is defined by 1.89% and 0% respectively. Koratagere exhibits an overall 13.26% match and 1.89% for moderate and 0.38% for severe drought. Kunigal has 0 for both severe and extreme while moderate drought makes a 0.38% correlation only. Madhugiri with an all-around 11.36% equivalence, has 1.52% for moderate and 0.38% for the extreme dry event being the only station with a slight value for extreme drought conditions. Pavagada has an overall of 15.53% harmony while there is absolutely no correlation for any of the drought categories at all. Sira has no match for severe and extreme drought categories while moderate drought is 0.38%. In total, Sira has a 7.95% match for all categories. Tiptur recorded a total of 7.2% similarity on the whole and 0.76% for a moderate and severe dry spell while extreme drought found no match. Both Tumakuru and Tumakuru-1 stations show a total of 6.82% correlation while both severe and extreme drought are 0. Moderate drought for Tumakuru and Tumakuru-1 is 0.38% and 0.76% respectively. Turuvekere station had a 14.03% match for all categories and 0.38% for moderate drought. There is no match for severe and extreme drought for this station. Koratagere had values for extreme, severe, and moderate wet scenarios respectively at 1.14%, 2.65%, and 2.27%. Pavagada holds the value of 1.52% for both extreme and severe wet conditions and 1.89% for moderate wet conditions.

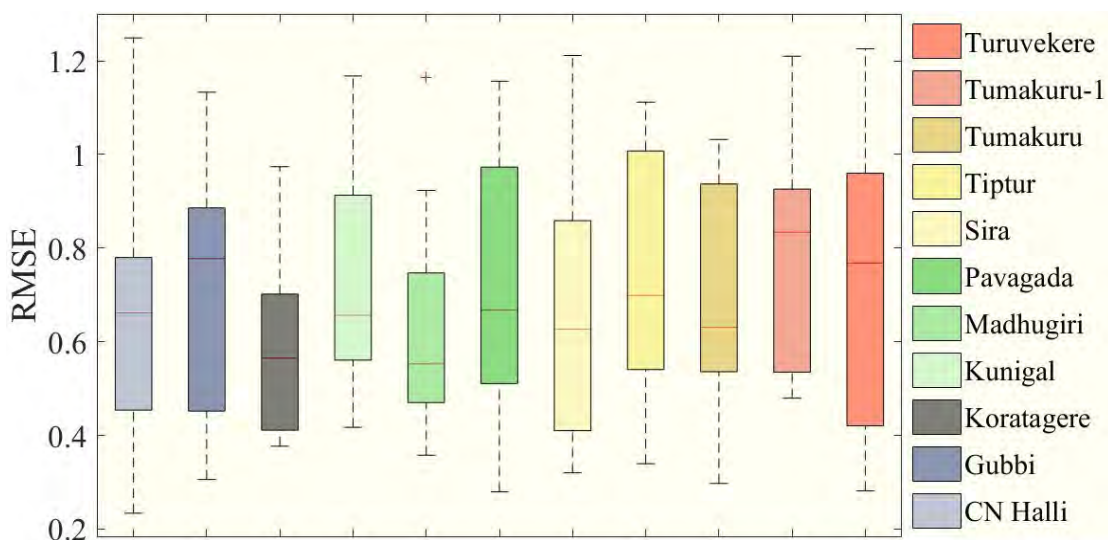


**Figure 39:** RMSE of 3B43 and rain gauge dataset for MCZI from 1998 to 2019

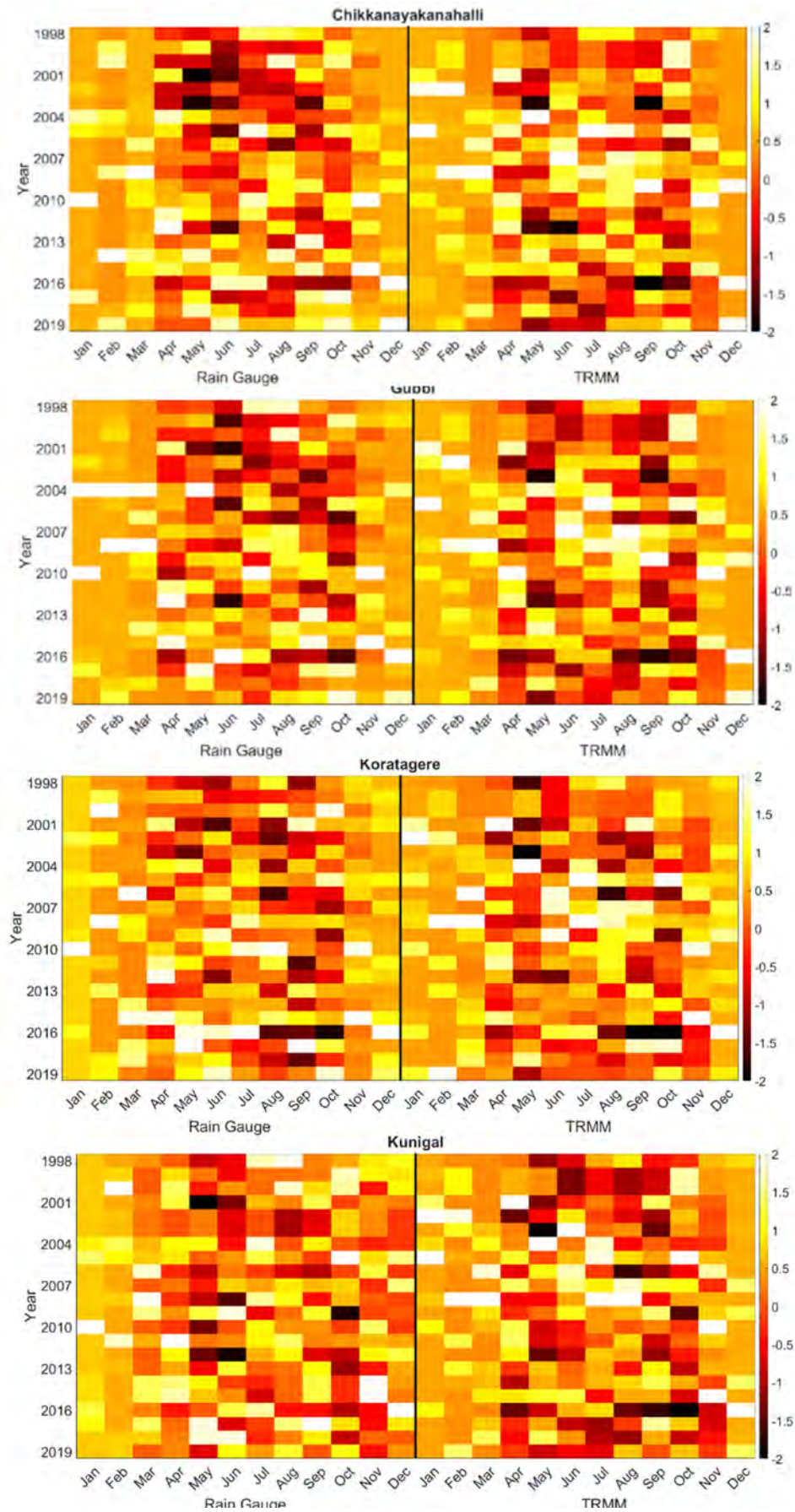


**Figure 40:** Monthly heat map for MCZI

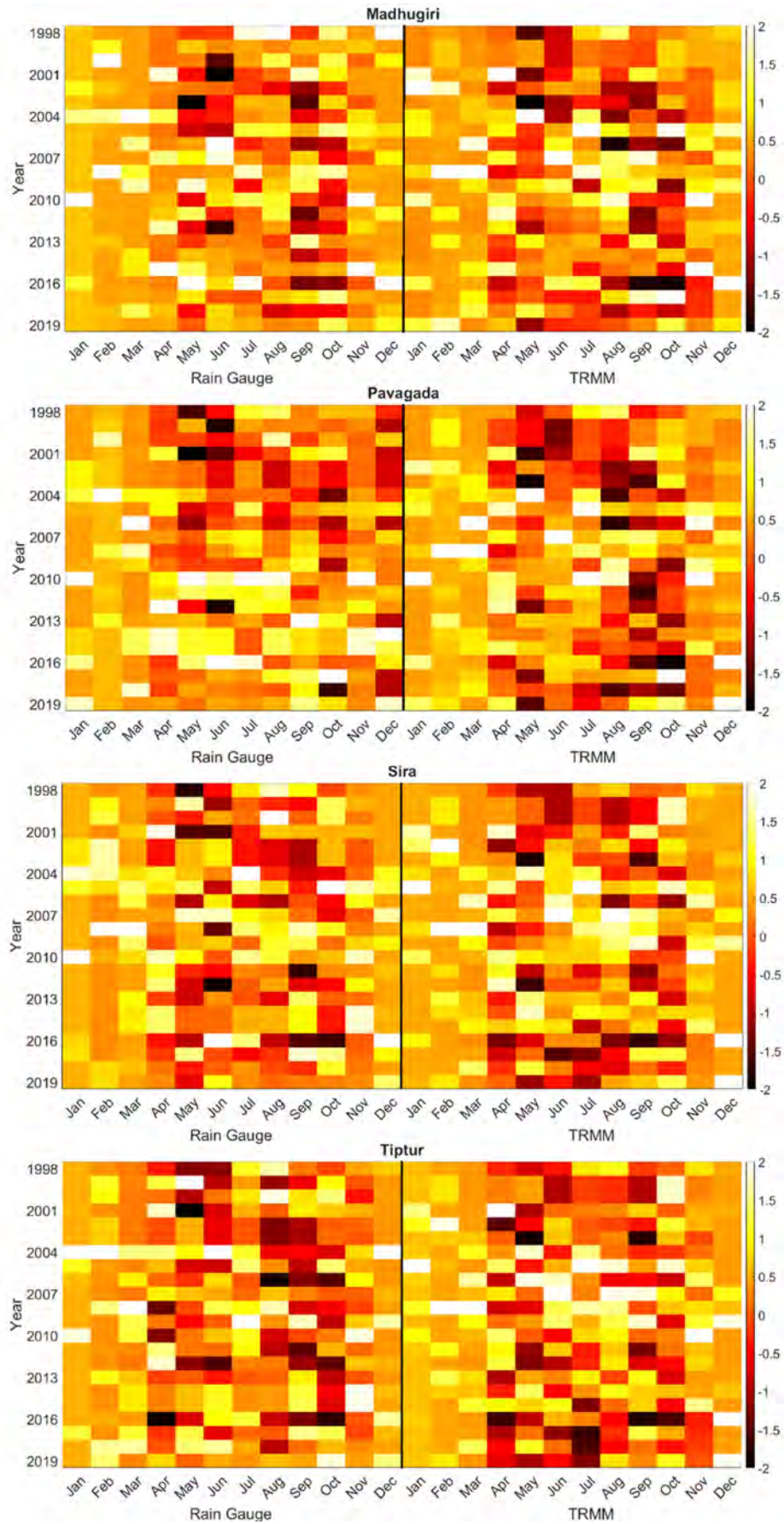
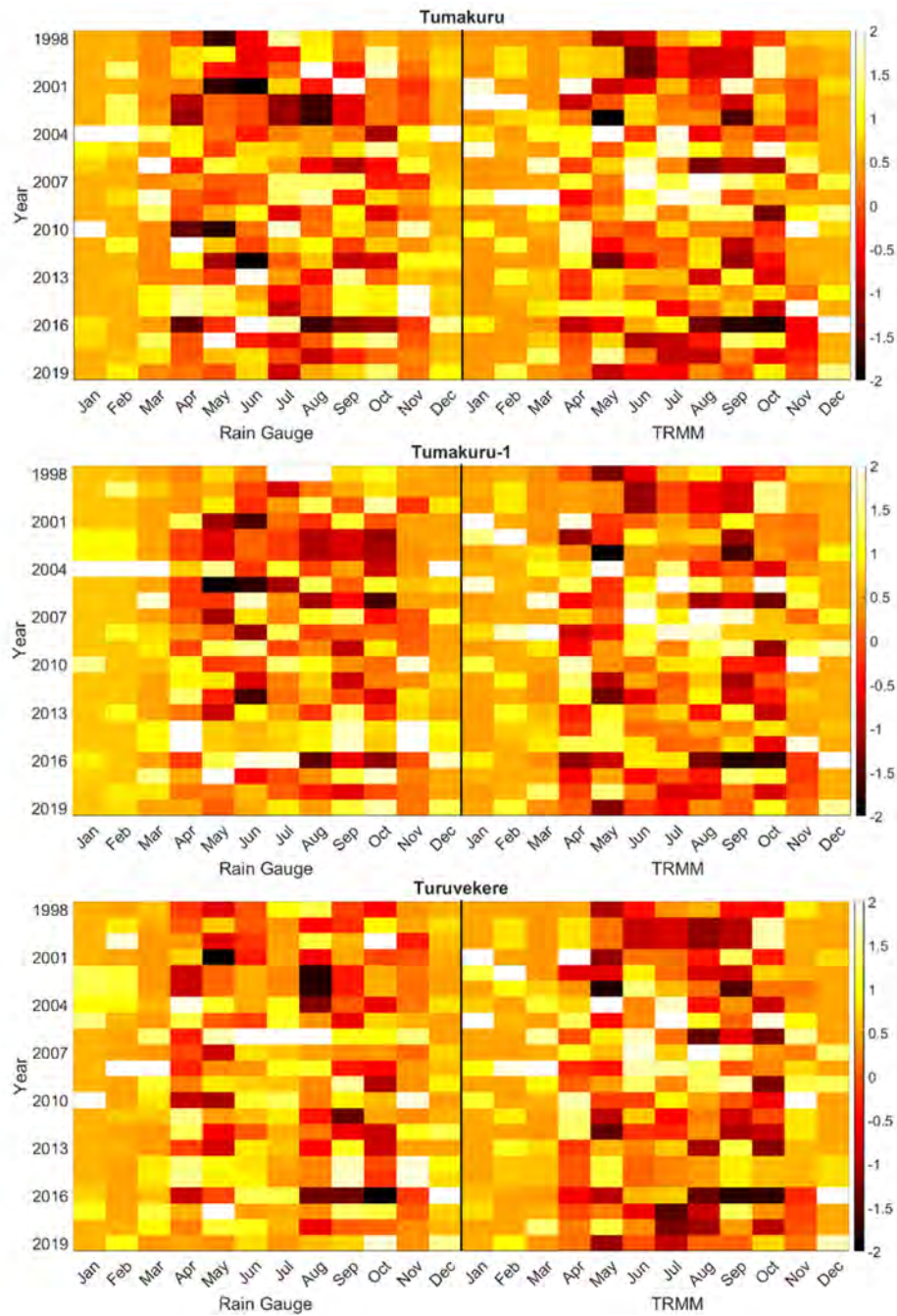


Figure 40: continued



**Figure 40:** continued

MCZI index shows greater similarity to the scatter diagram as the range of values is close to the defined range of -2 to +2. Few of the points reach up to +2.5. The rmse is fairly lower and again holds consistency for all the months of the year. The months indicating normal conditions match up to 61% of the datasets while all other category indicates a match of less than 1% when comparing the rain gauge and TRMM data of each month.

### 6.3.6. Percent of Normal

The percent of the normal index gives the percentage of rainfall at a particular time with respect to the long-term normal rainfall value. PN values for both rain gauge and TRMM-3B42 data were derived to verify the compatibility of the data to determine the drought conditions.

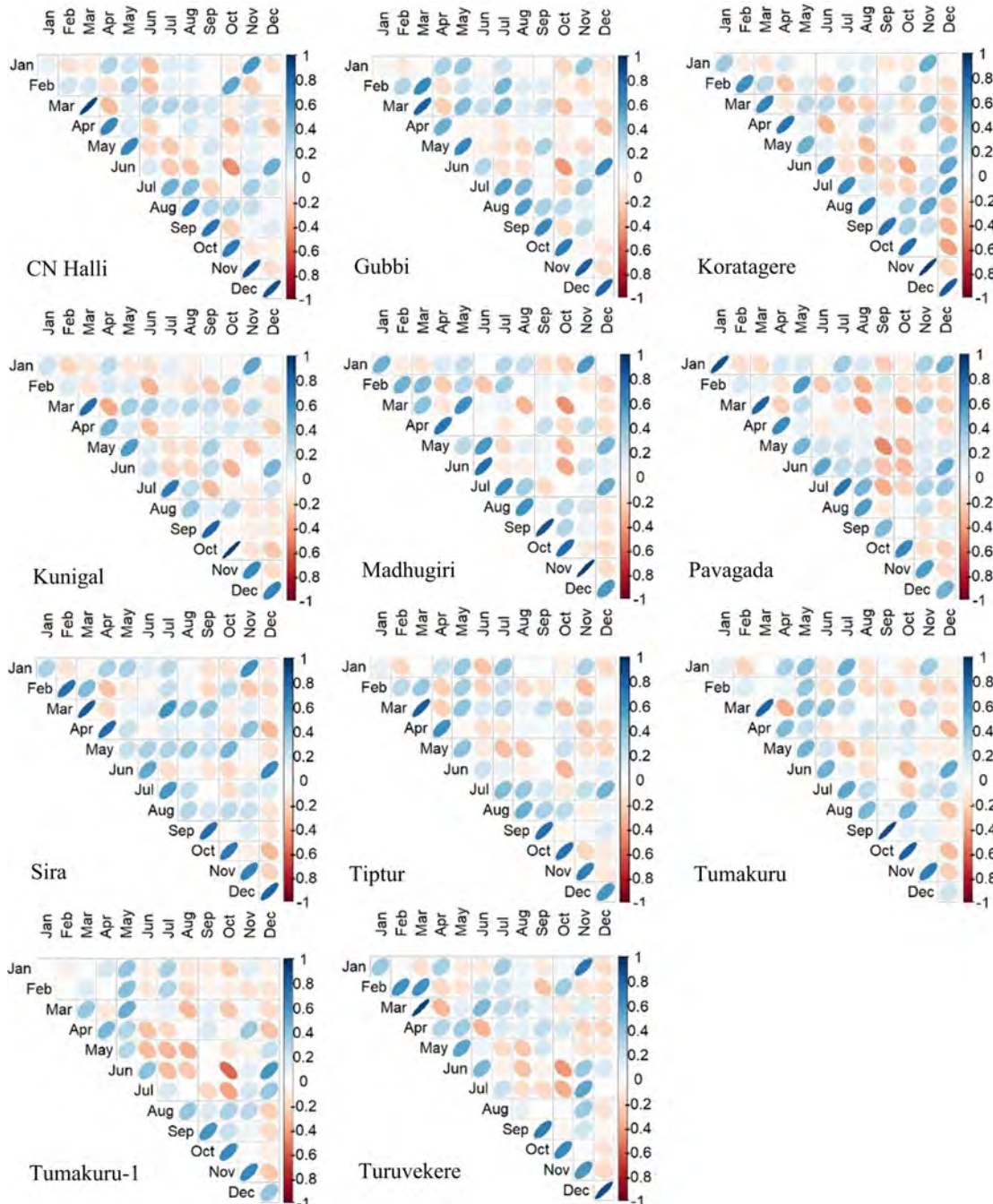


**Figure 41:** Pearson correlation of rain gauge and TRMM 3B43 for PN

None of the eleven stations shows an exact match of the PN value from two data sources as there are variations found throughout the output. At certain locations and times, TRMM depicts drought while the rain gauge describes flood-like

conditions and vice versa. Referring to Figure 43, Gubbi shows a good correlation between the two datasets while holding an apparent shift throughout the period at the same time following a similar pattern of graph While Tumakuru-1 shows polar opposite values in many instances. The error is maximum in January and February while the minimum is for September and October (Figure 42). All the values for the t-test resulted in a nearly zero value indicating a null hypothesis. Figure 41 indicates that January has the minimum correlation and March has the maximum correlation for various stations. Gubbi shows a negative coefficient for January. The maximum match found for overall value is at Chikkanayakanahalli station with 27.65%. The similarity for drought is 0.76%, 1.52%, and 26.89% for moderate, severe, and extreme events respectively. Gubbi has a total of 26.14% similarity and moderate, severe, and extreme events correlate 0.76%, 1.89%, and 25.76% respectively.

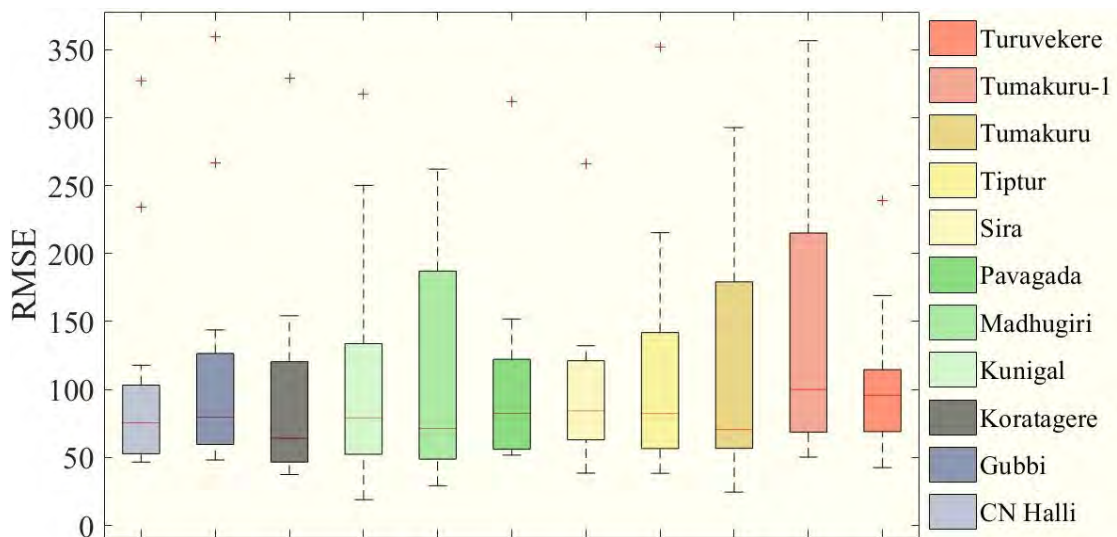


**Figure 42:** RMSE of 3B43 and rain gauge dataset for PN from 1998 to 2019

Koratagere holds a total of 26.14% for all and 0.383%, 1.14%, and 24.62% respectively for moderate, severe, and extreme dry spells. Kunigal has 1.52%, 0.76%, and 21.97% for moderate, severe, and extreme dry spells respectively, and 25.76% on the whole. Madhugiri station has a total of 24.24% while moderate, severe, and extreme events recorded 0.38%, 0.76%, and 26.52% respectively. Pavagada shows a total of 23.48% similarity while severe and extreme events find a similarity of 0.38% and 23.86% respectively. Moderate dry event finds no match for this station.

Sira finds a total of 26.52% harmony while moderate, severe, and extreme events are at 0.76%, 1.52%, and 26.14% respectively. Tiptur though having a total of 21.21% match, has no match for severe dry events. Moderate and extreme dry spells are defined with 1.52% and 23.86% respectively. Tumakuru has a total of 23.86% match for all categories and 0.38% match for both moderate and severe drought



and 21.97% for extreme drought conditions.

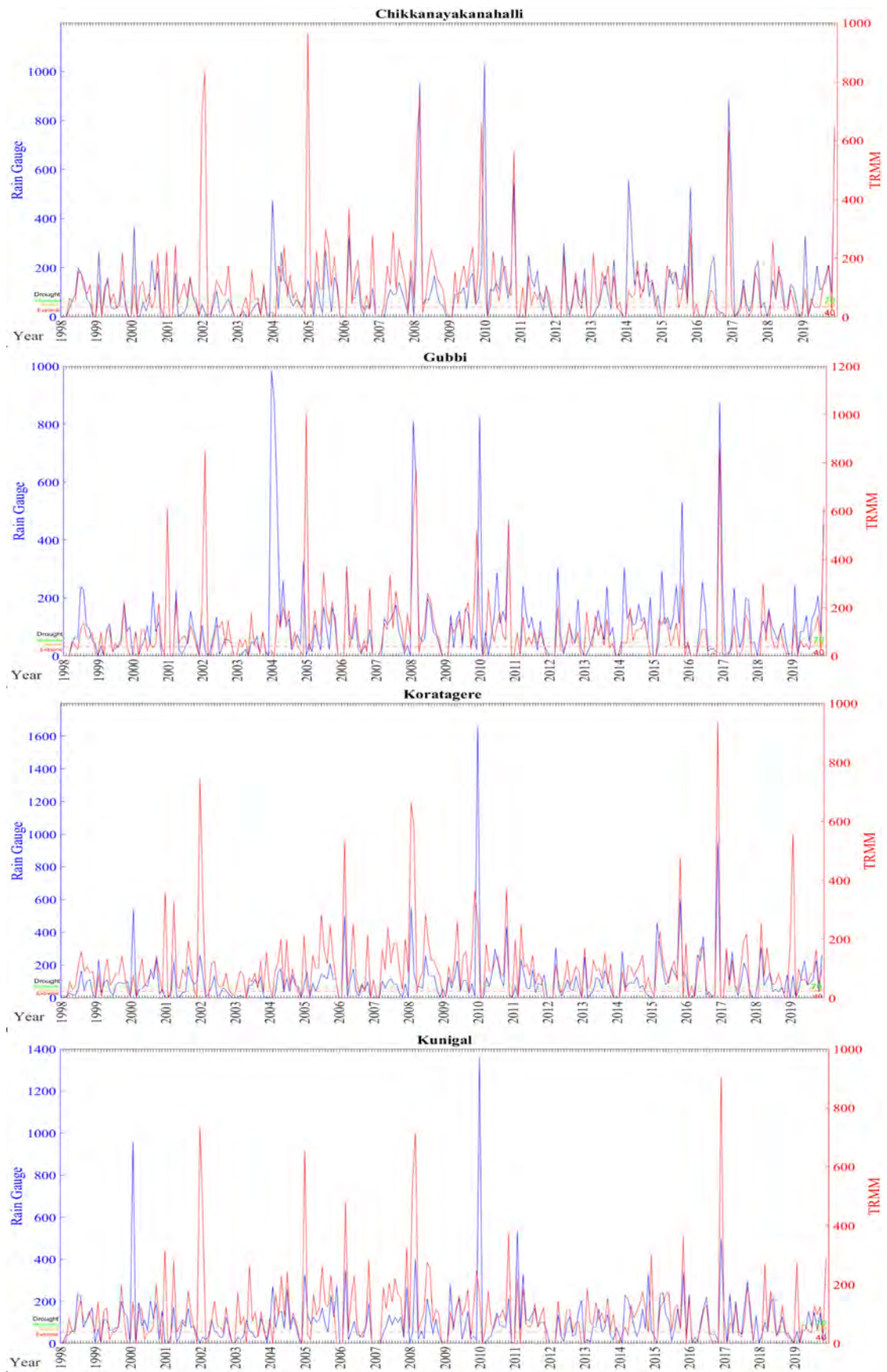


**Figure 43:** Overlapping temporal distribution of PN with drought severity

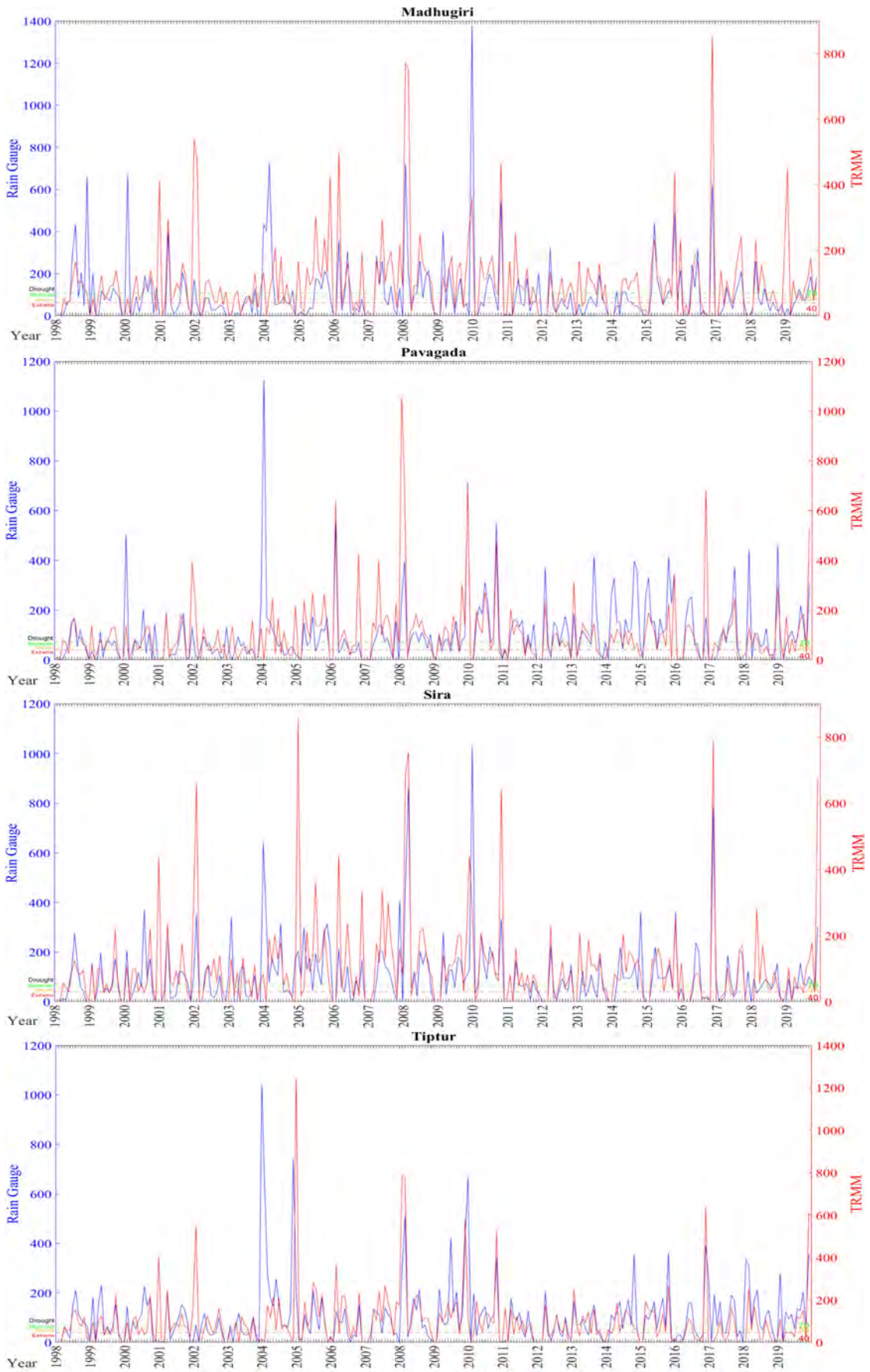
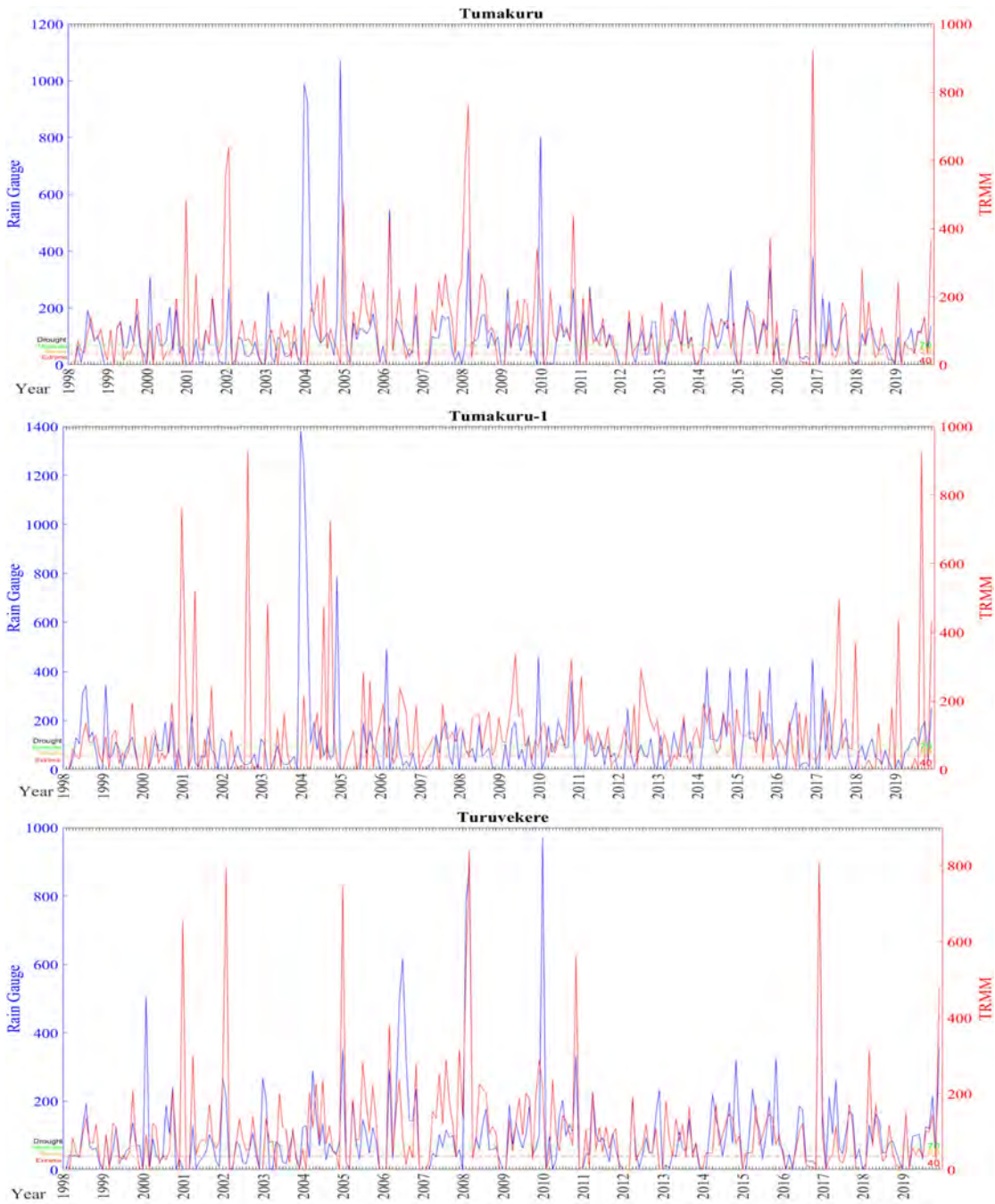


Figure 43: continued



**Figure 43:** continued

Tumakuru-1 has the least match for percent of normal index with a total of 10.23% on the whole. There is only a 0.76% and 13.26% match for a moderate and extreme dry period while the severe dry event has no match at all. Turuvekere has a 22.7% similarity while moderate, severe, and extreme events have 0.38%, 1.89%, and 22.73% respectively. To define the correlation for the wet events, most of the stations have 0% similarity when it comes to the severe wet event except for Kunigal, Madhugiri, and Tumakuru all at 0.38%. Gubbi station recorded 18.18% and 1.89% for extreme and moderate wet events respectively. Tumakuru-1 recorded the

least correlation of 10.98% for extreme and no match for the moderate event in the wet category. Percent of normal holds values way beyond the range reaching up to 400 on an average while scatters beyond 1000. We see a large fluctuation of the index value from the defined value. The rmse value also varies in the larger sense. The months matching for extremely wet and extremely dry conditions are 18% and 23% respectively. All the other conditions have a value of less than 1% when comparing the rain gauge and TRMM.

### 6.3.7. Deciles Index

The deciles plotted in Figure 46 show the example of Sira and Tumakuru-1 stations. While Sira shows a great correlation between TRMM and rain gauge especially in 2005 and 2010 following a very similar pattern, Tumakuru-1 witnesses a stark difference between the two datasets showing a greater difference. The plot of TRMM and gauge data for the time 1998 to 2019 shows a very good correlation. This is evident by the similar peaks found in the year 2004 and 2015 especially.

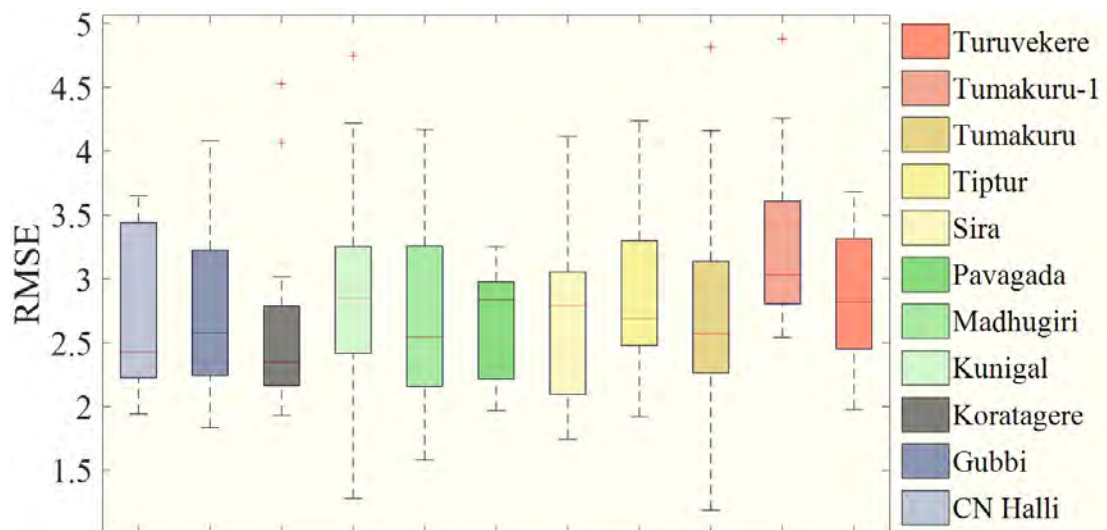


**Figure 44:** RMSE of 3B43 and rain gauge dataset for DI from 1998 to 2019

While comparing the total number of months for various categories, there is a very good correlation between the datasets. Most of the results agree with each other with a variation of not more than 5 months with an exception of normal and extremely dry conditions. While there is a certain match for the normal condition, extremely dry months do not match for any of the stations and there is a bigger gap between the values obtained.

The deciles as per Figure 44 show an average error of 2.81 while the maximum is seen in December and January. The t-test resulted in zero for the months April to November while the rest of the months recorded majorly negative values. The Pearson correlation coefficient in Figure 45 shows a good positive correlation of 0.6

on average. Chikkanayakanahalli station shows a good correlation of 28.41% on the whole. The extreme wet and extreme dry events show a match of 8.71% and 17.05% respectively. Moderate dry and severe dry showed 1.14% and 1.18% only.

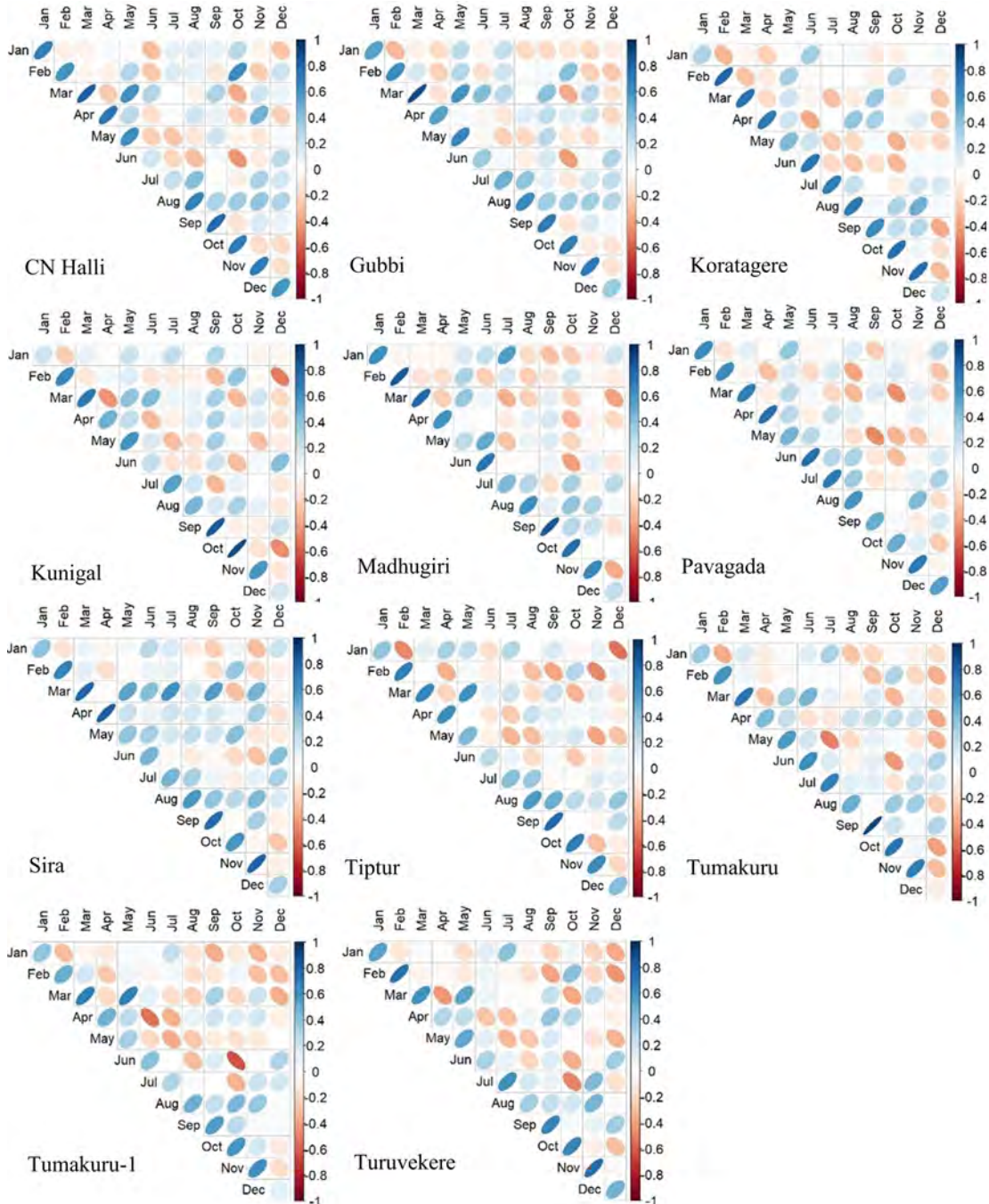


**Figure 45:** Pearson correlation of rain gauge and TRMM 3B43 for DI

There is no match at all for moderately wet conditions. Gubbi values also find an equivalence of 28.41% for all. 0.76%, 1.52%, and 16.67% are equal for moderate, severe, and extremely dry conditions respectively. Koratagere has an overall of 20.08% of the match.

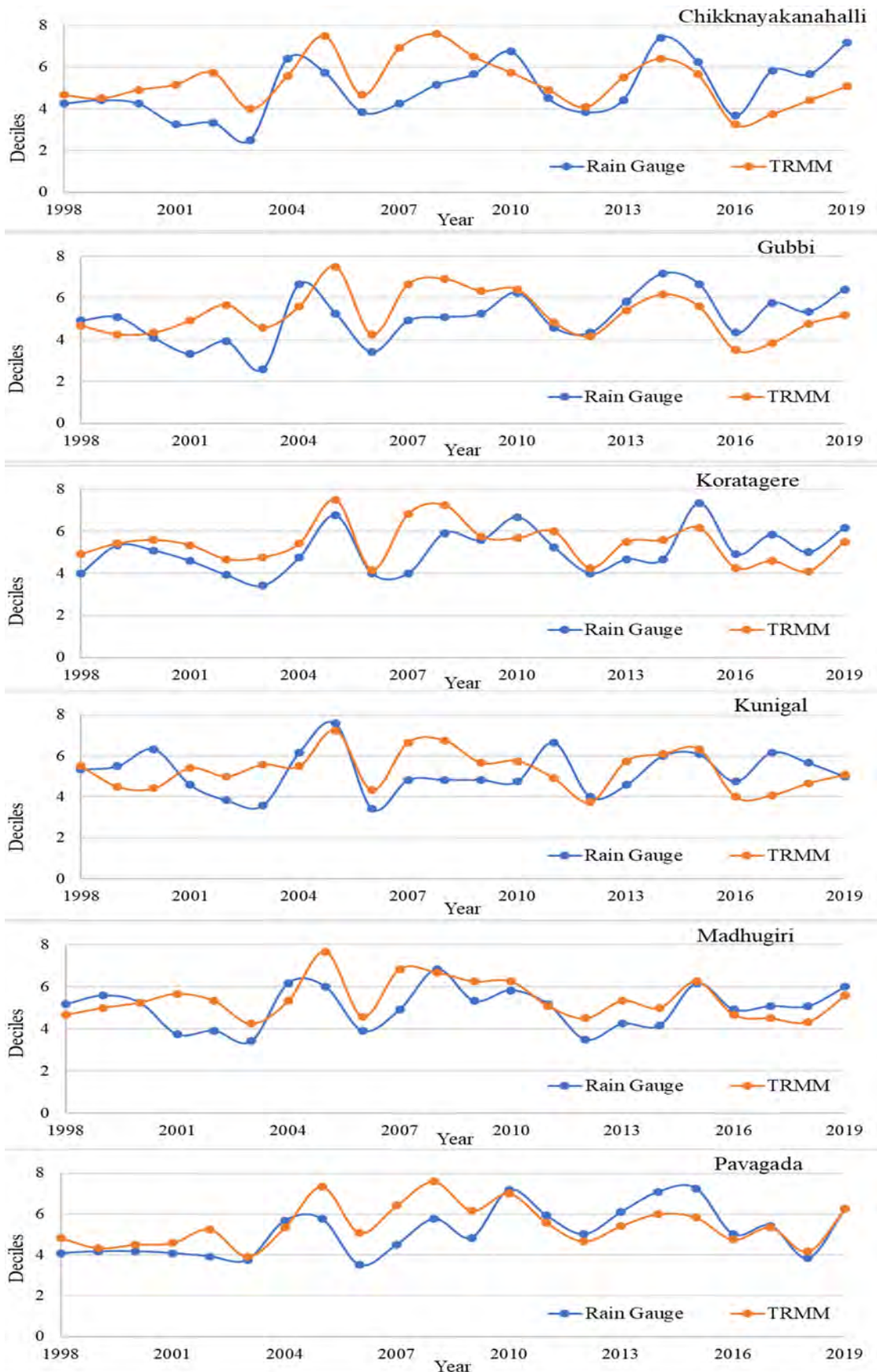


**Figure 46:** DI plot for rain gauge versus TRMM from 1998 to 2019

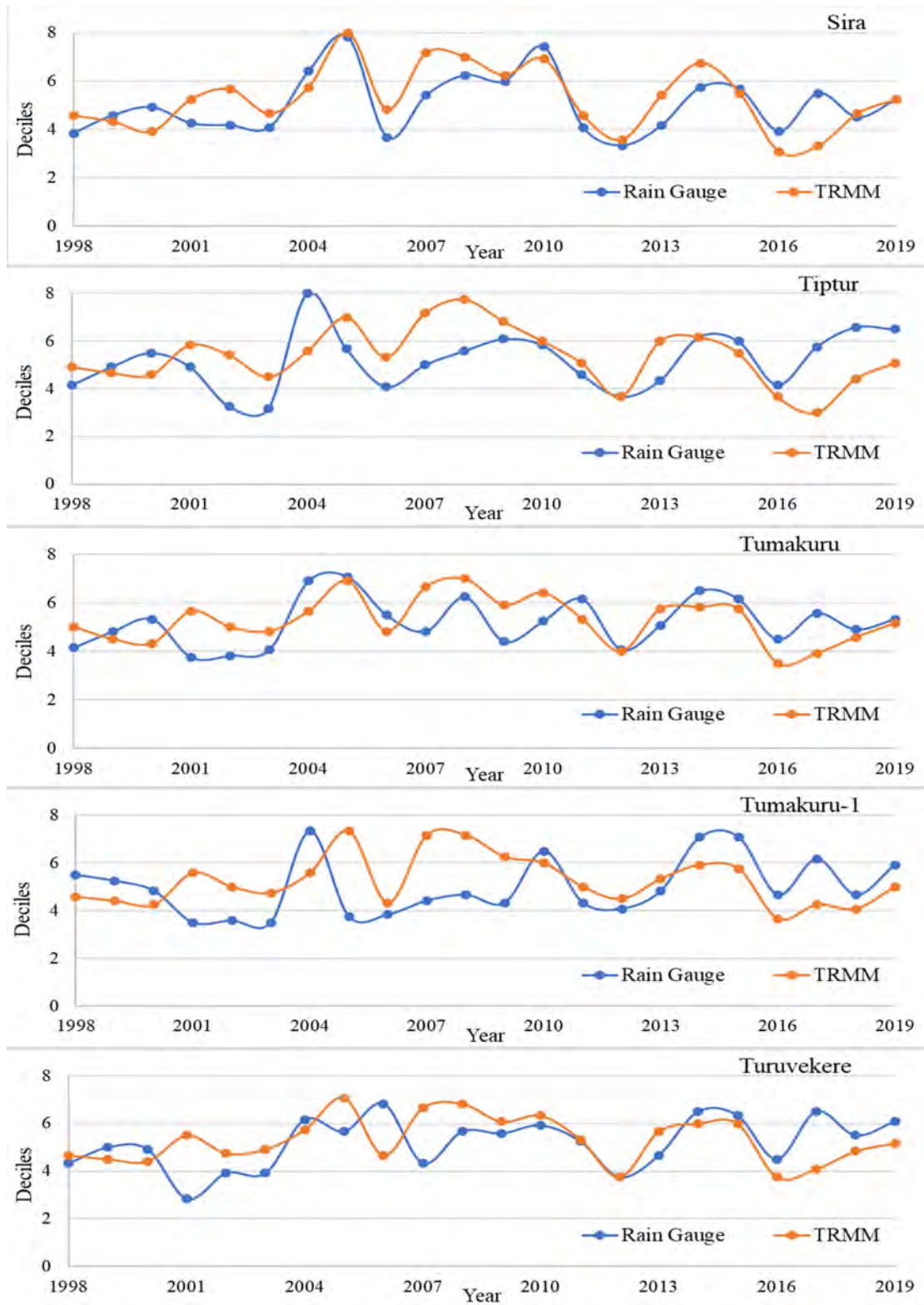


**Figure 46:** continued

The percentage match for the moderate, severe, and extreme dry spells is 1.14%, 1.52%, and 12.88% respectively. Kunigal displayed a total of 23.48% similarity. Also, the match for the moderate, severe, and extreme dry periods is 0.76%, 2.27%, and 14.02% respectively. Madhugiri portrays a total of 23.86% match between the

values. The similarities for the moderate, severe, and extreme dry period is 1.14%, 1.52%, and 12.12% respectively.

Pavagada shows an overall 20.45% similarity. For moderate, severe, and extreme dry events, there is 0.76%, 2.65%, and 9.85% harmony respectively. Sira in the total exhibits 25.38% common values. The percentage of similarity for the severe and extreme dry periods is 1.52% and 15.15% respectively. There is no match for the moderate dry event at all. 27.97% is the total match for Tiptur station. For moderate, severe, and extreme dry period is 0.76%, 1.14%, and 11.36% respectively. Tumakuru has a similarity of 25.76%. The dry period severity has a match of 1.14%, 1.89%, and 14.02% respectively for moderate, severe, and extreme. Tumakuru-1 displayed a total of 24.62% similarity. Also, the match for the moderate, severe, and extreme dry periods is 1.14%, 1.89%, and 13.26% respectively. Turuvekere on the whole shows 21.59% similarity. 0.76%, 2.27%, and 13.64% of equivalence are found for moderate, severe, and extreme dry spells respectively. Sira and Tumakuru-1 showed better responses with 9.47% and 8.71% respectively for extremely wet conditions, 3.79%, and 3.41% respectively for severe wet conditions, and 3.979% and 0.38% respectively for moderate dry conditions. The deciles index carries a comparatively lower value holding good for all seasons. The index exhibits 9% and 14% respectively for extremely wet and extremely dry conditions. Under severely wet, and normal conditions, there is about 3.5% of correlation while the rest of the value lies below 2% for the rain gauge and TRMM data.

#### 6.3.8. Comparison of rain gauge and TRMM through indices

The scatter plot for RAI, MCZI, and PN are utilized to draw a comparison between the indices. The plots indicate the index value obtained from both the rain gauge and TRMM. Figure 47 represents the scatter plot of RAI with the R2 value of 0.2599 indicating the variance in the data. For the MCZI, data falls on the trend line defined by  $y = 0.6125x + 0.1232$  with the variance not going beyond 0.3523 which indicates the similarity portrayed by the data (Figure 47). The index includes values that go way beyond the limits defined for it with the R2 being a low 0.1934 as seen in Figure 47 for the Percent of Normal Index. The result of the indices shows 26%, 35%, and 19% respectively for RAI, MCZI, and PN. For RAI, the values are mainly concentrated from -5 to +10 while MCZI ranges from -2 to +2.5 and PN ranges from 0 to 400 obtained in this research wherein we see the maximum accumulation of the correlated data.



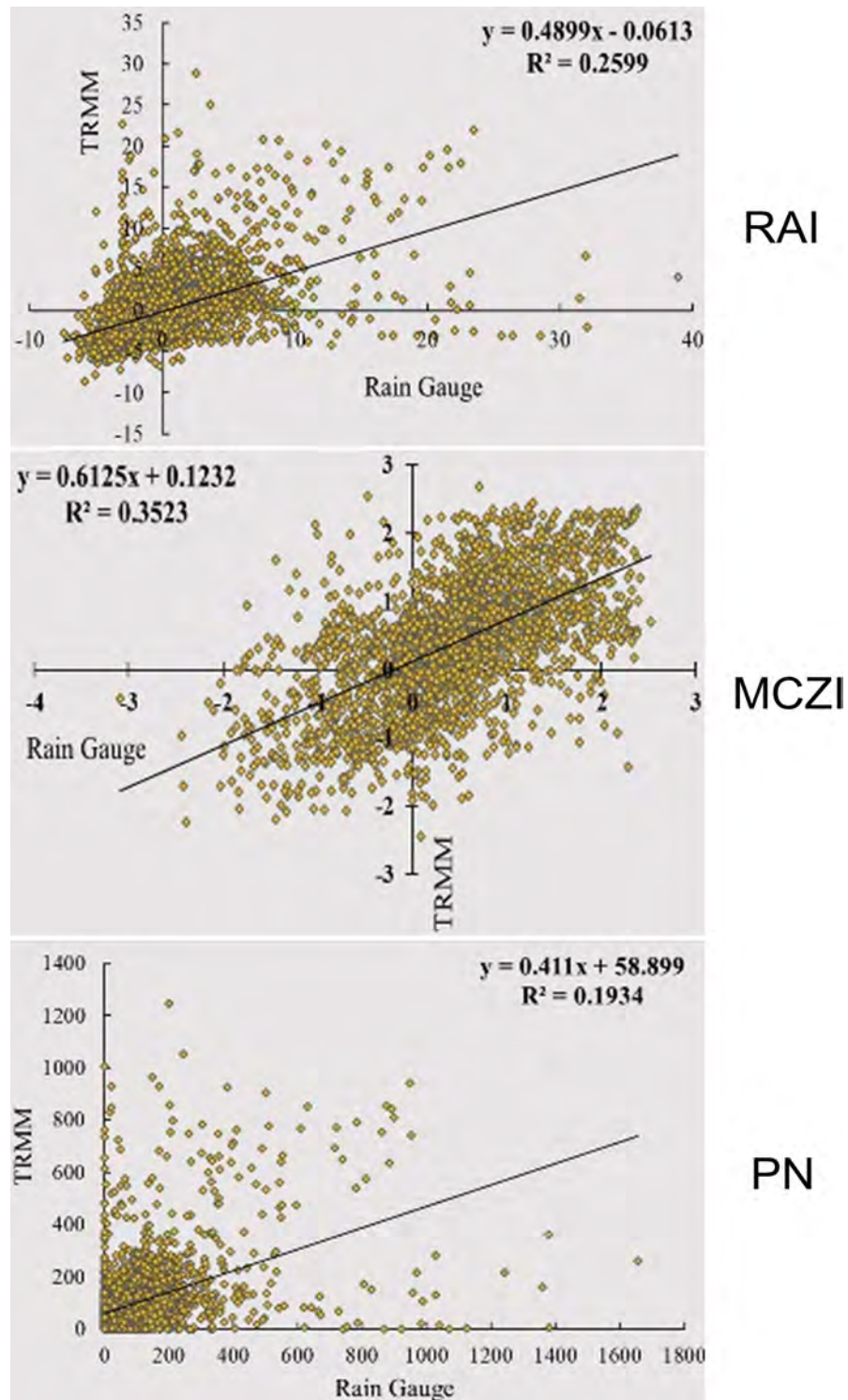


**Figure 47:** Scatter plot of indices

#### 6.4. Conclusion

Mitigating disasters like drought is a challenge requiring powerful tools. Precise data helps us determine the Spatio-temporal distribution and helps in monitoring the situation. The study aims at providing a suitable data source to determine the condition of meteorological drought.

- Although a clear result was not determined from the study regarding the effectiveness of the datasets, a lot is understood in terms of how different indices respond to different datasets. There is greater compatibility in long-term data and a bigger area.
- The result of PN shows a good match for moderate drought since the frequency of moderate drought is much higher. There are very few severe and extreme drought events and hence the probability of finding similarities becomes even slimmer.
- Among the four indices, MCZI bears the most similarity between the TRMM and gauge rainfall data.
- There are extreme variations in the index value, especially of TRMM data going way beyond the given range of the data which again poses difficulty in validation.
- While comparing each month data, all the drought indices show relatively low homogeneity between the two data sets which is represented in the percentage comparison of the datasets. But on the whole, when comparing the individual number of months for each station for each category of drought, there is a much higher similarity between the data sets. From this, we can concur that rain gauge and TRMM show a nearly equal amount of drought categories when talking about long-term data. Since the number of months of individual data for each category shows a good match.

The scope of the research lies in meteorological drought monitoring by using suitable data and also serves as a means to build atmospheric models of high accuracy and resolutions.

## 7. Conclusion

The objective of the study is to identify the drought prone area of Tumakuru district and carry out analysis of the spatio-temporal characterization of meteorological drought. Non-parametric tests were employed to understand the rainfall trend and change point analysis was done simultaneously. Different methods of measuring rainfall such as ground based rain gauge data was correlated with satellite based precipitation product using multiple drought indices and statistical methods.

### 7.1. Outcome of the study

The analysis and interpretation of the obtained results have helped to arrive at various conclusions about the drought scenario in the Tumakuru District. The outcome of the research has been presented specific to the objectives.

The drought hazard and prone area of Tumakuru District was investigated using the precipitation dataset through the means of SPI. The analysis revealed that instances of wet period in certain seasons of particular years but the abundance of dry spell was evident significantly. The years 1961, 1963, 2006, and 2007 showed prominent dryness in the annual scale. SPI has proven useful in identifying the pattern of drought in the region.

Characterization of the meteorological drought is interpreted by means of both SPI and SPEI. The use of SPEI which uses precipitation and evapotranspiration parameters while puts into perspective the role of temperature in drought study in comparison to SPI which uses only precipitation parameter. The study carried out at multiple timescales of 1-, 3-, 6-, 9-, 12-, and 24-month shows the fluctuations in seasonal drought at varying degrees. Both the indices gave consistent results at longer timescales but the correlation was very poor at shorter timescales.

Understanding the historical data is very important to understand the trend in the region and also to predict the future trend and take suitable measures to manage the water resources. MK and SS being the proven methods to study trend, MMK and ITA methods are newer and advanced methodologies for the same purpose. The advantage of ITA over MMK in the detection of long-term rainfall pattern is observed. The magnitude and the variability of the rainfall can be determined. In the annual and the seasonal timescales, MMK showed higher instances of significant increase in the trend in comparison to the ITA. A good correlation is also noticed for the z score of both ITA and MMK results while a consistent fluctuation is also witnessed for the stations.

Although there is a continuous change in the trend of rainfall observed throughout, the similar pattern can be seen, and this pattern tends to change periodically. The

change is obtained through the change point detection tests, to understand at what period, the trend began shifting. Change point was observed for a few stations and there is no regularities between the stations. Buishand and Pettitt test show similar results. ARIMA model helped provide a basic perspective on how the long term rainfall data can project the future pattern.

Basing off of reliable data source is important to arrive at accurate analysis and hence ground based and satellite based precipitation datasets are compared to understand the differences between them. Statistical techniques helped to analyse the deviation between the two products while the indices showed as to which was a better fit to study drought. MCZI showed the highest correlation for the data products.

## **7.2. Recommendations**

Based on the findings of the research, recommendations are proposed for the betterment of the Tumakuru District.

1. The available spatial distribution of the data points is 0.25 degrees which is much higher resulting in only 11 grid points within the study area. In order to understand the minor variation in the spatial distribution of the precipitation, an increase in the density of the ground points is suggested in order to rise the accuracy of the results.
2. The ARIMA model used to predict the rainfall is a very simple model considering only the precipitation parameter. Since various meteorological, climatological and anthropogenic factors influence the rainfall, a better suited model using multiple parameters can be used to do rainfall forecasting.
3. It is recommended that the influence of the urbanization, change in land cover, agricultural practices and other anthropogenic parameters be looked into since they have a huge role in inducing drought conditions.
4. Agricultural practices in the area are mostly dependent on rainfall and the fluctuation in the monsoon pattern has had a severe impact on the yield. Addition of soil moisture data in the drought analysis will provide a better perspective to understand the agricultural drought.
5. Crop yield decreases when rainfall fails and the socio-economic condition of the people is impacted. Farmers should be advised to grow crop which require less water and can adapt to fluctuation in monsoon.
6. To combat the growing stress on water requirement as a result of rapid urbanization and industrialization, water harvesting structures, rooftop rain water harvesting and other methods of preserving rain water must be made

mandatory.

7. The techniques used in the result though talks specifically about drought can also be extended to the study of flood. Furthermore, the fluctuation of groundwater should also be studied to know the full extent of drought on hydrological system.

## 8. Reference

- [1] Thomas B McKee, Nolan J Doesken, and John R Kleist. THE RELATIONSHIP OF DROUGHT FREQUENCY AND DURATION TO TIME SCALES. 1993.
- [2] Sergio M Vicente-Serrano, Santiago Beguería, and Juan I López-Moreno. A Multiscalar Drought Index Sensitive to Global Warming: The Standardized Precipitation Evapotranspiration Index. *Journal of Climate*, 23(7):1696–1718, 2010.
- [3] M P van Rooy. A RAINFALL ANOMALLY INDEX INDEPENDENT OF TIME AND SPACE, NOTOS. 1965.
- [4] E B Wilson and M M Hilferty. The Distribution of Chi-Square. *Proceedings of the National Academy of Sciences of the United States of America*, 17(12):684–688, dec 1931.
- [5] N Haied, A Foufou, S Chaab, M Azlaoui, S Khadri, K Benzahia, and I Benzahia. Drought assessment and monitoring using meteorological indices in a semi-arid region. *Energy Procedia*, 119:518–529, 2017.
- [6] Gene Willeke, J R M Hosking, James R Wallis, and Nathaniel B Guttman. The national drought atlas. *Proceedings of the Western Snow Conference, Colorado State University, Fort Collins*, 94, 1994.
- [7] India Meteorological Department. Statement on climate of india during 2020, Januray 2021.
- [8] MoEFCC India. Third biennial update report to the united nations framework convention on climate change, 2021.
- [9] R Krishnan, J Sanjay, Chellappan Gnanaseelan, Milind Mujumdar, Ashwini Kulkarni, and Supriyo Chakraborty. Assessment of climate change over the indian region, 2020.
- [10] Tom K. R. Matthews, Robert L. Wilby, and Conor Murphy. Communicating the deadly consequences of global warming for human heat stress. *Proceedings of the National Academy of Sciences*, 114(15):3861–3866, 2017.
- [11] Climate Research INDIA METEOROLOGICAL DEPARTMENT and Pune Services (CRS) Division. Observed monsoon rainfall variability and changes during recent 30 years (1989-2018), 2020.
- [12] Karumuri Ashok, Zhaoyong Guan, N. H. Saji, and Toshio Yamagata. Individual and combined influences of enso and the indian ocean dipole on the indian summer monsoon. *Journal of Climate*, 17(16):3141 – 3155, 2004.

- [13] Homero Paltan, Myles Allen, Karsten Haustein, Lena Fuldauer, and Simon Dadson. Global implications of 1.5 °c and 2 °c warmer worlds on extreme river flows. *Environmental Research Letters*, 13(9):094003, aug 2018.
- [14] UNISDR. Annual report 2014, 2014.
- [15] G. Naumann, L. Alfieri, K. Wyser, L. Mentaschi, R. A. Betts, H. Carrao, J. Spinoni, J. Vogt, and L. Feyen. Global changes in drought conditions under different levels of warming. *Geophysical Research Letters*, 45(7):3285–3296, 2018.
- [16] National Disaster Management Authority. National disaster management plan, 2016.
- [17] National Integrated Drought Information System (NIDIS). National integrated drought information system (nidis) strategic plan, 2022.
- [18] Karnataka State Health System Resource Center Department of Health Family Welfare. Draft of karnataka state action plan for climate change human health (ksapcchh), 2018.
- [19] Bonan GB, Levis S, Sitch S, Vertenstein M, and Oleson KW. A dynamic global vegetation model for use with climate models: concepts and description of simulated vegetation dynamics. *Global Change Biology*, 9(11):1543–1566, 2003.
- [20] Collins M, Tett S, and Cooper C. The internal climate variability of hadcm3, a version of the hadley centre coupled model without flux adjustments. *Climate Dynamics*, 17:61–81, January 2001.
- [21] D S Pai, Latha Sridhar, M Rajeevan, O P Sreejith, N S Satbhai, and B Mukhopadyay. Development of a new high spatial resolution ( 0 . 25 ° × 0 . 25 ° ) Long Period ( 1901-2010 ) daily gridded rainfall data set over India and its comparison with existing data sets over the region data sets of different spatial resolutions and time period. 1:1–18, 2014.
- [22] Jeanne Laurencelle, Tom Logan, and Rudi Gens. Alaska satellite facility (asf) radiometrically terrain corrected alos palsar products. page 12, 2015.
- [23] Susan K Jenson and Julia O Domingue. Extracting topographic structure from digital elevation data for geographic information-system analysis. *Photogrammetric Engineering and Remote Sensing*, 54:1593–1600, 1988.
- [24] Rajesh Sah and Apurba Das. Overcoming source limitations in drainage delineation by combining the streams of toposheet and dem in river

- morphometric studies. *Journal of the Geological Society of India*, 90:129–258, 08 2017.
- [25] Mehmet Dikici. Drought analysis with different indices for the Asi Basin (Turkey). *Scientific Reports*, 10(1):1–12, 2020.
- [26] Donald A. Wilhite and Michael H. Glantz. Understanding: the drought phenomenon: The role of definitions. *Water International*, 10(3):111–120, 1985.
- [27] A. K. Mishra and Vijay P. Singh. Analysis of drought severity-area-frequency curves using a general circulation model and scenario uncertainty. *Journal of Geophysical Research Atmospheres*, 114(6):1–18, 2009.
- [28] Giorgos Kallis. Droughts. *Annual Review of Environment and Resources*, 33:85–118, 2008.
- [29] Editorial. *Bulletin of the American Meteorological Society*, 78(5):797 – 802, 1997.
- [30] Peters E. Propagation of drought through groundwater systems-Illustrated in the Pang (UK) and Upper-Guadiana (ES) catchments, 2003.
- [31] Bilel Zerouali, Mohamed Chettih, Zaki Abda, Mohamed Mesbah, Celso Augusto Guimarães Santos, Reginaldo Moura Brasil Neto, and Richarde Marques Silva. Spatiotemporal meteorological drought assessment in a humid Mediterranean region: case study of the Oued Sebaou basin (northern central Algeria). *Natural Hazards: Journal of the International Society for the Prevention and Mitigation of Natural Hazards*, 108(1):689–709, August 2021.
- [32] Houquan Lu, Yihua Wu, Yijun Li, and Yongqiang Liu. Effects of meteorological droughts on agricultural water resources in southern China. *Journal of Hydrology*, 548:419–435, 2017.
- [33] S. Sangita Mishra and R. Nagarajan. Spatio-temporal drought assessment in tel river basin using standardized precipitation index (spi) and gis. *Geomatics, Natural Hazards and Risk*, 2(1):79–93, 2011.
- [34] Felicia Chiang, Omid Mazdiyasn, and Amir AghaKouchak. Evidence of anthropogenic impacts on global drought frequency, duration, and intensity. *Nature Communications*, 12(1):1–10, 2021.
- [35] Juan Du, Jian Fang, Wei Xu, and Peijun Shi. Analysis of dry/wet conditions using the standardized precipitation index and its potential usefulness for



- drought/flood monitoring in Hunan Province, China. *Stochastic Environmental Research and Risk Assessment*, 27(2):377–387, 2013.
- [36] M Naresh Kumar, C S Murthy, M V R Sesha Sai, and P S Roy. Spatiotemporal analysis of meteorological drought variability in the Indian region using standardized precipitation index. *Meteorological Applications*, 19(2):256–264, 2012.
- [37] Desalegn Chemed Edossa, Mukand Singh Babel, and Ashim Das Gupta. Drought analysis in the Awash River Basin, Ethiopia. *Water Resources Management*, 24(7):1441–1460, 2010.
- [38] P. Guhathakurta, Preetha Menon, P. M. Inkane, Usha Krishnan, and S. T. Sable. Trends and variability of meteorological drought over the districts of India using standardized precipitation index. *Journal of Earth System Science*, 126(8):1–18, 2017.
- [39] Subhajyoti Das. Natural Resources, Water Harvesting and Drought in Central India. *Journal of the Geological Society of India*, 95(3):321, 2020.
- [40] Ali Danandeh Mehr, Ali Unal Sorman, Ercan Kahya, and Mahdi Hesami Afshar. Climate change impacts on meteorological drought using SPI and SPEI: case study of Ankara, Turkey. *Hydrological Sciences Journal*, 65(2):254–268, 2020.
- [41] Javad Bazrafshan, Somayeh Hejabi, and Jaber Rahimi. Drought Monitoring Using the Multivariate Standardized Precipitation Index (MSPI). *Water Resources Management*, 28(4):1045–1060, 2014.
- [42] Khadija Diani, Ilias Kacimi, Mahmoud Zemzami, Hassan Tabyaoui, and Ali Torabi Haghighi. Evaluation of meteorological drought using the Standardized Precipitation Index (SPI) in the High Ziz River basin, Morocco. *Limnological Review*, 19(3):125–135, 2019.
- [43] G Rossi, M Benedini, G Tsakiris, and S Giakoumakis. On regional drought estimation and analysis. *Water Resources Management*, 6(4):249–277, 1992.
- [44] Ashok K. Mishra and Vijay P. Singh. A review of drought concepts. *Journal of Hydrology*, 391(1-2):202–216, sep 2010.
- [45] Ministry of Agriculture Farmers Welfare. Manual for Drought Management, 12 2019.
- [46] S. Mark Howden, Jean-François Soussana, Francesco N. Tubiello, Netra Chhetri, Michael Dunlop, and Holger Meinke. Adapting agriculture to climate

- change. *Proceedings of the National Academy of Sciences*, 104(50):19691–19696, 2007.
- [47] David Tilman, Christian Balzer, Jason Hill, and Belinda L Befort. Global food demand and the sustainable intensification of agriculture. 108(50):20260–20264, 2011.
- [48] Anne F. Van Loon. Hydrological drought explained. *WIREs Water*, 2(4):359–392, 2015.
- [49] Earth Sciences. Government of India Ministry of Earth Sciences ( MoES ) Climate Research and Services ( CRS ) Statement on Climate of India during 2020. 2010:1–5, 2021.
- [50] Ministry of Earth Science. Rainfall Statistics of India , 2019.
- [51] UNESCO IHE. Drought Vulnerability Assessment in Kenya. page 33, 2011.
- [52] River Development Ministry of Water Resources and Ganga Rejuvenation. *Ground Water Year Book*. Central Ground Water Board, 2017.
- [53] Hylke E. Beck, Niklaus E. Zimmermann, Tim R. McVicar, Noemi Vergopolan, Alexis Berg, and Eric F. Wood. Present and future köppen-geiger climate classification maps at 1-km resolution. *Scientific Data*, 5:1–12, 2018.
- [54] Lucas Eduardo de Oliveira Aparecido, Glauco de Souza Rolim, Jonathan Richetti, Paulo Sergio de Souza, and Jerry Adriani Johann. Köppen, Thornthwaite and Camargo climate classifications for climatic zoning in the State of Paraná, Brazil. *Ciencia e Agrotecnologia*, 40(4):405–417, 2016.
- [55] Rui Li, Atsushi Tsunekawa, and Mitsuru Tsubo. Index-based assessment of agricultural drought in a semi-arid region of Inner Mongolia, China. *Journal of Arid Land*, 6(1):3–15, 2014.
- [56] Boulos Abou Zakhem and Bassam Kattaa. Investigation of hydrological drought using cumulative standardized precipitation index (SPI 30) in the eastern Mediterranean region (Damascus, Syria). *Journal of Earth System Science*, 125(5):969–984, 2016.
- [57] A T M Sakiur Rahman, Chowdhury Sarwar Jahan, Quamrul Hasan Mazumder, Md. Kamruzzaman, and Takahiro Hosono. Drought analysis and its implication in sustainable water resource management in Barind area, Bangladesh. *Journal of the Geological Society of India*, 89(1):47–56, 2017.
- [58] Yi-Hwa (Eva) Wu and Ming-Chih Hung. Comparison of spatial interpolation techniques using visualization and quantitative assessment. In Ming-Chih

- Hung, editor, *Applications of Spatial Statistics*, chapter 2. IntechOpen, Rijeka, 2016.
- [59] W. R. Tobler. A Computer Movie Simulating Urban Growth in the Detroit Region. *Economic Geography*, 46:234, 1970.
- [60] Nathaniel B. Guttman. Accepting the standardized precipitation index: A calculation algorithm. *Journal of the American Water Resources Association*, 35(2):311–322, 1999.
- [61] G. Tsakiris and H. Vangelis. Towards a Drought Watch System based on spatial SPI. *Water Resources Management*, 18(1):1–12, 2004.
- [62] Nasrin Salehnia, Amin Alizadeh, Hossein Sanaeinejad, Mohammad Bannayan, and Azar Zarrin. Estimation of meteorological drought indices based on agmerra precipitation data and station-observed precipitation data. *Journal of Arid Land*, 9:797–809, 10 2017.
- [63] Danielle C. Edwards. Characteristics of 20th century drought in the united states at multiple time scales. 1997.
- [64] Herbert Conrad Schlueter Thom. *Some methods of climatological analysis*, volume 81. Secretariat of the World Meteorological Organization Geneva, 1966.
- [65] Jonathan Spinoni, Gustavo Naumann, Hugo Carrao, Paulo Barbosa, and Jürgen Vogt. World drought frequency, duration, and severity for 1951-2010. *International Journal of Climatology*, 34(8):2792–2804, 2014.
- [66] Zexi Shen, Qiang Zhang, Vijay P Singh, Peng Sun, Changqing Song, and Huiqian Yu. Agricultural drought monitoring across Inner Mongolia, China: Model development, spatiotemporal patterns and impacts. *Journal of Hydrology*, 571:793–804, 2019.
- [67] Hassan Moradi, M Rajabi, and M Faragzadeh. Investigation of meteorological drought characteristics in Fars province, Iran. *CATENA*, 84:35–46, 2011.
- [68] Santiago Begueria, Sergio M. Vicente-Serrano, and Marta Angulo-Martinez. A multiscalar global drought dataset: The speibase: A new gridded product for the analysis of drought variability and impacts. *Bulletin of the American Meteorological Society*, 91(10):1351 – 1356, 2010.
- [69] Shujun Guo. The Meteorological Disaster Risk Assessment Based on the Diffusion Mechanism. *Journal of Risk Analysis and Crisis Response*, 2:124, 2012.
- [70] C Giannakopoulos, P Le Sager, M Bindi, M Moriondo, E Kostopoulou, and C M Goodess. Climatic changes and associated impacts in the Mediterranean

- resulting from a 2°C global warming. *Global and Planetary Change*, 68(3):209–224, 2009.
- [71] W C Palmer. *Meteorological Drought*. Meteorological Drought. U.S. Department of Commerce, Weather Bureau, p.58, 1965.
- [72] Shraddhanand Shukla and Andrew W. Wood. Use of a standardized runoff index for characterizing hydrologic drought. *Geophysical Research Letters*, 35(2):L02405, 2008.
- [73] W J Werick, G E Willeke, N B Guttman, J R M Hosking, and J R Wallis. National drought atlas developed. *Eos, Transactions American Geophysical Union*, 75(8):89–90, 1994.
- [74] Anne K Fleig, Lena M Tallaksen, Hege Hisdal, and David M Hannah. Regional hydrological drought in north-western Europe: linking a new Regional Drought Area Index with weather types. *Hydrological Processes*, 25(7):1163–1179, 2011.
- [75] Sergio M Vicente-Serrano, Santiago Begueria, and Juan I López-Moreno. Comment on Characteristics and trends in various forms of the Palmer Drought Severity Index (PDSI) during 1900-2008 by Aiguo Dai. *Journal of Geophysical Research: Atmospheres*, 116:D19112, 2011.
- [76] S M Vicente-Serrano, A Zouber, T Lasanta, and Y Pueyo. Dryness is accelerating degradation of vulnerable shrublands in semiarid Mediterranean environments. *Ecological Monographs*, 82(4):407–428, 2012.
- [77] Sergio M Vicente-Serrano, Cesar Azorin-Molina, Arturo Sanchez-Lorenzo, Enrique Morán-Tejeda, Jorge Lorenzo-Lacruz, Jesús Revuelto, Juan I López-Moreno, and Francisco Espejo. Temporal evolution of surface humidity in Spain: recent trends and possible physical mechanisms. *Climate Dynamics*, 42(9):2655–2674, 2014.
- [78] Deepak Singh Bisht, Venkataramana Sridhar, Ashok Mishra, Chandranath Chatterjee, and Narendra Singh Raghuvanshi. Drought characterization over India under projected climate scenario. *International Journal of Climatology*, 39(4):1889–1911, 2019.
- [79] Changhong Liu, Cuiping Yang, Qi Yang, and Jiao Wang. Spatiotemporal drought analysis by the standardized precipitation index (SPI) and standardized precipitation evapotranspiration index (SPEI) in Sichuan Province, China. *Scientific Reports*, 11:1280, 2021.

- [80] Zhifang Pei, Shibo Fang, Lei Wang, and Wunian Yang. Comparative Analysis of Drought Indicated by the SPI and SPEI at Various Timescales in Inner Mongolia, China. *Water*, 12(7):1925, 2020.
- [81] Simone Falzoi, Emily Gleeson, Keith Lambkin, Jesko Zimmermann, Richa Marwaha, Robert O'Hara, Stuart Green, and Simona Fratianni. Analysis of the severe drought in Ireland in 2018. *Weather*, 74(11):368–373, 2019.
- [82] Masoud Irannezhad, Behzad Ahmadi, Bjørn Kløve, and Hamid Moradkhani. Atmospheric circulation patterns explaining climatological drought dynamics in the boreal environment of Finland, 1962-2011. *International Journal of Climatology*, 37(S1):801–817, 2017.
- [83] Liyan Tian and Steven M Quiring. Spatial and temporal patterns of drought in Oklahoma (1901-2014). *International Journal of Climatology*, 39(7):3365–3378, 2019.
- [84] Fernando Domínguez-Castro, Sergio M Vicente-Serrano, Miquel Tomás-Burguera, Marina Peña-Gallardo, Santiago Beguería, Ahmed El Kenawy, Yolanda Luna, and Ana Morata. High spatial resolution climatology of drought events for Spain: 1961-2014. *International Journal of Climatology*, 39(13):5046–5062, 2019.
- [85] Roberto Serrano-Notivoli, Ernesto Tejedor, Pablo Sarricolea, Oliver Meseguer-Ruiz, Mathias Vuille, Magdalena Fuentealba, and Martín de Luis. Hydroclimatic variability in Santiago (Chile) since the 16th century. *International Journal of Climatology*, 41(S1):E2015–E2030, 2021.
- [86] Daniele Secci, Maria Giovanna Tanda, Marco D'Oria, Valeria Todaro, and Camilla Fagandini. Impacts of climate change on groundwater droughts by means of standardized indices and regional climate models. *Journal of Hydrology*, 603:127154, 2021.
- [87] Hafzullah Aksoy, Mahmut Cetin, Ebru Eris, Halil Ibrahim Burgan, Yonca Cavus, Isilsu Yildirim, and Murugesu Sivapalan. Critical drought intensity-duration-frequency curves based on total probability theorem-coupled frequency analysis. *Hydrological Sciences Journal*, 66(8):1337–1358, 2021.
- [88] Sanjay Kumar, S A Ahmed, N Harishnaika, and M Arpitha. Spatial and Temporal Pattern Assessment of Meteorological Drought in Tumakuru District of Karnataka during 1951-2019 using Standardized Precipitation Index. *Journal of the Geological Society of India*, 98(6):822–830, 2022.

- [89] Ranjeet John, Jiquan Chen, Zu-Tao Ou-Yang, Jingfeng Xiao, Richard Becker, Arindam Samanta, Sangram Ganguly, Wenping Yuan, and Ochirbat Batkhishig. Vegetation response to extreme climate events on the Mongolian Plateau from 2000 to 2010. *Environmental Research Letters*, 8(3):35033, aug 2013.
- [90] Santiago Begueria, Sergio M. Vicente-Serrano, Fergus Reig, and Borja Latorre. Standardized precipitation evapotranspiration index (spei) revisited: parameter fitting, evapotranspiration models, tools, datasets and drought monitoring. *International Journal of Climatology*, 34(10):3001–3023, 2014.
- [91] Myles Allen, O P Dube, W Solecki, F Aragón-Durand, W Cramer, S Humphreys, M Kainuma, J Kala, N Mahowald, and Y Mulugetta. Global warming of 1.5°C. An IPCC Special Report on the impacts of global warming of 1.5°C above pre-industrial levels and related global greenhouse gas emission pathways, in the context of strengthening the global response to the threat of climate change. *Sustainable Development, and Efforts to Eradicate Poverty*, 2018.
- [92] Mohd Sayeed Ul Hasan and Abhishek Kumar Rai. Groundwater quality assessment in the Lower Ganga Basin using entropy information theory and GIS. *Journal of Cleaner Production*, 274:123077, 2020.
- [93] Bushra Praveen, Swapan Talukdar, Shahfahad, Susanta Mahato, Jayanta Mondal, Pritee Sharma, Abu Reza Md. Towfiqul Islam, and Atiqur Rahman. Analyzing trend and forecasting of rainfall changes in India using non-parametrical and machine learning approaches. *Scientific Reports*, 10(1):10342, 2020.
- [94] Dickson Mbigi and Ziniu Xiao. Analysis of rainfall variability for the October to December over Tanzania on different timescales during 1951–2015. *International Journal of Climatology*, 41(14):6183–6204, nov 2021.
- [95] K Ibrahim-Bathis, S A Ahmed, V Nischitha, and M A Mohammed-Aslam. Crop Water Requirements Analysis Using Geoinformatics Techniques in the Water-Scarce Semi-Arid Watershed. In *Advances in Remote Sensing for Natural Resource Monitoring*, chapter 6, pages 81–93. John Wiley Sons, Ltd, 2021.
- [96] Henry B Mann. Nonparametric Tests Against Trend. *Econometrica*, 13(3):245–259, 1945.
- [97] Zekâi Sen, Eyüp Sisman, and Ismail Dabanli. Innovative Polygon Trend Analysis (IPTA) and applications. *Journal of Hydrology*, 575(November 2018):202–210, 2019.

- [98] Naomi Altman and Martin Krzywinski. Simple linear regression. *Nature Methods*, 12(11):999–1000, 2015.
- [99] Zekâi Sen. Innovative Trend Analysis Methodology. *Journal of Hydrologic Engineering*, 17(9):1042–1046, sep 2012.
- [100] Mohd Sayeed Ul Hasan, Abhishek Kumar Rai, Zeesam Ahmad, Faisal M Alfaisal, Mohammad Amir Khan, Shamshad Alam, and Meheebub Sahana. Hydrometeorological consequences on the water balance in the Ganga river system under changing climatic conditions using land surface model. *Journal of King Saud University - Science*, 34(5):102065, 2022.
- [101] Zichen Hu, Shuguang Liu, Guihui Zhong, Hejuan Lin, and Zhengzheng Zhou. Modified Mann-Kendall trend test for hydrological time series under the scaling hypothesis and its application. *Hydrological Sciences Journal*, 65(14):2419–2438, 2020.
- [102] Murat San, Fatma Akçay, Nguyen Thi Thuy Linh, Murat Kankal, and Quoc Bao Pham. Innovative and polygonal trend analyses applications for rainfall data in Vietnam. *Theoretical and Applied Climatology*, 144(3-4):809–822, 2021.
- [103] Sinan Jasim Hadi and Mustafa Tombul. Long-term spatiotemporal trend analysis of precipitation and temperature over Turkey. *Meteorological Applications*, 25(3):445–455, 2018.
- [104] Priya Narayanan, Sumana Sarkar, Ashoke Basistha, and Kamna Sachdeva. Trend analysis and forecast of pre-monsoon rainfall over India. *Weather*, 71(4):94–99, 2016.
- [105] Brototi Biswas, Ratnaprabha S Jadhav, and Nilima Tikone. Rainfall Distribution and Trend Analysis for Upper Godavari Basin, India, from 100 Years Record (1911-2010). *Journal of the Indian Society of Remote Sensing*, 47(10):1781–1792, 2019.
- [106] Jayanta Das, Tapash Mandal, A. T.M.Sakiur Rahman, and Piu Saha. Spatio-temporal characterization of rainfall in Bangladesh: an innovative trend and discrete wavelet transformation approaches. *Theoretical and Applied Climatology*, 143(3-4):1557–1579, 2021.
- [107] Yujie Liu, Jie Chen, and Tao Pan. Spatial and temporal patterns of drought hazard for China under different RCP scenarios in the 21st century. *International Journal of Disaster Risk Reduction*, 52:101948, 2021.

- [108] Yiliner Alifujiang, Jilili Abuduwaili, Balati Maihemuti, Bilal Emin, and Michael Groll. Innovative trend analysis of precipitation in the Lake Issyk-Kul Basin, Kyrgyzstan. *Atmosphere*, 11(4):1–16, 2020.
- [109] Bilel Zerouali, Nadhir Al-Ansari, Mohamed Chettih, Mesbah Mohamed, Zaki Abda, Celso Augusto Guimarães Santos, Bilal Zerouali, and Ahmed Elbeltagi. An enhanced innovative triangular trend analysis of rainfall based on a spectral approach. *Water (Switzerland)*, 13(5):727, 2021.
- [110] Atul Saini, Netrananda Sahu, Pankaj Kumar, Sridhara Nayak, Weili Duan, Ram Avtar, and Swadhin Behera. Advanced Rainfall Trend Analysis of 117 Years over West Coast Plain and Hill Agro-Climatic Region of India. *Atmosphere*, 11(11):1–25, 2020.
- [111] Lalit Pal, Chandra Shekhar P Ojha, Surendra K Chandniha, and Amit Kumar. Regional scale analysis of trends in rainfall using nonparametric methods and wavelet transforms over a semi-arid region in India. *International Journal of Climatology*, 39(5):2737–2764, 2019.
- [112] Melkamu Meseret Alemu and Getnet Taye Bawoke. Analysis of spatial variability and temporal trends of rainfall in Amhara region, Ethiopia. *Journal of Water and Climate Change*, 11(4):1505–1520, 10 2019.
- [113] RN Singh, Sonam Sah, Bappa Das, Lata Vishnoi, and H Pathak. Spatio-temporal trends and variability of rainfall in Maharashtra, India: Analysis of 118 years. *Theoretical and Applied Climatology*, 143(3):883–900, 2021.
- [114] W D S Nisansala, N S Abeysingha, Adlul Islam, and A M K R Bandara. Recent rainfall trend over Sri Lanka (1987-2017). *International Journal of Climatology*, 40(7):3417–3435, 2020.
- [115] Jesper Rydén. Statistical analysis of possible trends for extreme floods in northern Sweden. *River Research and Applications*, 38(6):1041–1050, 2022.
- [116] Jeffrey Denzil K Marak, Arup Kumar Sarma, and Rajib Kumar Bhattacharjya. Innovative trend analysis of spatial and temporal rainfall variations in Umiam and Umtru watersheds in Meghalaya, India. *Theoretical and Applied Climatology*, 142(3):1397–1412, 2020.
- [117] R N Singh, Sonam Sah, Bappa Das, Sunil Potekar, Amresh Chaudhary, and H Pathak. Innovative trend analysis of spatio-temporal variations of rainfall in India during 1901-2019. *Theoretical and Applied Climatology*, pages 821–838, 2021.



- [118] S Jain, Vijay Kumar, and M Saharia. Analysis of rainfall and temperature trends in northeast India. *International Journal of Climatology*, 33:968–978, 2013.
- [119] Hans Von Storch. Misuses of statistical analysis in climate research. In *Analysis of climate variability*, pages 11–26. Springer, 1999.
- [120] Maurice G Kendall. *Rank correlation methods*. Griffin, London, 1975.
- [121] Khaled H Hamed and A Ramachandra Rao. A modified Mann-Kendall trend test for autocorrelated data. *Journal of Hydrology*, 204(1):182–196, 1998.
- [122] Pranab Kumar Sen. Estimates of the Regression Coefficient Based on Kendall's Tau. *Journal of the American Statistical Association*, 63(324):1379–1389, jul 1968.
- [123] Zekai Sen. Innovative trend significance test and applications. *Theoretical and Applied Climatology*, 127(3-4):939–947, feb 2017.
- [124] Sadik Alashan. Testing and improving type 1 error performance of Åžen's innovative trend analysis method. *Theoretical and Applied Climatology*, 142(3):1015–1025, 2020.
- [125] Hao Wu and Hui Qian. Innovative trend analysis of annual and seasonal rainfall and extreme values in Shaanxi, China, since the 1950s. *International Journal of Climatology*, 37(5):2582–2592, 2017.
- [126] Paul Dankwa, Eugene Cudjoe, Ebenezer Ebo Yahans Amuah, Raymond Webrah Kazapoe, and Edna Pambour Agyemang. Analyzing and forecasting rainfall patterns in the Manga-Bawku area, northeastern Ghana: Possible implication of climate change. *Environmental Challenges*, 5:100354, 2021.
- [127] J. Malley et al. P.R. Shukla, J. Skea, R. Slade, A. Al Khourdajie, R. van Diemen, D. McCollum, M. Pathak, S. Some, P. Vyas, R. Fradera, M. Belkacemi, A. Hasija, G. Lisboa, S. Luz. IPCC, 2022: Climate Change 2022: Mitigation of Climate Change. Contribution of Working Group III to the Sixth Assessment Report of the Intergovernmental Panel on Climate Change. Technical report.
- [128] Yavuz Selim Güçlü. Improved visualization for trend analysis by comparing with classical Mann-Kendall test and ITA. *Journal of Hydrology*, 584:124674, 2020.
- [129] Sanjay Kumar, Syed Ashfaq Ahmed, and Jyothika Karkala. Evaluating the Consistency of TRMM over the Rain Gauge for Drought Monitoring in the Semi-Arid Region of Karnataka, India using Statistical Methods. *Environ. Sci.: Adv.*, 1:517–529, 2022.

- [130] Huiling YANG, Hui XIAO, Chunwei GUO, Yue SUN, and Ruina GAO. Innovative trend analysis of annual and seasonal precipitation in Ningxia, China. *Atmospheric and Oceanic Science Letters*, 13(4):308–315, 2020.
- [131] A N Pettitt. A Non-Parametric Approach to the Change-Point Problem. *Journal of the Royal Statistical Society: Series C (Applied Statistics)*, 28(2):126–135, 1979.
- [132] T A Buishand. Some methods for testing the homogeneity of rainfall records. *Journal of Hydrology*, 58(1):11–27, 1982.
- [133] S Swain, S Nandi, and P Patel. Development of an ARIMA Model for Monthly Rainfall Forecasting over Khordha District, Odisha, India. In Pankaj Kumar Sa, Sambit Bakshi, Ioannis K Hatzilygeroudis, and Manmath Narayan Sahoo, editors, *Recent Findings in Intelligent Computing Techniques*, pages 325–331, Singapore, 2018. Springer Singapore.
- [134] G E P Box and D R Cox. An Analysis of Transformations. *Journal of the Royal Statistical Society: Series B (Methodological)*, 26(2):211–243, 1964.
- [135] Wayne C Palmer. Keeping Track of Crop Moisture Conditions, Nationwide: The New Crop Moisture Index. *Weatherwise*, 21(4):156–161, 1968.
- [136] Qiaohong Sun, Chiyuan Miao, Qingyun Duan, Hamed Ashouri, Soroosh Sorooshian, and Kuo-Lin Hsu. A Review of Global Precipitation Data Sets: Data Sources, Estimation, and Intercomparisons. *Reviews of Geophysics*, 56(1):79–107, 2018.
- [137] Mehdi Mahbod, Amin Shirvani, and Fabio Veronesi. A comparative analysis of the precipitation extremes obtained from tropical rainfall-measuring mission satellite and rain gauges datasets over a semiarid region. *International Journal of Climatology*, 39(1):495–515, 2019.
- [138] Anoop Kumar Shukla, Chandra Shekhar Prasad Ojha, Rajendra Prasad Singh, Lalit Pal, and Dafang Fu. Evaluation of TRMM Precipitation Dataset over Himalayan Catchment: The Upper Ganga Basin, India. *Water*, 11(3), 2019.
- [139] Venkatraman Prasanna, Juvy Subere, Dwijendra K Das, Srinivasan Govindarajan, and Tetsuzo Yasunari. Development of daily gridded rainfall dataset over the Ganga, Brahmaputra and Meghna river basins. *Meteorological Applications*, 21(2):278–293, 2014.
- [140] Vivek Gupta, Manoj K Jain, Pushpendra K Singh, and Vishal Singh. An assessment of global satellite-based precipitation datasets in capturing precipitation extremes: A comparison with observed precipitation dataset in India. *International Journal of Climatology*, 40(8):3667–3688, 2020.

- [141] Manoj Thakur, T Kumar, M Narayanan, Koteswara, and Humberto Barbosa. Analytical study of the performance of the IMERG over the Indian landmass. *Meteorological Applications*, 27:1–11, 2020.
- [142] U V Murali Krishna, Subrata Kumar Das, Sachin M Deshpande, S L Doiphode, and G Pandithurai. The assessment of Global Precipitation Measurement estimates over the Indian subcontinent. *Earth and Space Science*, 4(8):540–553, 2017.
- [143] Xianghu Li, Qi Zhang, and Xuchun Ye. Dry/Wet Conditions Monitoring Based on TRMM Rainfall Data and Its Reliability Validation over Poyang Lake Basin, China. *Water*, 5(4):1848–1864, 2013.
- [144] S E Nicholson, D Klotter, L Zhou, and W Hua. Validation of Satellite Precipitation Estimates over the Congo Basin. *Journal of Hydrometeorology*, 20(4):631–656, 2019.
- [145] Diogo Costa Buarque, Rodrigo Cauduro Dias de Paiva, Robin T Clarke, and Carlos André Bulhões Mendes. A comparison of Amazon rainfall characteristics derived from TRMM, CMORPH and the Brazilian national rain gauge network. *Journal of Geophysical Research (Atmospheres)*, 116(D19):D19105, oct 2011.
- [146] Yancong Cai, Changjie Jin, Anzhi Wang, De-Xin Guan, Jiabing Wu, Fenghui Yuan, and Leilei Xu. Comprehensive precipitation evaluation of TRMM 3B42 with dense rain gauge networks in a mid-latitude basin, northeast, China. *Theoretical and Applied Climatology*, 126:659–671, 2015.
- [147] A Ochoa, L Pineda, P Crespo, and P Willems. Evaluation of TRMM 3B42 precipitation estimates and WRF retrospective precipitation simulation over the Pacific–Andean region of Ecuador and Peru. *Hydrology and Earth System Sciences*, 18(8):3179–3193, 2014.
- [148] Ming Pan, Haibin Li, and Eric Wood. Assessing the Skill of Satellite-Based Precipitation Estimates in Hydrologic Applications. *Water Resources Research - WATER RESOUR RES*, 46:535, 2010.
- [149] Abd. Rahman As-syakur, T Tanaka, Rakhmat Prasetia, Swardika Ketut, and I Kasa. Comparison of TRMM Multisatellite Precipitation Analysis (TMPA) Products and Daily-Monthly Gauge Data over Bali Island. *International Journal of Remote Sensing*, 32:8969–8982, 2011.
- [150] Roongroj Chokngamwong and Long Chiu. Comparisons of Daily Thailand Rain Gauge with GPCC and TRMM Satellite Precipitation Measurements. 2022.

- [151] Wilhelm Kirch, editor. *Student's t-Test*, page 1358. Springer Netherlands, Dordrecht, 2008.
- [152] Wilhelm Kirch, editor. *Pearson's Correlation Coefficient*, pages 1090–1091. Springer Netherlands, Dordrecht, 2008.

## Publication

1. **Sanjay Kumar**, Syed Ashfaq Ahmed and Jyothika Karkala (2022) *Intensity and Spatiotemporal Variations of Drought in Tumakuru District, India using drought Indices*. Geocarto International
2. **Sanjay Kumar**, Syed Ashfaq Ahmed, Harish Naika N and Arpitha M (2022) *Spatial and Temporal Pattern Assessment of Meteorological Drought in Tumakuru District of Karnataka during 1951–2019 using Standardized Precipitation Index*. Journal of the Geological Society of India 98, 822–830. <https://doi.org/10.1007/s12594-022-2073-3>
3. **Sanjay Kumar**, Syed Ashfaq Ahmed and Jyothika Karkala (2022) *Evaluating the Consistency of TRMM over the Rain Gauge for Drought Monitoring in the Semi-Arid Region of Karnataka, India using Statistical Methods*. Environmental Science: Advances
4. Harish Naika N, Syed Ashfaq Ahmed, **Sanjay Kumar** and Arpitha M (2022) *Computation of the spatio-temporal extent of rainfall and long-term meteorological drought assessment using standardized precipitation index over Kolar and Chikkaballapura districts, Karnataka during 1951-2019*. Remote Sensing Applications: Society and Environment, 27, 100768. <https://doi.org/https://doi.org/10.1016/j.rsase.2022.100768>
5. Harish Naika N, Syed Ashfaq Ahmed, **Sanjay Kumar** and Arpitha M (2022) *Spatio-Temporal Rainfall Trend Assessment Over a Semi-Arid Region of Karnataka State, Using Non-Parametric Techniques*. Arabian Journal of Geosciences

## Papers in communication

- 6. Sanjay Kumar**, Syed Ashfaq Ahmed and Jyothika Karkala (2022)  
*Time Series Data and Rainfall Pattern Subjected to Climate Change using Non-Parametric Tests over Vulnerable Region of Karnataka, India.*  
Journal of Water and Climate Change
- 7. Sanjay Kumar**, Syed Ashfaq Ahmed and Jyothika Karkala (2022)  
*Statistical Approach to Visualize the Seven-Decadal Rainfall Variation as response to Climate Change in a semiarid region of Karnataka, India.*  
Arabian Journal of Geosciences
- 8. Sanjay Kumar**, Syed Ashfaq Ahmed and Jyothika Karkala (2022)  
*Variation in the response of ground and satellite-based precipitation products in the interpretation of drought in Tumakuru District, Karnataka.* World Development Sustainability

## Paper Presented in International Conferences

1. Presented research paper entitled "*Implementing Standardized Precipitation Index for Assessing the Spatio-Temporal Meteorological Drought pattern in Tumakuru District, India*" in three-day International Conference on **Earth and Environment in Anthropocene (ICEEA-2021)** held on 29th – 31st October, 2021 organised by the Department of Geology, School of Earth Sciences, Central University of Karnataka, India jointly with Centre for Environmental Sciences, and Department of Geology, University of Madras, Chennai, India
2. Presented research paper entitled "*Correlation of SPI and SPEI for the Spatiotemporal Analysis of Drought Characteristics in Tumakuru District, Karnataka, India*" in the International Conference on **Extreme weather events under changing climate (ICEWECC - 2022)**, Jointly organised by G.B. Pant National Institute of Himalayan Environment, Himachal region centre, Kullu along with CSIR -Fourth paradigm Institute, Bangalore and District Disaster Management Authority, Kullu, Himachal Pradesh, India held during March 10 – 11, 2022.
3. Presented research paper entitled "*Analyzing the Seven Decadal Rainfall Patterns through a Non-parametric Statistical Approach in Southeast Karnataka*" in the International Conference on **Only One Earth-Save Our Mother Earth** on 4th -5th June 2022 organised by centre for Environmental Sciences, University of Madras and National Polytechnic Institute (IPN), Mexico City, Mexico

## Paper Presented in National Conferences

1. Presented research paper entitled "*Spatio-Temporal Characterization and Trend Analysis of Rainfall over Tumakuru District, Karnataka*" in the National Conference on **Recent Trend in Earth Science and Geoinformatics Application in Engineering Practices** held during 9th and 10th March – 2022 at Department of Earth Science, University of Mysore, Manasagangotri, Mysore-570006, Karnataka, India